Division of Marine Engineering,
School of Naval Architecture and Marine Engineering,
National Technical University of Athens

DIPLOMA THESIS

Modeling of Ammonia Combustion Emissions in a Dual-Fuel Engine

Georgios Pontikakos

Examination Committee:

L. Kaiktsis, Professor NTUA (Supervisor)
G. Papadakis, Assistant Professor NTUA
C. Papadopoulos, Associate Professor NTUA

In collaboration with:

Winterthur Gas & Diesel Ltd, Winterthur, Switzerland

Athens, February 2023

Abstract

The strict regulations dictated by the International Maritime Organization (IMO) regarding the decarbonization of the shipping sector have initiated worldwide research and development for using alternative fuels for ship propulsion. Among them, ammonia (NH_3) is an attractive candidate, due to its wide availability and the potential of being produced by means of renewable energies, its non-explosive character, as well as its good thermophysical properties, which include a volumetric energy density in the range of other alternative fuels. Potential challenges associated with the adoption of ammonia for marine propulsion include its resistance to autoignition, its corrosive and toxic characteristics, the potential for nitrogen oxides (NOx) formation due to fuel bound nitrogen, as well as the production of nitrous oxide (N_2O), associated with a very high global warming potential.

The main objective of the present study is to develop and validate a computational tool for assessing the production of emissions from ammonia combustion in dual-fuel engines. To this end, a thermodynamic model is developed in the frame of the GT-POWER computational tool, and is coupled with a Detailed Chemical Kinetics Mechanism (DCKM). The latter consists of a detailed mechanism for n-dodecane ($C_{12}H_{26}$) combustion, assembled with a mechanism for NOx-NH_3 chemistry; it includes approximately 190 species and 2800 elementary reactions.

The computational tool developed has been tested for the case of a heavy-duty four-stroke dual-fuel engine, for which experimental data are available in the open literature. The engine can operate (i) in the diesel mode, and (ii) using simultaneously diesel fuel and ammonia, with the former directly injected and the latter introduced upstream the intake manifold. The present computational results were compared against experimental data for a ”Constant Power - Constant Speed” operation stencil; as the percentage of ammonia in the fuel mixture increases, the engine operation transitions from a diesel mode to a lean premixed ammonia combustion mode. The parameters of the thermodynamic tool developed were properly adapted to match the experimental pressure traces, yielding an overall good comparison for all cases considered. Further, predictions of emitted carbon dioxide (CO_2) were also in good agreement with experiments. Predicted nitric oxide (NO) emissions were in reasonably good agreement with experiments for high and intermediate percentage of diesel in the diesel-ammonia mixture, and less so for low contribution of diesel fuel (high percentage of ammonia), suggesting that the chemical kinetics mechanism should be further tested in the corresponding operation range. Low exhaust concentration was predicted for nitrogen dioxide (NO_2) and N_2O. Overall, the present development forms a solid basis towards characterizing ammonia combustion and predicting associated emissions in marine engines operating with ammonia, in an effective manner.

Σύνοψη

Οι κανονισμοί που θεσπίστηκαν πρόσφατα από τον Διεθνή Ναυτιλιακό Οργανισμό (International Maritime Organization - IMO) σχετικά με την απανθρακοποίηση της ναυτιλίας έχουν δώσει το έναυσμα για έρευνα και ανάπτυξη με στόχο τη χρήση εναλλακτικών καυσίμων στην πρόωση πλοίων. Μεταξύ αυτών, η αμμωνία (NH_3) είναι μια ελκυστική δυνατότητα, εξαιτίας της ευρείας διαθεσιμότητάς της και της δυνατότητας παραγωγής της μέσω ανανεώσιμων πηγών ενέργειας, της χαμηλής της εκρηκτικότητας, καθώς και των καλών θερμοφυσικών ιδιοτήτων της. Οι τελευταίες περιλαμβάνουν ενεργειακό κατ' όγκον περιεχόμενο στο εύρος άλλων εναλλακτικών καυσίμων. Πιθανές προκλήσεις που σχετίζονται με την υιοθέτηση της αμμωνίας ως ναυτιλιακό καύσιμο περιλαμβάνουν την αντίσταση σε αυτανάφλεξη, τον διαβρωτικό - τοξικό χαρακτήρα της, τον σχηματισμό οξειδίων του αζώτου (NOx) ως επακόλουθο της παρουσίας αζώτου στο μόριο, καθώς και την παραγωγή υποξειδίου του αζώτου (N_2O), που αποτελεί πολύ ισχυρό αέριο του θερμοκηπίου.

Ο κύριος στόχος της παρούσας εργασίας είναι η ανάπτυξη και επαλήθευση ενός υπολογιστικού εργαλείου για τον υπολογισμό των παραγόμενων αέριων ρύπων από την καύση αμμωνίας σε κινητήρες διπλού καυσίμου, οι οποίοι ενδιαφέρουν άμεσα στο πλαίσιο εφαρμογών της ναυτιλίας. Για τον σκοπό αυτόν, αναπτύχθηκε στο περιβάλλον του υπολογιστικού πακέτου GT-POWER ένα θερμοδυναμικό μοντέλο, και έγινε σύζευξή του με έναν λεπτομερή μηχανισμό χημικής κινητικής. Ο τελευταίος αποτελείται από έναν λεπτομερή μηχανισμό για την καύση κανονικού δωδεκανίου ($C_{12}H_{26}$), σε συνδυασμό με έναν μηχανισμό της χημείας NOx-NH_3, που περιλαμβάνει συνολικά περίπου 190 ενώσεις και 2800 στοιχειώδεις αντιδράσεις.

Στο πλαίσιο της παρούσας εργασίας, το αναπτυχθέν υπολογιστικό εργαλείο εφαρμόστηκε στην περίπτωση ενός τετράχρονου κινητήρα διπλού καυσίμου βαρέως τύπου, για τον οποίο υπάρχουν διαθέσιμα πειραματικά δεδομένα στη βιβλιογραφία. Ο κινητήρας μπορεί να λειτουργεί (i) ως κινητήρας Diesel, και (ii) με ταυτόχρονη χρήση καυσίμου diesel (απευθείας έγχυση) και αμμωνίας (προσθήκη στην πολλαπλή εισαγωγής). Τα παρόντα υπολογιστικά αποτελέσματα συγκρίθηκαν με πειραματικά δεδομένα για ένα σύνολο περιπτώσεων λειτουργίας με κοινό χαρακτηριστικό "Σταθερή Ισχύς - Σταθερές Στροφές". Στο παραπάνω πλαίσιο, με αύξηση του ποσοστού της αμμωνίας στο μείγμα του καυσίμου, η λειτουργία του κινητήρα μεταπίπτει από την καύση τύπου diesel σε καύση με φλόγα προαναμείξης. Οι παράμετροι του θερμοδυναμικού μοντέλου που αναπτύχθηκε προσαρμόστηκαν κατάλληλα, επιτυγχάνοντας συνολικά καλή σύγκλιση με τα πειραματικά δεδομένα για τις καμπύλες πίεσης, στις περιπτώσεις που εξετάστηκαν. Οι προβλέψεις για το εκπεμπόμενο διοξείδιο του άνθρακα (CO_2) ήταν επίσης σε καλή συμφωνία με τα πειράματα. Για υψηλό και ενδιάμεσο ποσοστό καυσίμου diesel στο μείγμα diesel-αμμωνίας, οι υπολογισθείσες τελικές συγκεντρώσεις μονοξειδίου του αζώτου (NO) ήταν σε αρκετά καλή συμφωνία με τα πειραματικά δεδομένα, και λιγότερο για χαμηλή περιεκτικότητα του καυσίμου diesel (υψηλό ποσοστό αμμωνίας), γεγονός που υποδηλώνει ότι ο μηχανισμός χημικής κινητικής θα πρέπει να εξεταστεί περαιτέρω στο αντίστοιχο εύρος λειτουργίας. Τέλος, οι υπολογισθείσες τελικές συγκεντρώσεις διοξειδίου του αζώτου (NO_2) και N_2O ήταν σε όλες τις περιπτώσεις σε χαμηλά επίπεδα. Συνολικά, η παρούσα εργασία συνιστά μια ουσιαστική βάση για περαιτέρω έρευνα για τον χαρακτηρισμό της καύσης της αμμωνίας και τον υπολογισμό των εκπομπών αέριων ρύπων σε κινητήρες με ενδιαφέρον για εφαρμογές πρόωσης στη ναυτιλία.

Contents

List of Figures

List of Tables

Chapter 1

Introduction

1.1 Emissions and corresponding Regulations in the maritime domain

Ever since man made the first floating craft, the sea has been used extensively for the transportation of both people and goods.From wind energy to steam, and from steam to the Internal Combustion Engine(ICE), mankind is continuously looking for new ways in order to make maritime transportation faster and more efficient. With the wide adoption of the Diesel engine from ships in the early 20^{th} century, the world trade has changed radically over the years. However, with the implementation of the Diesel technology, many problems have risen concerning both the human health and the environment, due to the emissions produced from the engine operation. Today, with well over a century of use, the large 2-Stroke Marine Diesel Engine has been established as the main propulsive force of the world's trading fleet. Although the engine itself has undergone substantial changes and developments in order to become even more efficient and environmentally friendly, further actions are needed in order to address the current environmental and energy needs.

The continuous abatement of the available fossil fuels, and ultimately their depletion, as well as the severe environmental impact of the emissions produced during their combustion, have troubled the global community for decades; today, the need to take action is more urgent than ever. The main emissions produced from marine engines are the following: Nitrogen Oxides (**NOx**), which contribute to the formation of smog and acid rain, Sulfur Oxides (**SOx**), which have an acidifying effect on the environment, Carbon Dioxide ($\mathbf{CO_2}$), which is the main GreenHouse Gas(GHG), Carbon Monoxide (**CO**), which is poisonous to humans, and finally **soot** and **particulate matter**. The first worth important regulation concerning the air pollution from ships is MARPOL's Annex VI, titled "Prevention of air pollution from ships"[1], which entered into force on May 19, 2005.

The GHG emissions produced from the maritime sector , which are of main interest at the present study,have reportedly increased over the last few years. More specifically, as shown in **Fig.1.1**, in the time period between 2012-2018 there has been a substantial increase of **9.6%** in **Total GHG** emissions (including CH_4, N_2O in CO_2 equivalent). Correspondingly, the CO_2 emitted in the atmosphere was also found to have increased by **9.3%** over the same time period, according to the IMO's Fourth GreenHouse Gas Study ([2]). Furthermore, GHG emissions are projected to increase by **30%** with reference to 2008, if a "business as usual" scenario is to be followed **(Fig.1.2)** [2],[3].

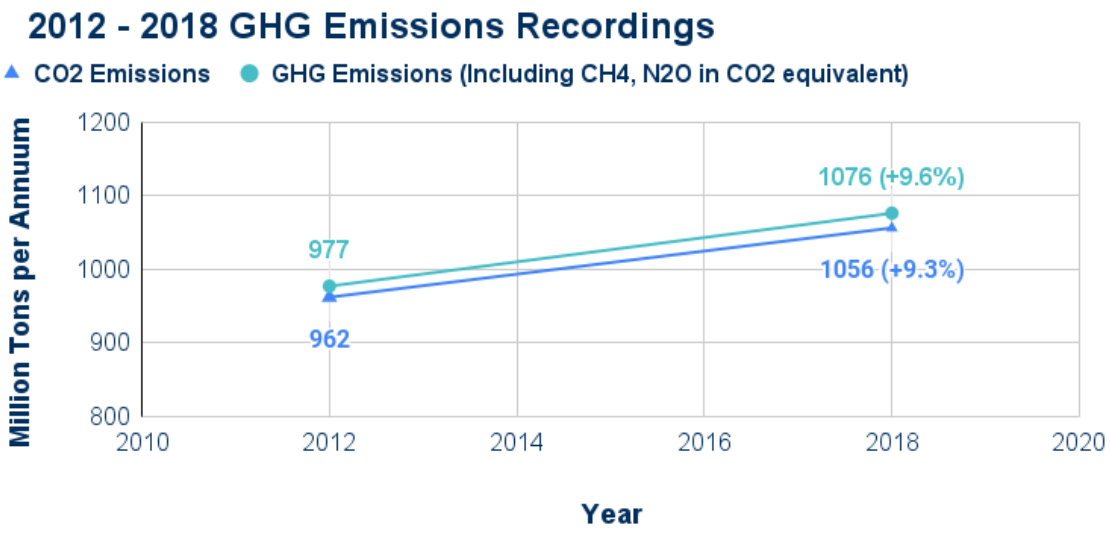

Figure 1.1: 2012 - 2018 Global GHG Emissions Recordings (in equivalent CO_2 tons per annum) from the maritime sector.

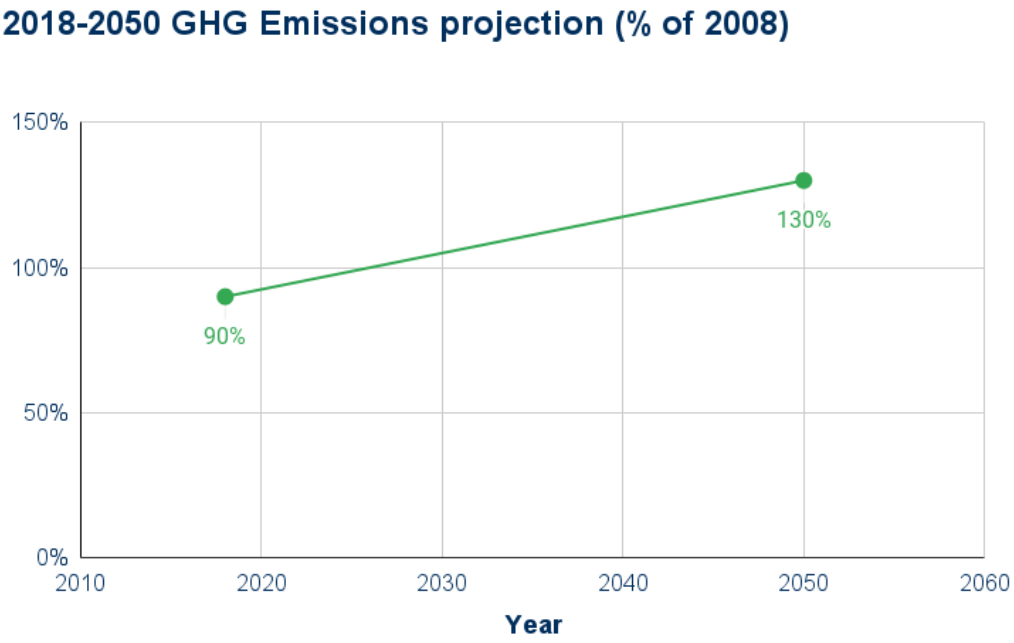

Figure 1.2: 2018-2050 GHG Emissions projection, in equivalent CO_2 tons per annum, (% of 2008).

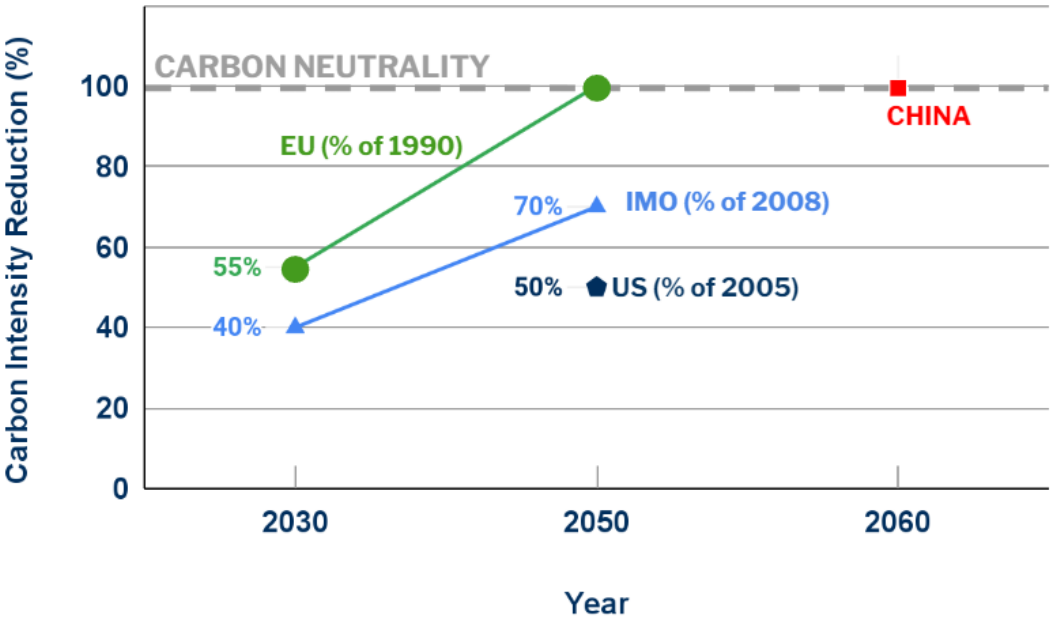

Figure 1.3: Regulations for decreasing Carbon Intensity from shipping.

In order to address the issue, the global regulators have decided to take action, implementing strategies for reducing the Carbon Intensity of the shipping industry. The most significant regulator of them all, the International Maritime Organization(IMO), dictates a solid **55**% and **70**% decrease by 2030 and 2050 respectively (compared to 2008), and aspires for a Carbon Neutral(CN) global fleet as soon as possible within this century **(Fig.1.3)**.

1.2 Objective of the present work

There are many ways for mitigating GHG emissions from ICEs. One of the most widely discussed is the transition towards non-carbon based fuels. **Ammonia** (chemical formula $\mathbf{NH_3}$), is one of the most well known candidates among these fuels, and is continuously gaining more attention in the present day. Many researchers and scientists have studied extensively the behavior of ammonia as a fuel and its combustion characteristics, both in experiment and in simulation. Computational Fluid Dynamics(CFD) along with Detailed Chemical Kinetics(DCK) have been used as tools in many studies. However, the precise results of CFD analysis come with a penalty in the need for computational power. Thus, this study uses a more simple yet efficient approach, **Thermodynamic Modeling**.

More specifically, the aim of the present work was to develop and calibrate a Thermodynamic model using the Gamma Technologies' **GT-POWER** software[4]. The model is paired with a **Detailed Chemical Kinetics Mechanism(DCKM)**, and is used for predicting the main emissions produced during the combustion of Ammonia-Diesel mixtures in a Dual-Fuel engine. In the time the present work was conducted, no experimental data concerning large 2-Stroke marine engines running on ammonia-diesel fuel mixtures were available in the open literature. Thus, an experimental work [5] on a heavy duty, 4-Stroke engine modified to operate in a dual-fuel mode was used as a reference study for the development of the model.

The structure of the present work is as follows:

- **Chapter 2:** A review of ammonia as a fuel for ICEs. A short analysis on the production methods of ammonia, its advantages and the potential challenges that may come with its use. An extensive recap of the development in the use of ammonia as a fuel during the last decades, and lastly a review of the current research status is conducted.
- **Chapter 3:** A walkthrough in the experimental apparatus. First of all, a description of the modified engine used in the experiments is done. Then, the test protocol is explained and the basic concept is presented. An introduction to the GT-POWER software is done and the theoretical background is explained. After that, the model development is presented in terms of: (a) setup, (b) DCKM introduction and (c) calibration.
- **Chapter 4:** The main results concerning the emission species as well as the matching of the pressure traces are presented in this chapter, followed by a short discussion.
- **Chapter 5:** Main conclusions presentation and discussion. Having presented the emission results, the main conclusions are extracted and presented. Lastly, a discussion about future work is conducted.

Chapter 2

Ammonia: a promising alternative fuel

2.1 Molecular structure, physical and chemical properties of Ammonia

Ammonia is a chemical compound that is gaseous at room temperature and has a distinct pungent smell. The ammonia chemical name (as determined by the IUPAC) is azane, its chemical formula is $\mathbf{NH_3}$, and is also sometimes called nitrogen trihydride[6].

Ammonia's molecule consists of three(3) Hydrogen atoms and one(1) Nitrogen atom. More specifically, the ammonia molecular structure involves a central nitrogen atom that is covalently bonded to three hydrogen atoms. An important feature of the ammonia molecule is that the nitrogen has a lone pair of electrons, which can accept a proton (i.e., hydrogen ion) to form an ammonium ion ($\mathbf{NH_4^+}$). This lone pair results in the molecule's shape, which is described as a trigonal pyramid [6], Fig.2.1.

At room temperature and pressure, ammonia exists as a clear and colorless gas. The chemical's boiling and freezing points are **240K** and **195.5K**, respectively, with a density of $\mathbf{0.73kg/m^3}$, which makes its vapor lighter than air, and autoignition temperature of **924K** under atmospheric conditions[7].

It has a distinct odor that is often characterized as pungent, sharp, or suffocating. While it is generally considered non-flammable, it may burn at high vapor concentrations or in the presence of a strong ignition source, platinum catalyst, or combustible materials[6].

Ammonia is an alkali compound and when dissolved in water, it forms a basic solution with a pH of around 10. The molecular weight or molar mass of ammonia is $\mathbf{17g/mol}$, and it can be easily calculated by summing the atomic masses of the individual atoms that form a single molecule. More specifically:

- Atomic Masses:
  - **H** : **1**
  - **N** : **14**

$$\textbf{Molecular Weight} = 3 \cdot 1 + 14 = \mathbf{17g/mol} \tag{2.1}$$

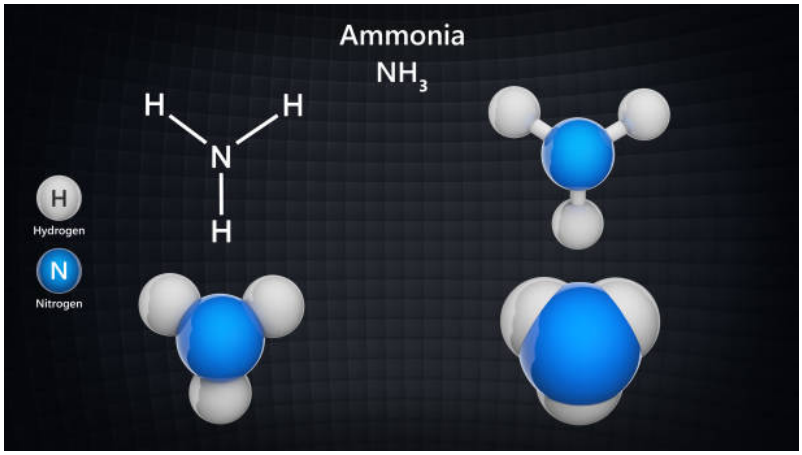

Figure 2.1: Ammonia Molecule in its distinctive trigonal pyramid shape.

Lastly, Ammonia is considered as highly toxic, not only to humans, but to aquatic flora and fauna as well. Furthermore, it is strongly corrosive, and thus special piping and handling equipment is needed (e.g. teflon piping and seals) for handling Ammonia safely, both onboard and on land. The inhalation of Ammonia is dangerous for humans, and can be potentially fatal in higher concentrations. However, the substance's distinctive and strong odour enables for its easy detection, even in concentrations well below the danger zone (0.6-53 ppm) [7]. The human exposure limit is 50 ppm, whereas concentrations of up to 300 ppm may cause instantaneous respiratory damage ("Immediately Dangerous to Life or Health" (IDLH) limit). Furthermore, due to being lighter than the air, Ammonia dissipates quickly to the upper atmosphere, in case of accidental leakage. In the following Table2.1, the toxicity levels of Ammonia and the corresponding exposure effects can be seen in detail.

Table 2.1: **Ammonia toxicity exposure levels**[8];[9]

Concentration / time	**Effect**
10000 ppm	Promptly lethal
5000 – 10000 ppm	Rapidly fatal
700 – 1700 ppm	Incapacitation from tearing of the eyes and coughing
500 ppm for 30 minutes	Upper respiratory tract irritation, tearing of the eyes
134 ppm for 5 minutes	Tearing of the eyes, eye irritation, nasal irritation, throat irritation, chest irritation
140 ppm for 2 hours	Severe irritation, need to leave the exposure area
100 ppm for 2 hours	Nuisance eye and throat irritation
50 – 80 ppm for 2 hours	Perceptible eye and throat
20 – 50 ppm	Mild discomfort, depending on whether an individual is accustomed to smelling ammonia

2.2 Methods of Ammonia Production

One of the main reasons why ammonia is considered an attractive alternative to conventional carbon-based fuels, is its abundance in the global market. Ammonia is a widely produced chemical, mainly used as a fertilizer component in the agricultural industry, and thus it is readily accessible worldwide. Specifically speaking, about 80% of the global ammonia production is used in agriculture as fertiliser. The remaining 20% is used in refrigeration, purification of water supplies, and industrial manufacture of various products including plastics, explosives, textiles, pesticides, dyes, and other chemicals[7];[10];[11]. Furthermore, a well established worldwide network for storage and distribution of Ammonia already exists, and the safe handling of the chemical in large quantities is well documented as well.

Pure ammonia was first prepared by English physical scientist Joseph Priestley in 1774, and its exact composition was determined by French chemist Claude-Louis Berthollet in 1785 [10]. Ammonia is consistently the second most widely produced chemical in the world [**giddey**], with an annual global production of **147 Million Metric Tons** in 2021. Furthermore, the annual global production capacity of Ammonia is expected to increase to up to **290 Million Metric Tons** by 2030 (Fig.2.2), making it even more readily available in the global market.

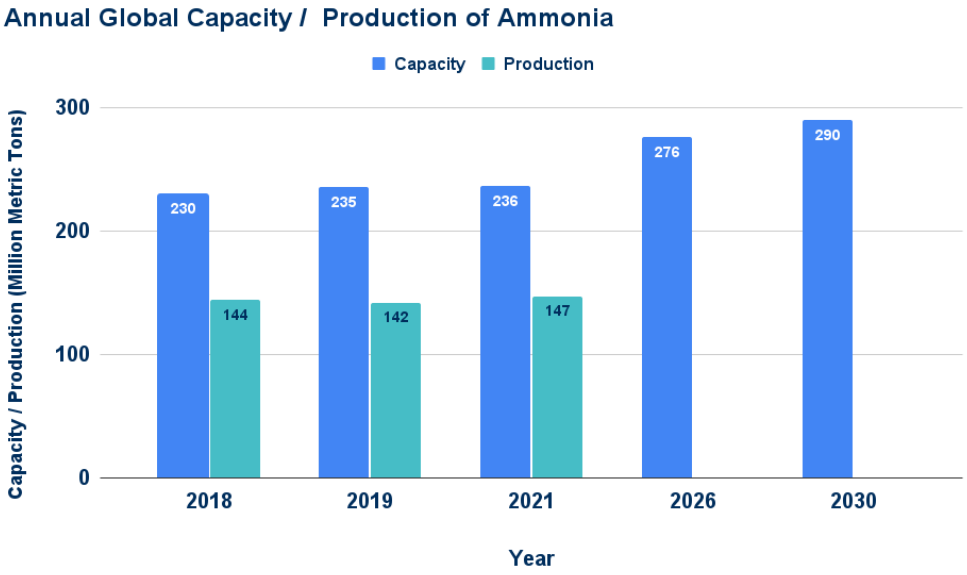

Figure 2.2: Annual Global Capacity - Production of Ammonia [12]

In an industrial scale, Ammonia is mainly produced via the following two methods:

2.2.1 Thermocatalytic Ammonia Synthesis - The Haber Bosch Method

The first, and most commercially successful process, was developed by Fritz Haber using an iron catalyst discovered by Carl Bosch and Alwin Mittasch [13]. The production of ammonia from hydrogen and nitrogen is an exothermic reaction favoured at lower temperature and higher-pressure conditions, however high temperature is required to achieve a satisfactory rate of ammonia formation [7];[10]. The so-called **Haber Bosch process** combines hydrogen and nitrogen at a ratio of **3:1** to produce ammonia in the presence of an iron-based catalyst within a temperature range of **400** – **550°C** and high pressure range of **100** – **1000 atm** [7];[10], Fig.2.3. The reactants to ammonia efficiency of Haber Bosch process is about 15-25% conversion per single run, but the unreacted gases are recycled, and eventually an **overall conversion of 97%** and a **peak power-to-ammonia efficiency of 60-64%** is achieved.

The process follows the basic reaction of ammonia synthesis which is shown below:

$$\mathbf{N_2} + \mathbf{3H_2} \iff \mathbf{2NH_3}, \quad \triangle\mathbf{H} = -\mathbf{92.5\ kJ/mol}\ [14] \tag{2.2}$$

The above reaction is strongly kinetically restricted due to the triple bond in the Nitrogen molecule (N≡N), which has a significantly high binding energy of **911 kJ/mol** [7];[**giddey**]. Therefore, high temperature is required in order for the Nitrogen molecule to be separated. Furthermore, high pressure is applied in order for the chemical equilibrium to be favorably promoted towards the Ammonia synthesis side, and to eliminate the reverse process rate of Ammonia being decomposed into Nitrogen.

The **Nitrogen** needed for the Haber Bosch process is obtained by an air separation unit, while the **Hydrogen** is obtained from steam reforming of methane, according to the following reaction:

$$\mathbf{CH_4} + \mathbf{2H_2O} \iff \mathbf{4H_2} + \mathbf{CO_2} \tag{2.3}$$

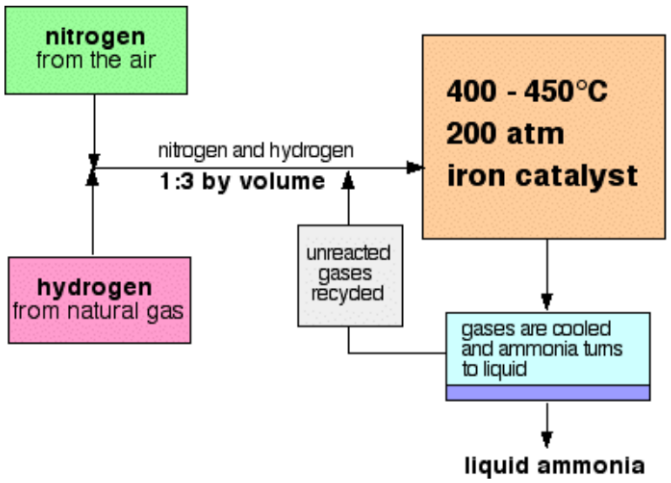

Figure 2.3: Scheme of the Haber Bosch process [15].

Up to **72%** of the world's Hydrogen for Ammonia production is obtained using Natural Gas, however other sources such as coal, heavy fuel oils, coke oven gas and naphtha are also used in lower percentages [7], as it can be seen in the pie chart below (Fig.2.4). Whereas in the most countries the main source used is Natural Gas, China's production of Ammonia is mainly based on the use of coal, which entails higher GHG emissions and power consumption.

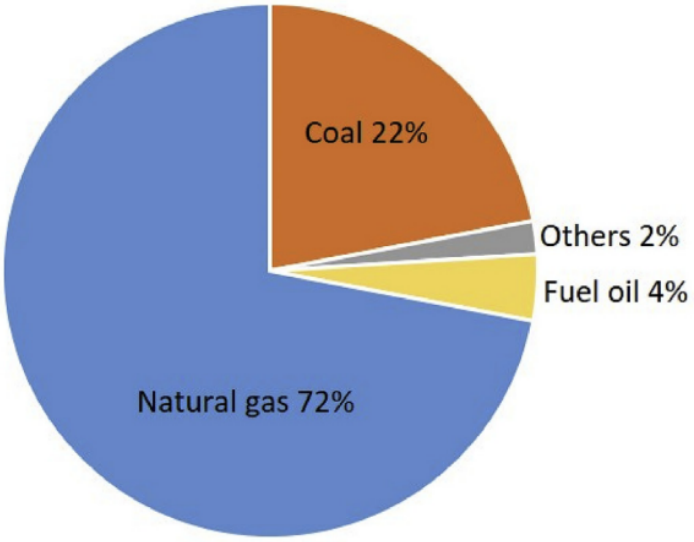

Figure 2.4: Various sources of Hydrogen used for Ammonia production [7].

2.2.2 Electrochemical Ammonia Synthesis

The second process, applicable in an industrial scale, is the Electrochemical Synthesis process. This process typically involves the supply of Hydrogen to the anode, the formation of protons at the electrolyte/electrode interface, the migration of protons through the electrolyte and the reaction with Nitrogen at the cathode to form Ammonia with the uptake of electrons[7]. This method can be divided into four(4) categories, accordingly to the type of the electrolyte used. The categories are the following [**giddey**]:

- **Liquid electrolytes** operating near room temperatures
- **Molten salt electrolytes** operating in temperature zones of $300 - 500^oC$
- **Composite electrolytes** consisting of a solid electrolyte combined with a low melting salt operating in temperature zones of $300 - 500^oC$
- **Solid electrolytes** operating in a wide temperature zone (from room temperature to up to 800^oC), depending of the type of the electrolyte membrane used.

The production of Ammonia is achieved at cathode via the electrochemical reaction 2.4 [14], and a **peak efficiency of 60%** can be achieved. However, one must bear in mind that this technology is still under evaluation.

$$\mathbf{N_2 + 6H^+ + 6e^- \Longleftrightarrow 2NH_3} \tag{2.4}$$

2.2.3 Green Ammonia

The so-called ”Green Ammonia”, is the Ammonia which is produced without the use of fossil or carbon-based fuels in general. What is of interest in this concept, is that on the road towards the decarbonization of the maritime sector, having zero upstream GHG emissions sets the basis for a completely carbon free shipping industry. However, with the growth of the production of Green Ammonia also come some issues. First of all, Green Ammonia is (at least in the short term) much more expensive than the fossil based one. Thus, a need for certifying that Ammonia bought by a customer, to say a ship operator, is produced in a ”green” way is created, so the buyer ensures that his capital is well spent. If an Ammonia production plant includes an electrolyzer to produce Hydrogen and uses renewable energy for the whole Ammonia production process, the produced Ammonia could be certified or the certificate for using renewable electricity would need to be passed on to the end-consumer [9].

For the production of Green Ammonia, the Hydrogen needed is obtained by water electrolysis, using a renewable energy source, such as solar and wind, in order to produce the needed electricity. After electrolysing water, the Hydrogen obtained can be used in both the already mentioned Haber Bosch and the Electrochemical processes. The Hydrogen and Nitrogen (the latter obtained from an air separation unit), are then combined under specific conditions, and Green Ammonia is synthesized (Fig.2.5). In the case of the Electrochemical Synthesis of Ammonia, using Hydrogen derived from renewable energy sources has a double benefit. Not only it eliminates the production of CO_2 emissions, but it also prevents the poisoning of the catalyst from traces of sulphur compounds and CO, which are common impurities in the Hydrogen produced via steam reforming of natural gas [7]. However, utilizing water electrolysis also comes with a penalty in the energy demand as well as with increased energy losses, resulting in an overall power-to-ammonia efficiency of $\mathbf{50-60}$%, which is actually lower than that of the classical Haber Bosch method.

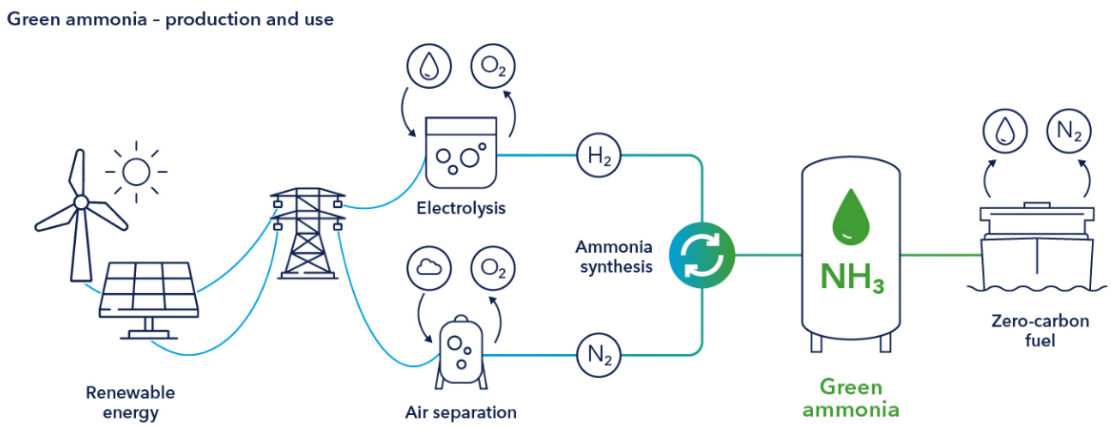

Figure 2.5: Green Ammonia production process [16].

2.3 Ammonia as a fuel

Hydrogen is considered as the successor of the carbon-based fuels. Its superb combustion behaviour alongside its sustainable production process, have placed it on top of the alternative fuels' candidates' list. However, the direct utilization of hydrogen as a transport fuel is faced with several safety and storage challenges due to its physio-chemical properties like boiling point (-252.87^oC) and flammability range (4% to 75% concentration in air) [17]. The most common technique for Hydrogen storage is by utilizing highly pressurized gas cylinders (lightweight cylinders made of composite materials with a maximum pressure allowance of up to 80 MPa). The overall volumetric efficiency of the pressurized gas system can be improved by further increasing the storage pressure, however this comes with a penalty in the gravimetric efficiency of the system, as an increase of the walls' thickness is also required for the tank to withstand the elevated pressure. So, the main drawbacks of this storage method is the poor volumetric efficiency of the system, even in high pressure, diffusion leading to leakages and tank stability issues. An alternative to the previously mentioned storage method, is storing liquid Hydrogen in cryogenic tanks under ambient pressure ($\mathbf{-251.9^oC}$, $\mathbf{70.8kg/m^3}$). However, this technique also comes with major drawbacks, the most significant of them being the lower energy efficiency of the liquefaction process and the boiling off of hydrogen from cryogenic containers. Lastly, the use of Hydrogen in ICEs applications also poses concerns related to Hydrogen embrittlement of engine components. This phenomenon comprises the intrusion of Hydrogen atoms in the surfaces' imperfections, accelerating the movement of molecules through metal interstices, ultimately leading to cracking of the engines' components [17].

The potential challenges concerning the pure Hydrogen's transportation and storage conditions, can be overcome by the utilization of the so-called Hydrogen carriers, which are substances with significant Hydrogen content, yet more favourable and efficient storage and transportation properties

2.3.1 Advantages of Ammonia as a fuel

Ammonia is seen as an excellent fuel due to its favorable physio-chemical properties and easy and efficient production, transportation and storage processes. It is considered as a superb hydrogen carrier, with a gravimetric Hydrogen content of **17.7%**, and can be easily reformed at either low temperature with the use of a catalyst or at high temperature without the catalyst's presence [18]. To be more specific, the volumetric Hydrogen content of liquefied Ammonia is even higher than that of pure liquefied Hydrogen, with the former being equal to $\mathbf{106kg - H_2/m^3}$ and the latter being equal to $\mathbf{71kg - H_2/m^3}$. Furthermore, liquefied Ammonia has a Volumetric Energy Density of $\mathbf{11.3MJ/L}$ at liquid form (at pressures higher than 0.8MPa), which is significantly higher than that of pure liquefied Hydrogen ($4.7MJ/L$, at 35MPa pressure) [17].

Ammonia has a very **low viscosity**, which helps greatly in the atomization and the formation of droplets during the injection of the fuel. Moreover, Ammonia's very low freezing point (**-77.73^{o}C**) makes it a suitable fuel for applications in extremely cold environments. Furthermore, it is lighter than air, thus it can dissipate quickly, avoiding human poisoning in case of spillage. Also, it is highly soluble to water, which also prevents undesired effects in case of an accident in handling. Last but not least, Ammonia has a very high octane rating (**RON $\approx$ 130**), which eliminates any unfavorable knocking effect, making Ammonia a suitable fuel for Spark Ignition(SI) engine applications.

What makes ammonia an attractive solution especially for marine applications, is that in terms of storage conditions, it can be stored at room temperature (25^{o}) at just 10.2 atm of pressure, which is well below the storage pressure of LPG and LNG. This means that the already existing handling infrastructure onboard LPG/LNG carriers can be used for ammonia handling only with slight modifications. A comparison between the fuel properties of NH_3, Methane and MGO can be seen in Table2.2.

Calculation of the tank volume required for ammonia storage onboard a vessel

To show the benefit of ammonia in terms of storage, a quick calculation and comparison of the tank volumes needed for ammonia, methane and Marine Gas Oil(MGO) is made.

Table 2.2: **Fuel properties comparison between ammonia-MGO-methane**

Fuel	**Natural Gas**	**MGO**	**Ammonia**
Formula	CH_4	$C_{10}H_{20}$–$C_{15}H_{28}$	**NH_3**
Storage Method	Comp. Gas	Liquid	**Liquid**
Storage Temp. (^{o}C)	25	25	**25**
Storage Pressure (atm)	245	1.0	**10.2**
Fuel Density (kg/m^3)	187.1	855	**602.8**
LHV (MJ/kg)	**47.1**	**42.7**	**18.8**

Fuel No.1: MGO
Fuel No.2: Ammonia
Fuel No.3: Methane

Considering the same chemical energy content **Q** for all three fuel cases:

$$\mathbf{Q_1 = Q_2 = Q_3}$$

$$\mathbf{m_1 \cdot LHV_1 = m_2 \cdot LHV_2 = m_3 \cdot LHV_3}$$

$$\rho_1 \cdot \mathbf{V_1 \cdot LHV_1} = \rho_2 \cdot \mathbf{V_2 \cdot LHV_2} = \rho_3 \cdot \mathbf{V_3 \cdot LHV_3} \tag{2.5}$$

Substituting the fuel density and LHV values according to Table2.2, equation2.5 gives the following results:

$$\frac{V_{MGO}}{V_{NH_3}} \approx 0.3 \tag{2.6}$$

$$\frac{V_{NH_3}}{V_{CH_4}} \approx 0.77 \tag{2.7}$$

From equation 2.6, it is concluded that to store ammonia with the shame chemical energy content as MGO, the tank volume required is 70% greater.

On the other hand, equation 2.7 shows that compared to methane, ammonia needs $\approx$ **23**% less space for the same energy content to be provided.

2.3.2 Disadvantages of Ammonia as a fuel

Ammonia as a fuel, however, is far from ideal. Its unfavorable thermodynamic properties, such as its **low laminar flame speed** ($\approx$ **0.07 m/s**, at an equivalence ratio equal to $\phi \approx$ **1.1**, as it can be seen in Fig.2.6), **narrow flammability limits**, **low adiabatic flame temperature** compared to other fuels, and its very high auto-ignition temperature, make the utilization of Ammonia in IC engines quite challenging. A direct comparison of the thermodynamic properties of Ammonia and other fuels can be seen in Table2.3.

Table 2.3: **Thermodynamic Properties of Ammonia and other fuels - a comparison**[17]

Property	**Ammonia** NH_3	**Gasoline (iso-Octane)** C_8H_{18}	**Diesel (n-Dodecane)** $C_{12}H_{26}$	**Methane** CH_4	**Hydrogen** H_2
Lower Heating Value (MJ/kg)	**18.8**	≈ 42.5	≈ 44.5	47.1	120.1
Density at 1 bar and 25^{o}C (kg/m^3)	**0.718**	736	849	0.667	0.0837
Specific heat C_p (kJ/kg K)	**2.190**	2.22	1.75	2.483	14.30
Latent heat of vaporization (kJ/kg)	**1370**	348.7	232.4	511	455
Auto-ignition temperature (K)	**930**	503	527–558	859	773–850
Laminar Burning Velocity at ϕ = 1 (m/s)	**0.07**	0.58	0.86	0.38	3.51
Flammability limit (Equivalence ratio - φ)	**0.63–1.4**	0.55-4.24	0.8–6.5	0.5–1.7	0.1 – 7.1
Stoichiometric AF ratio by mass	**6.05**	15	14.5	17.3	34.6
Boiling point (^{o}C)	**–33.34**	35–200	282–338	-161.5	-252.7
Melting point (^{o}C)	**–77.73**	$-90 \longrightarrow -95$	$-30 \longrightarrow -18$	-182	-259
Octane rating (RON)	**130**	90–98	–	120	>100
Volumetric Energy Density (GJ/m^3)	**11.3(>0.8MPa)**	33(STP)	36.4(STP)	9.35(35MPa)	4.7(69Mpa)
Adiabatic flame temperature (^{o}C)	**1800**	2138	2300	1950	2110

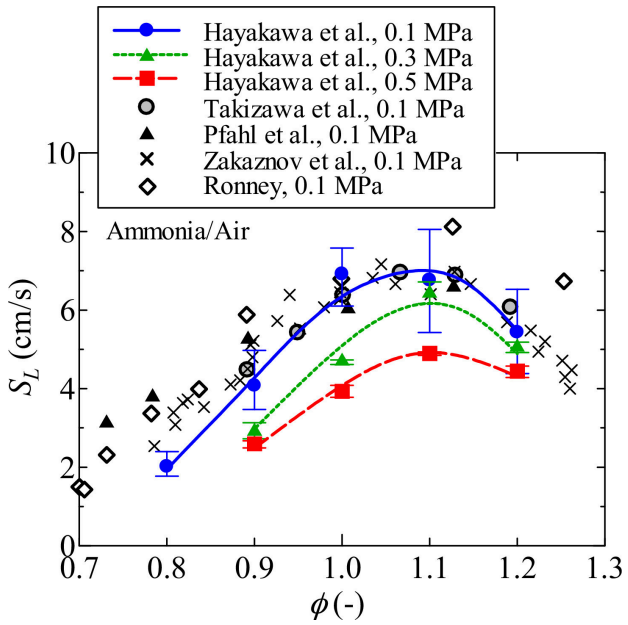

Figure 2.6: Unstretched laminar burning velocity, $\mathbf{S_L}$, of $\mathbf{NH_3/air}$ premixed flames in terms of equivalence ratio - ϕ, at mixture temperature of **298K**. Results from [19];[20];[21];[22];[23]. Reprinted from [24].

2.3.3 Basic combustion theory

For the completeness of the present work, a short introduction into the basics of combustion terminology and chemistry is made. The main term discussed here is the so-called **Equivalence Ratio -** ϕ (or the reverse fraction, called the **lambda ratio -** λ).

Air - Fuel Ratio (AFR)

As its name suggests, AFR is a fraction, representing the mass analogy of fuel and air existing at a certain moment at a specific engine location (usually it is referred to the combustion chamber). Mathematically, it is represented as shown below:

$$\mathbf{AFR} = \frac{\mathbf{m_{AIR}}}{\mathbf{m_{FUEL}}} \tag{2.8}$$

The reverse fraction is also used, and is called **Fuel-Air Ratio (FAR)**:

$$\mathbf{FAR} = \frac{\mathbf{m_{FUEL}}}{\mathbf{m_{AIR}}} = \frac{\mathbf{1}}{\mathbf{AFR}} \tag{2.9}$$

The **stoichiometric AFR**, represents the analogy of the air and fuel masses, in order for stoichiometric combustion of this particular fuel to be achieved. In the stoichiometric combustion, the entire amount of fuel is oxidized with just the right amount of air. So there is neither excess of air nor abundance of fuel. This is called a **stoichiometric** air-fuel mixture. The mathematical representation of the **stoichiometric AFR** is as follows:

$$\mathbf{AFR_{ST}} = \frac{\mathbf{m_{AIR_{ST}}}}{\mathbf{m_{FUEL_{ST}}}} \tag{2.10}$$

Equivalence Ratio - φ

However, in realistic combustion conditions (e.g. during the operation of an ICE), stoichiometric mixtures are one of the cases encountered. More specifically, usually in ICE applications, the mixture composition varies depending on the current operating conditions. So a differentiation is made between the two different mixture types that can occur:

- **Rich mixture:** it is the type of mixture where the fuel is in abundance. There is more fuel than what is needed (indicated by the stoichiometric AFR), and thus it is called **fuel-rich** mixture.
- **Lean mixture:** in this case, an excess of air is observed. There is a larger amount of air than what is indicated by the stoichiometric AFR, so the mixture is characterized as **fuel-lean**.

For convenience and practicality reasons, in order for an air-fuel mixture to be easily characterized as either rich or lean, a new ratio was invented, the so called **equivalence ratio** or ϕ, as is more commonly seen in the literature. The equivalence ratio is again a fraction, with the numerator being the real FAR (the one representing the specific conditions in each particular application), and the denominator being the stoichiometric FAR. Its calculation formula is presented below:

$$\phi = \frac{\mathbf{FAR}}{\mathbf{FAR_{ST}}} \tag{2.11}$$

The ratio of the real AFR to the stoichiometric one is also extensively used in the literature, and it is the so called **lambda ratio -** λ:

$$\lambda = \frac{\mathbf{AFR}}{\mathbf{AFR_{ST}}} \tag{2.12}$$

In Table2.4, an easy way to characterize an air-fuel mixture, depending on the values of the ϕ or λ ratios is presented:

Table 2.4: **Characterization of air-fuel mixtures depending on the λ and ϕ ratios**

Mixture Composition	**Lambda Ratio - λ**	**Equivalence Ratio - φ**
Lean	>1	<1
Stoichiometric	**1**	**1**
Rich	<1	>1

Calculation of the stoichiometric AFR for Ammonia combustion

In order to calculate the stoichiometric AFR for any fuel, the chemical reaction of its combustion must be known. The overall reaction for the oxidation/combustion of Ammonia is the following [24]:

$$\mathbf{4\,NH_3 \;+\; 3\cdot(O_2 \;+\; \frac{79}{21}\,N_2) \;\longrightarrow\; 6\,H_2O \;+\; 3\cdot\frac{121}{21}\,N_2} \tag{2.13}$$

As indicated in 2.13, in order for **4 moles** of NH_3 to be oxidized, **3 moles** of air are needed. Furthermore, the Molar Weight of Ammonia is (as calculated previously) equal to $\mathbf{MW_{NH_3} = 17\,g/mol}$, whereas that of Oxygen (the atomic mass of Oxygen is 16g/mol) is easily calculated as shown below:

$$\mathbf{MW_{O_2} = 2\cdot 16 = 32\,g/mol} \tag{2.14}$$

So, in a gravimetric basis, the ratio of Ammonia and Oxygen needed for stoichiometric combustion to occur is equal to:

$$\mathbf{\frac{m_{O_2}}{m_{NH_3}} = \frac{3\cdot 32}{4\cdot 17} \approx 1.41176} \tag{2.15}$$

Equation2.15 indicates that for **1 kg of Ammonia** to be burned, **1.41176 kg of Oxygen** is needed. In order to calculate the exact mass of air needed, the content in Oxygen of air by weight must be taken into account. The gravimetric content of air in Oxygen is approximately equal to **23.14%**[25]. So the mass ratio of Oxygen and air is equal to:

$$\mathbf{\frac{m_{O_2}}{m_{air}} = 23.14\%\ or\ 0.2314} \tag{2.16}$$

The substitution of equation 2.16 in 2.15 results in the following relation:

$$\mathbf{\frac{m_{air}}{m_{NH_3}} = \frac{1.41176}{0.2314} \rightarrow AFR_{ST}^{NH_3} \approx 6.1} \tag{2.17}$$

2.3.4 Chemical Kinetics of Ammonia combustion and fuel NOx

Ammonia oxidation chemistry has been extensively studied over the past several decades, mainly due to its relevance to fuel NOx formation and Selective non-Catalytic Reduction of NOx (SNCR), which uses Ammonia as a reducing agent for NO species [24];[26];[27];[28];[29].

One of the most significant early efforts to set the basis for detailed kinetics description of Ammonia oxidation, was the work of Miller and his co-workers [30];[31];[32]. In [32], a computational investigation in a variety of burner-stabilized and freely propagating NH_3/O_2 and $NH_3/H_2/O_2$ flames was made, and a detailed kinetics mechanism for NH_3 oxidation was proposed, which consisted of **22 species and 98 elementary reactions**. The model was found to perform well in lean and moderately rich conditions, satisfactorily predicting the species profiles measured by MacLean and Wagner [33], Green and Miller [34], Fenimore and Jones [35], and the burning velocity measured by Murray and Hall [36]. However, the model was found inadequate in predicting the measurements at rich flame conditions, and this was attributed to the Ammonia pyrolysis mechanism being incomplete [24].

The understanding of ammonia oxidation has improved since the pioneering works by Miller and co-workers and the kinetics models have improved in comprehensiveness and accuracy over the years [24]. The most recent and well-established chemical mechanisms concerning the oxidation of Ammonia are presented in Table2.5 [37].

Table 2.5: **Most recent and well-established Chemical Kinetics Mechanisms for Ammonia Oxidation**

Mechanism	Species	Reactions	Ref.
Klippenstein	33	211	[38]
Dagaut	26	133	[39]
Zhang	37	229	[40]
Shrestha	34	261	[41]
Nakamura	38	232	[42]
Okafor	60	359	[43]
Otomo	32	213	[44]
Stagni	31	203	[45]
Mathieu	33	159	[46]

Some worth-mentioning mechanisms that are not exclusively used for Ammonia oxidation modeling, but for Nitrogen related chemistry in general are the following:

- **Konnov's mechanism (v0.6)**: Detailed mechanism for CH_4/air flame modeling with NCN pathway for prompt-NO formation (201 species, 2300 reactions) [47];[48].
- **Lindstedt's mechanism**: Detailed mechanism for $NH_3/H_2/O_2$, $NH_3/NO/H_2/O_2$ and NH_3/O_2 flames, specialized in NO formation and DeNOx chemistry [49].
- **Tian's mechanism**: Detailed mechanism for nitromethane flame modeling, and prediction of N_2 and NO related species (69 species and 314 reactions) [50].
- **GRI-Mech 3.0 mechanism**: a mechanism developed by the Berkley combustion team (as an updated version of GRI-Mech 2.11. It is a detailed kinetic mechanism for methane/air combustion including nitric species for NOx predictions (53 species and 325 reactions) [51].

Nevertheless, the reaction pathway proposed by Miller et al. [32], as seen in Fig.2.7, provides an adequate tool for understanding the chemistry of NH_3 oxidation and fuel NO formation and reburn. Fig. 2.7 is thoroughly explained below.

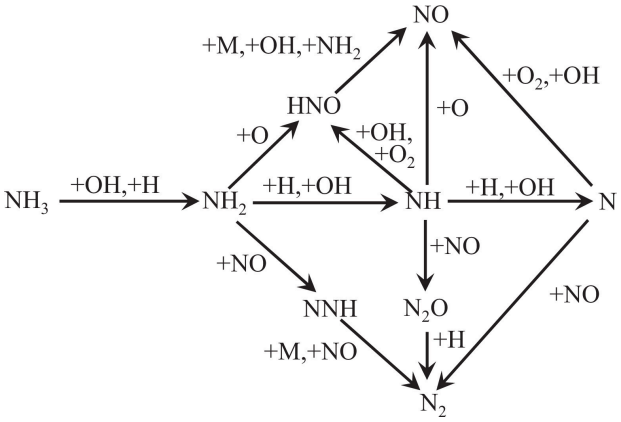

Figure 2.7: NH_3 oxidation pathway by Miller et al. [32]. Reprinted by [24].

Lean Ammonia flame Kinetics

Ammonia is consumed by H abstraction, **mainly through the reaction with OH** under all conditions of equivalence ratio - φ. Other secondary consumption steps include the reaction with H and O, the common product of these reactions being NH_2. Depending on the concentration of the O/H radicals, NH_i (i=0,1,2) oxidation may primarily lead to NO formation, with HNO as an intermediate step, or to NO reduction, via NH_i-NO reactions. In the lean flame conditions, there is an abundance in the O/H radical pool (with a peak concentration around φ = 0.9) which favors the conversion of NH_i to NO, and simultaneously potentially inhibits the reduction of NO. As a result, in these flame conditions, the NO concentration is high and peaks around the same equivalence ratio (φ = 0.9). On the one hand, Skreiberg [52] noted that by adding CO in lean $NH_3/NO/N_2/O_2$ flames at 1273K temperature, the O/H radical pool was increased, and thus the overall NO formation via the HNO route was promoted to higher levels.

On the other hand, Mendiara and Glarborg [53] reported that the addition of CO_2 in NH_3/CH_4/air flames caused the depletion of the O/H radical pool, ultimately leading to significant NO reduction, as the CO_2 reacts with H radicals to form CO.

HNO is primarily produced through the reaction of NH2 with O atoms. The NH$\rightarrow$ HNO path constitutes a secondary route for HNO production. HNO is then solely oxidized to NO. Recent kinetics studies show that HNO is converted to NO in the flame mainly through reactions with H, OH, O_2, and through thermal dissociation. **The HNO intermediate channel is the dominant NO production path in NH_3/air flames under all conditions** [24].

Rich Ammonia flame Kinetics

As the flame becomes richer, the tendency for **NH_i (i=0,1,2) to be oxidized** through **reactions with H** increases significantly. This is because, despite the overall decrease of the O/H concentration in richer conditions, the relative concentration of H radicals in the O/H radical pool is increased. The reaction between NH_i and H atoms, leads to a substantial H_2 production, mainly from the NH_2 species, and ultimately to the production of N atoms. The relative abundance of N atoms in rich flames promotes the set of reactions known as the extended Zeldovich mechanism (Thermal NO formation), which will be discussed in depth later on [24].
The lower concentration of O/H radicals in richer Ammonia flames leads also to lower NO production levels from NH_i oxidation. Additionally, the promotion of NH_i combination reactions significantly decreases the available NH_i radicals for NO production and thus contributing to lower overall NO formation [28];[32];[54]. Haynes [28] studied routes for NO formation and reduction in ammonia flames and suggested that N_2 formation through NH_i + NH_i reactions may be relatively greater in richer lower temperature flames where NH_3 is more stable. Subsequent studies by Dean et al. [54], found that NH_i combination reactions dominate the kinetics of rich ammonia flames and contribute to the low NO production. Combination reactions of the type NH_i + NH_i provide an alternative route for the conversion of NH_i to N_2, without the involvement of NO [24]. These reactions mainly follow the path shown below:

$$\mathbf{NH_2} \xrightarrow{+\mathbf{NH_2},\mathbf{NH}} \mathbf{N_2H_2} \xrightarrow{+\mathbf{M},\mathbf{H}} \mathbf{NNH} \xrightarrow{+\mathbf{M},\mathbf{O},\mathbf{O_2}} \mathbf{N_2}$$

with NNH being primarily consumed by the dissociation reaction, whereas the reactions with O and O_2 are of secondary importance.

Dean and Bozzeli [55] proposed that NNH may lead to substantial NO production through the so-called NNH mechanism, which involves the reaction of NNH with an O atom. This suggests that a substantial amount of NO may result from the NH_i combination pathway.

According to Klippenstein et al. [56], between the above three channels, **the N_2 + OH is the most dominant**, whereas the N_2O + H is competitive. The NH + NO channel was found to be a relatively minor channel even at high temperatures due to the endothermicity of the reaction [24].

Extended Zeldovich mechanism in NH_3 combustion

During the combustion of non-nitrogen containing fuels, the main route for thermal NOx production is the so-called extended Zeldovich mechanism. It is a chemical mechanism that describes the oxidation of Nitrogen and the formation of NOx species and it was first proposed by the Russian physicist Y.B. Zeldovich in 1946 [57]. The mechanism consists of three reactions and has the following structure:

$$\mathbf{N_2 + O \overset{k1}{\longleftrightarrow} NO + N}$$

$$\mathbf{N + O_2 \overset{k2}{\longleftrightarrow} NO + O}$$

$$\mathbf{N + OH \overset{k3}{\longleftrightarrow} NO + H}$$

with the forward rate constants of the above reactions being equal to:

$$\mathbf{k_{1f} = 1.47 \cdot 10^{13} \cdot T^{0.3} \cdot e^{-75286.81/RT}}$$
$$\mathbf{k_{2f} = 6.4 \cdot 10^{9} \cdot T \cdot e^{-6285.5/RT}}$$
$$\mathbf{k_{3f} = 3.8 \cdot 10^{13}}$$

where the pre-exponential factor is measured in units of cm, mol, s and K, temperature in Kelvins, and the activation energy in cal/mol; R is the universal gas constant.

The overall reaction rate is mostly governed by the first reaction (i.e., rate-determining reaction), as it requires the cleavage of the covalent N$\equiv$N triple bond, and thus it is favored in elevated temperatures above 1800K. Therefore, for hydrocarbon fuels and even low-nitrogen-containing fuels such as natural gas in which the extended Zeldovich mechanism is the main contributor to NOx formation, temperature control is the most important factor in NOx control [24]. Since the second reaction is much faster than the first, it occurs immediately following the first reaction. At fuel-rich conditions, due to lack of oxygen, the second reaction becomes weak, hence, the third reaction is included in the mechanism, and thus it is called the extended Zeldovich mechanism.

In ammonia flames, however, the extended Zeldovich mechanism is active even at low temperatures, although its net contribution to NO concentration may be negligible. In Fig.2.8 the percent contribution of each step of the mechanism to the total rate of NO production (positive values) or reduction (negative values) in NH_3/air flames can be seen. Note that $N_2 + O \rightarrow$NO+N is a reduction step for NO in ammonia flames because the abundance of NO and N atoms favors the backward reaction.

All the kinetics models, except GRI Mech 3.0, show that the importance of the extended Zeldovich mechanism is promoted in rich flames. In the models of Miller [32] and Konnov [47], $N_2 + O \rightarrow NO+N$ is the primary NO reduction step in rich flames, and these kinetics models predict that the net influence of the extended Zeldovich mechanism in rich NH_3/air flames is a reduction of NO. The predictions made by Okafor's mechanism [43], which is a detailed CH_4/NH_3 oxidation kinetics model based on GRI Mech 3.0 with the addition of important N/H chemistry from Tian's mechanism, agrees with that of Tian's mechanism, as shown in Fig.2.8 [24].

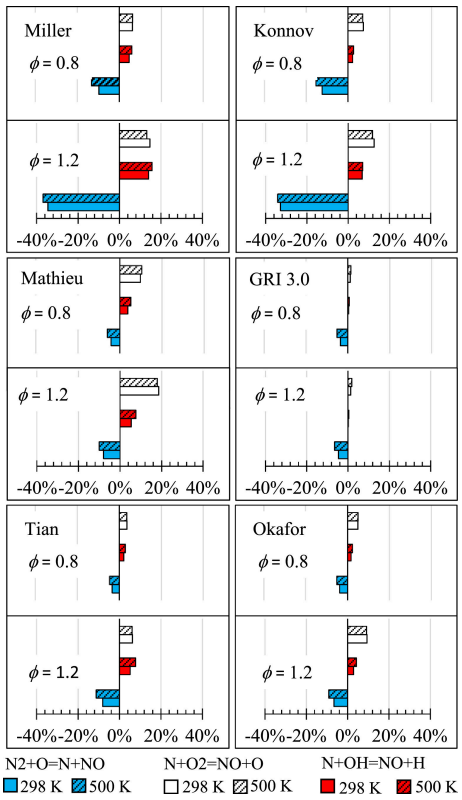

Figure 2.8: Percent contribution of the extended Zeldovich mechanism to total NO production or reduction in NH_3/air flames at different initial mixture temperatures. Reprinted by [24].

An increase in temperature enhances the O/H radical pool due to promotion of the temperature-sensitive chain branching reactions. Consequently, total NO production and reduction increases and decreases, respectively. However, the net contribution of the extended Zeldovich mechanism to NO concentration may not be significantly affected by temperature. As shown in Fig2.8, the rates of NO reduction via $N_2 + O \rightarrow NO+N$ and production via $N + OH \rightarrow NO+H$ increase with temperature, while NO production via $O_2 + N \rightarrow NO+O$ does not respond significantly to an increase in temperature [24].

NO reduction Kinetics

The reaction of NO with NH_i (i=0, 1, 2) leads to the reduction of NO to N_2. These reactions take place under all conditions but are promoted under particular conditions. The reaction of NO with N atoms, as discussed previously, is promoted in rich flames and at elevated temperatures. NO reduction by NH primarily produces N_2O via NH+NO $\rightarrow N_2O$+H. N_2O is then largely consumed through N_2O+H $\rightarrow N_2$+OH [58]. The dominant NO reduction step under all conditions, especially in lean flames, is the reaction of NO with NH_2, which has two product channels, NH_2+NO $\rightarrow$NNH+OH - (R1) and NH_2+NO $\rightarrow N_2$+H_2O - (R2).

Lyon [26];[27] found that within a certain temperature range and oxygen concentration, NOx reduction in flames can be enhanced using NH_3 in a process called Thermal DeNOx.The self-sustaining character of the DeNOx mechanism is due to the direct or indirect production of OH and O from R1 at a rate controlled by the branching ratio, $\alpha = \frac{\mathbf{k_1}}{\mathbf{k_1 + k_2}}$, and the lifetime of NNH. The sensitivity of the thermal DeNOx process to the concentration of O/H radicals contributes to its dependence on temperature. At the lower boundary of the effective thermal DeNOx temperature window, the chain terminating reaction H + O_2+M $\rightarrow HO_2$+M competes with H + O_2 $\rightarrow$O+OH and hence inhibits the thermal DeNOx process. On the other hand, above the upper temperature boundary, there is significant growth in the O/H radical pool, leading to net NO production rather than reduction. It can thus be understood that the NO formation/reduction in ammonia flames, as well as the reactivity of the N/H/O chemistry, may be significantly dependent on α and the lifetime of NNH. Nakamura et al. [42] concluded that **α** is a key parameter controlling ammonia reactivity [24].

2.3.5 Main emissions from ammonia combustion

During the combustion of pure NH_3/air mixtures, no carbon-based emissions are produced. After all, that is the main reason why the whole ”alternative fuel” campaign was launched in the first place. However, the use of ammonia as a fuel leads to the production of nitrogen related emission species that must be taken seriously into consideration.

NOx emission species

When ammonia is being combusted, as is the case with every other fuel, **nitrogen oxides or NOx** are produced. However, the fuel-bound nitrogen in the case of ammonia constitutes a significant additional source of NOx. The total NOx can be divided in the following three categories:

- **Thermal NOx**: Thermal NOx are produced via the already mentioned extended Zeldovich mechanism. The production of thermal NOx is present in every combustion case, as it requires only nitrogen from the air and O-O/H radicals, which are in abundance in a flame. The reactions are highly temperature dependent, so the hotter the combustion, the more NOx is formed.

The NOx formation rate is also pressure and residence time dependent. Decreasing any of these three reduces the NOx, but the exponential dependence on temperature makes reducing combustion temperature the key strategy to low NOx combustion. Fortunately, the thermal NOx formation rates are relatively slow; equilibrium concentrations are never reached in practical combustion devices.

- **Fuel NOx**: When nitrogen is chemically bonded to the fuel, essentially all of it converts to NOx in the exhaust.
- **Prompt NOx**: The presence of a second mechanism leading to NOx formation was first identified by Fenimore [35] and was termed ”prompt NOx”. There is good evidence that prompt NOx can be formed in a significant quantity in some combustion environments, such as in low-temperature, fuel-rich conditions and where residence times are short. Surface burners, staged combustion systems, and gas turbines can create such conditions. At present the prompt NOx contribution to total NOx from stationary combustors is small. However, as NOx emissions are reduced to very low levels by employing new strategies (burner design or furnace geometry modification), the relative importance of the prompt NOx can be expected to increase.

Unburned Ammonia - Ammonia Slip

Due to ammonia’s challenging combustion characteristics, mainly implying its lower adiabatic flame temperature, which as a consequence leads to overall lower combustion temperatures, an amount of fuel to be directly emitted to the exhaust without being combusted. The phenomenon of ammonia directly being released in the exhaust gases is the so-called ammonia slip and its mainly due to the entrapment of fuel in the cylinders’ crevice volume (the main reason is ammonia’s low burning velocity and long quenching distance). Due to the toxicity of the chemical, ammonia slip is a major issue and special care should be taken for its prevention.

Nitrous Oxide - N_2O

Nitrous oxide, also known as ”laughing gas”, is a very potent GHG, with almost 300 times higher Global Warming Potential(GWP) than CO_2 ($GWP_{CO_2} = 1$). N_2O emissions can occur under certain conditions during the combustion as tests with ammonia-diesel mixtures have shown [24];[59]. It has been shown that N_2O formation is favoured in lower combustion temperatures, and thus in order to mitigate its production, the implementation of higher cylinder temperatures and multiple injections has been found effective [60]. The high GWP of N_2O poses a major challenge for the adoption of ammonia as an alternative fuel, as it can mitigate any positive effect that ammonia may have in the decrease of the GHG emissions.

2.3.6 Emission trends in ammonia/Hydrocarbon(HC) dual-fuel applications

As will be discussed extensively in the following sections, the utilization of ammonia is mainly following a dual-fuel approach, with ammonia/HC/air mixtures being way more favorable than pure NH_3/air mixtures. The concept of dual-fuel operation mainly consists of ammonia being the main fuel, and a more reactive HC-based secondary fuel (e.g. diesel) being used as an ignition promoter, in order for better combustion characteristics to be achieved. However, even when a small amount of HC fuel is inserted into the combustion process, carbon-based emissions are to be expected as well.

- **CO_2**: The carbon dioxide amount produced is directly proportional to the HC-based fuel used. Thus in the case of fuel substitution by ammonia, the overall CO_2 are decreased.
- **CO**: carbon monoxide is showing a more complex trend. Although the carbon content of the total fuel mixture is decreased when ammonia is used as a fuel, the incomplete combustion due to lower combustion temperatures ultimately has been found to increase the total CO emissions [61].
- **Soot**: in the case of diesel usage as a pilot/secondary fuel, the formation of soot is also present. As fuel rich zones in the cylinder are the major sources for soot emission in diesel combustion, the introduction of ammonia has been found to have a controversial effect. In the case when ammonia substitutes the diesel fuel in high percentages (>40% in an energy basis), the soot emissions where found to decrease. On the other hand, in lower substitution percentages ($\approx$ 20% ammonia), it was observed that there was sufficient amount of diesel for ”diesel-rich” zones to be created, and in combination with the overall lower combustion temperature, the soot formation was increased [5];[17].
- **Unburned Total Hydrocarbons(UTHC)**: once again, the introduction of ammonia has a controversial impact. In high ammonia fueling percentages, although the HC fueling was consequently decreased, the UTHC emissions were found to increase. This was again, due to the lower combustion temperature and the subsequent lower total combustion efficiency [61].

2.3.7 Conclusions regarding the emissions from ammonia combustion

The relationship between NOx and ammonia slip is unfortunate. Literature on CI engines shows that NOx emissions tend to be produced at high combustion temperatures and unburned ammonia at low temperatures, with no “ideal” temperature level eliminating both of these emission species [7]. Additionally, emissions of unburned ammonia can occur during unstable combustion conditions.

However, there is insufficient research on the exact ammonia slip levels in large marine engines. Solutions to both NOx emissions and ammonia slip exist. There are ammonia slip catalysts which are already developed for land-based and road transport. Unburned ammonia and NOx emissions can be reduced through engine calibration and more controlled combustion conditions,e.g. by applying exhaust gas recirculation(EGR).

Exhaust gas after-treatment systems to reduce NOx emissions, like the selective catalytic reduction (SCR), are already widely used in the maritime sector. In the SCR system, ammonia is used as a reducing agent to reduce NOx to nitrogen (N_2) and water vapour in presence of a catalyst. The advantage of ammonia-fuelled ships is that the reducing agent is already onboard and thus readily available [8].

As far as the **N_2O** is concerned, it has been shown that the minimization of the species is possible by operating at higher combustion temperatures.

So, all in all, This indicates that future engines could minimize N_2O and ammonia slip by operating on high temperatures, whereas NOx would be reduced by SCR for compliance with ECAs. Interestingly, catalysts for the combined removal of NOx and N_2O are commercially available according to Alfa Laval [8]. **Optimizing the combustion process and eliminating any remaining emissions with exhaust gas after-treatment systems might therefore be a way forward** [9].

2.4 Implementation of Ammonia in ICEs

2.4.1 Ammonia through the ages

The research concerning the utilisation of Ammonia as a fuel for ICEs could be divided into two main time periods. The early period, from the beginning of the Second World War to the late 1970s, and the recent period from the beginning of the second millennium to the present day. The main difference between these two periods is the ultimate objective of the research. During the former period, the global scientific and engineering community was focusing on developing new engine technologies, running on alternative, non-carbon based fuels, in order to face any future oil crisis. During the latter period, the main objective of the international research community is to minimize global GHG emissions, by utilising non-fossil fuels for ICE operation, in order to cope with the international regulations, and ultimately to protect the environment.

The early years of research

The first implementation of ammonia as a fuel for automotive applications, dates as far back as 1822. In Thurston's book [62], it is mentioned that Sir Goldsworthy Gurney was the first to propose and develop an ammonia-powered engine for a small locomotive. Several decades later, at the beginning of the 20th century, the use of Ammonia as an anti-knock element, due to its significantly high octane number (**RON** $\approx$ **130**), was proposed, in order to operate ICEs with high average pressures and smooth combustion at high speeds [63]. In 1933, Norsk Hydro was one of the leading companies to run a truck with a modified engine running on hydrogen, with an ammonia reformer being installed on the vehicle [64], (Fig.2.9).

Figure 2.9: Truck ran on Hydrogen, with onboard Ammonia converter, by Norsk Hydro, 1933

In 1938, Ammonia Casale Ltd patented an Ammonia-Hydrogen ICE, which by the 1940s was installed in about 100 vehicles [64];[65].

Moving on to the next decade, the 1940s was a landmark decade for the ammonia-fuelled ICE [7]. During World War II, the oil stockpiles were running dry, mainly due to the oil campaign deployed from the Allies against the occupation forces. The shortage of hydrocarbon fuels, created the need for alternative solutions for powertrain operation, especially for military and armoured fighting applications. This is when ammonia decisively steps in as a favourable candidate among the alternative fuels. In 1945, Kroch [66] published the findings of a one-year study performed by the Belgian State-supervised system of suburban and countryside transportation by rail and road, together with Belgian scientists. In the work published, it is mentioned that the first successful implementation of liquid anhydrous ammonia as a fuel for motorised buses was achieved in 1943. More specifically, the author underlined the excellent results obtained by burning ammonia combined with coal gas, without any power loss, corrosion or increased lubricating oil consumption compared to the gas oil engine [7].

Last but not least, the author suggests that the ignition promoter, which in this particular case was the coal gas, could easily be replaced by other gases, such as Hydrogen, resulting in a completely coal-free engine operation.

After the Second World War ended and the global oil supplies were restored, there was a slight decline in the interest in Ammonia as a power source. In the post-World War era, and more specifically in the 1960s, the Energy Depot Project, funded by the US Military was launched, with its main objective being the development of alternative solutions for power generation, in order to face any future fuel oil crisis [67]. In this project various alternative fuels, such as ammonia, hydrogen and hydrazine, were tested in a single-cylinder Waukesha engine [7]. In their study, the researchers proved that Ammonia is a feasible option compared to fossil fuels, for fueling the civilian market [68]. Furthermore, in the frame of the same project, in 1967, anhydrous ammonia was used as a fuel for an ICE operated in two different modes [69]. The first approach was to maintain a Compression Ignition(CI) operation, using a dual-fuel mixture of ammonia and diesel oil, whereas the second was to transition to Spark Ignition(SI) mode, by converting the engine in an appropriate manner. The main observation of this work was that for the same power output, the cost of Ammonia operation was approximately ten times higher than that of hydrocarbon fueling scenario. However, a steady operation of the engine was achieved.

After the Energy Depot Project ended, not many steps forward have been made in the research domain of ammonia being used as a fuel for ICEs, and the whole idea was basically scrapped and remained buried for several decades. However, with the recent need for GHG emissions reduction, the road towards alternative fuels was re-opened once again, and Ammonia, being a carbon-free and easy to store and handle fuel has been restored in the spotlight of the international research community.

Recent Progress and Development

Various companies and research groups have been working on the ”ammonia utilisation” project in the last decades. In 1981, a converted Chevrolet Impala, running on ammonia was in-house presented by Greg Vezina in the company Hydrofuel Inc. [70]. In 2007, an ammonia fueled pickup car traveled all the way from Detroit, Michigan to San Francisco (USA) to prove the feasibility of the ammonia-fueling concept [71]. Presented in 2013’s Geneva Motor Show, the Marangoni Toyota GT86 ECO Explorer was the first racing car powered by ammonia [72]. The car could operate in Ammonia-only mode for a range of 111 miles ($\approx$ **180km**), claiming a completely CO_2 free operation. However, the Bigas system (responsible for the ammonia-fueling operation) could operate only for engine speeds up to 2,800 rpm. At higher speeds, and when a more fun-to-drive experience was desired, a switch to direct-injected gasoline fuel could be easily achieved.

In 2014, the Hydrogen Energy Center announced the development of a hydrogen-ammonia operated tractor [73], and in the same year, a research group of the Korean Institute of Energy Research presented their accomplishment, which was a vehicle operated in a dual-fuel mode. The first fuel was gasoline, directly injected into the cylinder, and the second was port-injected ammonia. The ammonia fueling percentage achieved was up to 70% on an energy basis. In 2018, Ezzat and Dincer [74], proposed the development of a carbon-free fueling system, for vehicles running on ammonia-Hydrogen fuels, Fig.2.10. The system proposes a unique solution for onboard hydrogen production via the electrochemical decomposition of ammonia [7].

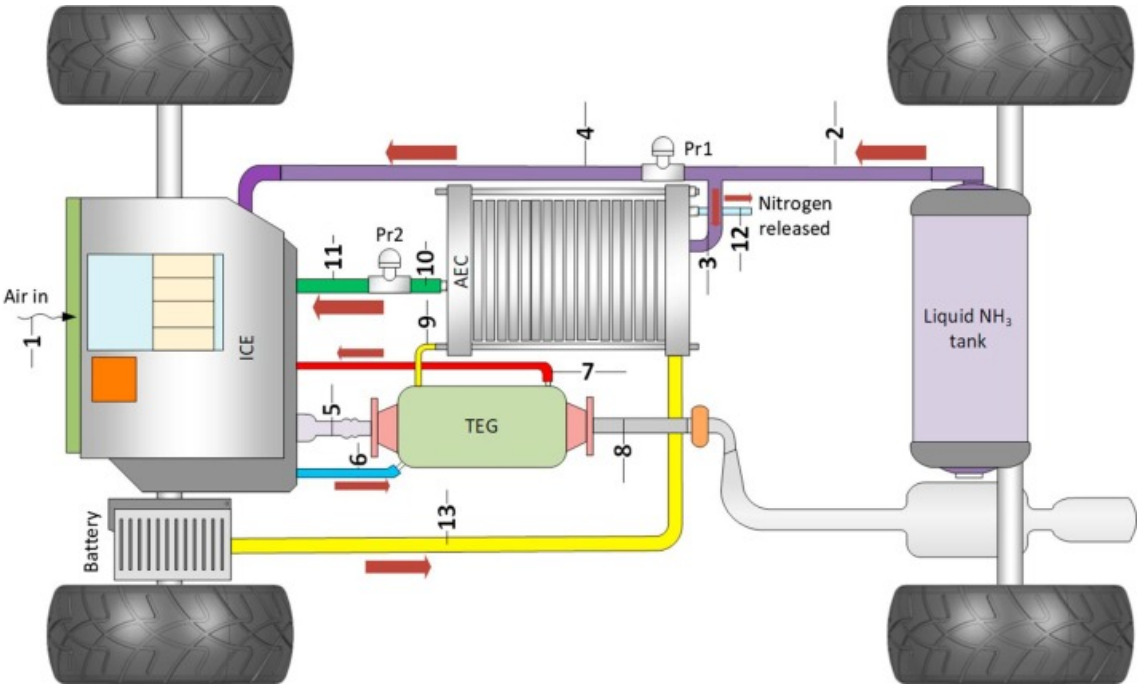

Figure 2.10: Schematic of the proposed integrated system comprising ICE, Thermoelectric Generator(TEG) and Ammonia Electrolyte Cell(AEC) unit by Ezzat and Dincer [74].

Ammonia is a favourable fuel, not only for the automotive industry, but for the power generation and marine sectors as well. In contrast to the former, in the power generation and marine industries, the space sonstraints are not an issue. Thus, the implementation of catalytic equipment for handling the unfavourable emissions from the combustion of ammonia (e.g. SCR System for the reduction of NOx downstream of the engine) is a viable option.

As far as the maritime sector is concerned, the two leading companies in the marine engine development have already decided to take action. MAN Energy Solutions has announced their first ammonia-fueled engine to be developed by 2024, both as a complete new package and as a retrofitting option for their already existing engines, currently running on LPG [75]. Winterthur Gas and Diesel (WinGD), has also announced the development of their ammonia-running 2-Stroke engine, in collaboration with Hyundai Heavy Industries(HHI), by the year 2025 [76].

2.4.2 Required engine system modifications

In order for a conventional ICE to operate on ammonia, only minor changes to the engine's geometry are required [77]. The main modifications are the Ammonia fuel container and the supply system, which create the need for more available space and also increase the overall weight of the layout. In most of the experimental cases, ammonia is port-injected in vapor form into the intake manifold or close to the intake valves. However, alternative methods for importing Ammonia into the cylinder, such as direct in-cylinder injection or cooled liquid Ammonia injection, can be found in the literature, although they are not so common.

Moreover, in order for a smooth engine operation to be maintained, other minor modifications, such as altering the compression ratio or the spark ignition system, may be required. In the case of a CI engine, the high resistance of ammonia to auto-ignition makes the smooth operation of the engine highly dependent on the air-fuel mixture ignition source and the Cetane Number(CN) of the secondary fuel(in a dual-fuel mode scenario). Furthermore, ammonia is highly corrosive to some materials such as copper, nickel and plastics. These materials should be avoided, and the fuel line system should be made out of corrosion resistant materials (e.g. teflon or stainless steels). Introducing the Ammonia downstream the engine's boosting device's compressor can prevent its corrosion, whereas using a mixer can increase the air/ammonia homogeneity and cylinder-to-cylinder distribution [7]. Lastly, in the case of partial cracking of ammonia to hydrogen before it being supplied to the engine, changes to the spark plug materials and the overall spark plug system may be required in order to avoid backfiring. Backfiring is the phenomenon where any residual electric energy remaining in the spark cable leads to a secondary discharge during the intake stroke, ultimately resulting in the ignition of the air-fuel mixture at the intake port. This phenomenon is due to the Hydrogen's minimum ignition energy [7];[77].

2.4.3 Ammonia as a fuel for CI engines

In diesel engines, fuel is atomized into small droplets inside the combustion chamber by injecting it at high pressure with the help of fuel injectors at the end of compression stroke [78]. It forms a combustible mixture with inlet air at high temperature and pressure during the compression stroke, which raises its temperature to the auto-ignition temperature and hence results in spontaneous ignition [79].

CI engines have higher Compression Ratios(CR)($\approx$ **14** : **1** $-$ **25** : **1**) and thermal efficiencies (η : **45** $-$ **55%**) compared to their SI counterparts (CR: 8:1-12:1, η: 28-42%). Combustion in the CI engine is different from that of the SI engine since the CI engine combustion consists of four distinct stages [80]:

1. ignition delay
2. pre-mixed burning
3. mixing controlled combustion
4. after burning

The presence of NH_3 affects the combustion process at each stage and influences the reaction at the subsequent stages as a result [81].

Furthermore, the annual installed capacity of CI is an order of magnitude larger than that of SI engines [81], since it finds wider application in transportation and power generation sectors. In the transportation sector, the shipping industry consumes approximately 330 million metric tons of fossil fuels annually, resulting in higher levels of toxic exhaust emissions polluting the environment, and thus creating the need for alternative fuel utilization.

However, the outcomes of the early year research period on ammonia were disappointing for CI engines due to the poor combustion characteristics of the fuel such as high auto-ignition temperature, low flame speed, narrow flammability limits and high heat of vaporisation (Table 2.3). More specifically, for pure NH_3/air mixture auto-ignition to be achieved and for a smooth engine operation to be maintained, extremely high CR of **35:1 - 100:1** are needed. Of course, this is not a viable option for commercial CI engines, and it even poses a challenge for testing in laboratory conditions. Therefore, the long pose in literature after the, already mentioned, first phase of research is well justified. However, in the last few years, ammonia is once again gaining the global community's attention, with the research objectives mainly focusing on the reduction of greenhouse emissions by partially replacing diesel fuel with alternative carbon-free solutions in a dual-fuel operation [7];[17].

Some of the potential strategies for utilizing ammonia as a CI engine fuel are the following:

- **High CR** implementation, which, as previously mentioned, is quite challenging and commercially restricted.
- **Preheating intake air combined with higher CR.**
- **Dual-fuel operation with hydrocarbon fuels as ignition promoters.**
- **Partial dissociation into H_2**. The H_2 is again used as a combustion promoter.
- **Implementation of alternative combustion strategies**. Low pressure techniques (e.g. HCCI and PCCI), and alteration of the injection timing.

Ammonia as a single fuel for CI engine combustion

The importance of ammonia based CI engine combustion was highlighted by Wagner in 1965 (in his review comments to publications [67], [68], [82]), where he disclosed the experimental results of his studies (1963) on ammonia combustion (pure ammonia and ammonia with additives) in a Cooperative Fuel Research (CFR) engine. Compatibility study on ammonia injection techniques were covered in the army laboratory program and the compatibility of ammonia fuel with the engine (engineering materials and lubricants) were assessed by Gray et al., which revealed no substantial issues and the ammonia combustion was observed to be achievable only at 35:1 compression ratio [83]. Converting the CI engine to spark ignited mode by igniting the injected fuel with the help of a spark plug was also considered to be short term solution by researchers at US Army tank automotive center in 1966 to address the difficulties to burn ammonia by meeting its higher auto-ignition temperature [84], [85]. Direct injection of ammonia is faced with the challenge related to vaporisation of fuel and efforts to address this challenge was taken up by Pearsall [69], where modifications were made to the design of the injection system by incorporating a heat exchanger for cooling the fuel, but even then the researchers failed to achieve combustion. **Ammonia only operation as a single fuel in CI engine is very challenging as it would require very high CRs** and very limited literature from the early stage of research (1960–1970) has reported ammonia only combustion in CI mode [17].

Ammonia-Diesel dual-fuel applications

The combustion of ammonia in dual-fuel operation is a realistic conception as the secondary fuel, with lower auto-ignition temperature, can be used to trigger the combustion of the mixture. Diesel was one of the first fuels tested as the ignition source in a dual-fuel engine back in 1966 by Gray et al. [83]. The researchers managed to operate a diesel-ammonia dual-fuel compression ignition engine with a compression ratio as low as 15.2:1 compared to the 35:1 they used for the ammonia-only operation. When diesel was replaced by amyl nitrate (CN>100) and dimethylhydrazine (CN=67) the minimum compression ratio where smooth combustion was observed was reduced down to 12:1 and 13.7:1 respectively. As highlighted by the researchers, the minimum compression ratio for a stable operation was highly dependent on the cetane number of the secondary fuel. The authors also observed that satisfactory combustion could only be observed when ammonia was injected into the cylinder no later than 40 crank angle degrees before the end of the diesel injection. Whereas, a late ammonia injection (at or slightly before the end of diesel injection) resulted in misfiring. Pearsall and Garabedian [69] also investigated the effects of the cetane number of diesel fuel. The authors operated their engine with Military Compression Ignition and Turbine Engine (CITE) fuel with a cetane number of 38 and two alternative-diesel types of CN44 and CN50. The diesel fuel with a cetane number of 50 provided optimum performance with the shortest ignition delay, highest power and combustion efficiency[7].

Pearsall [86] tested a two-cylinder version of the 12 cylinder AVDS-1790 Vee-Twin engine ([87]) with diesel pilot injection and ammonia gas port-injection at a compression ratio of 18.6:1. The author conducted experiments to determine the effects of varying the quantity of the diesel fuel supplied to the engine while holding all other conditions constant[7].

It was found that when the engine was operating at relatively lean conditions (ϕ = 0.64), the increase of the diesel fuel amount led to a more intense increase in power output and reduction of the brake specific fuel consumption (BSFC) compared to the case where the engine was operating at richer conditions (ϕ = 0.85). The increase in power output for the lean condition was three times the heat content of the diesel fuel, which according to the authors indicated the necessity of much higher ignition energy. Despite achieving optimum conditions of operation, the performance output of the dual-fuel engine tested by the authors was nowhere near the converted spark plug ammonia-only operated engine. The author concluded in his work that the power output of a supercharged diesel-ammonia engine could be easily achieved by a naturally aspirated ammonia-only spark ignition engine. Pearsall and Charles Garabedian of the U.S, Army-Tank Automotive Command, [69] showed the benefits of the spark ignition ammonia engine over the dual-fuel application. The authors highlighted the inherent advantages of spark ignition operation such as the ability to run throttled at part load, the superior reliability of the ignition source and the lower system complexity as storage of a secondary fuel is not required[7].

Comparative study on the suitability of four different fuels (methane, ammonia, methanol and ethanol) on a high speed direct injection diesel engine (with constant amount diesel pilot injection) was performed by Bro and Pedersen [88], and the results can be seen in Fig.2.11. Results of study indicated ammonia as the least suitable alternate fuel for dual fuel combustion in CI engines owing to its slow combustion, higher ignition delay and emission of unburnt ammonia. Research studies on ammonia fuelled CI engines took a long pause after this specific study in 1977 (also due to restoration of the hydrocarbon fuel economy by addressing the existing logistic issues).

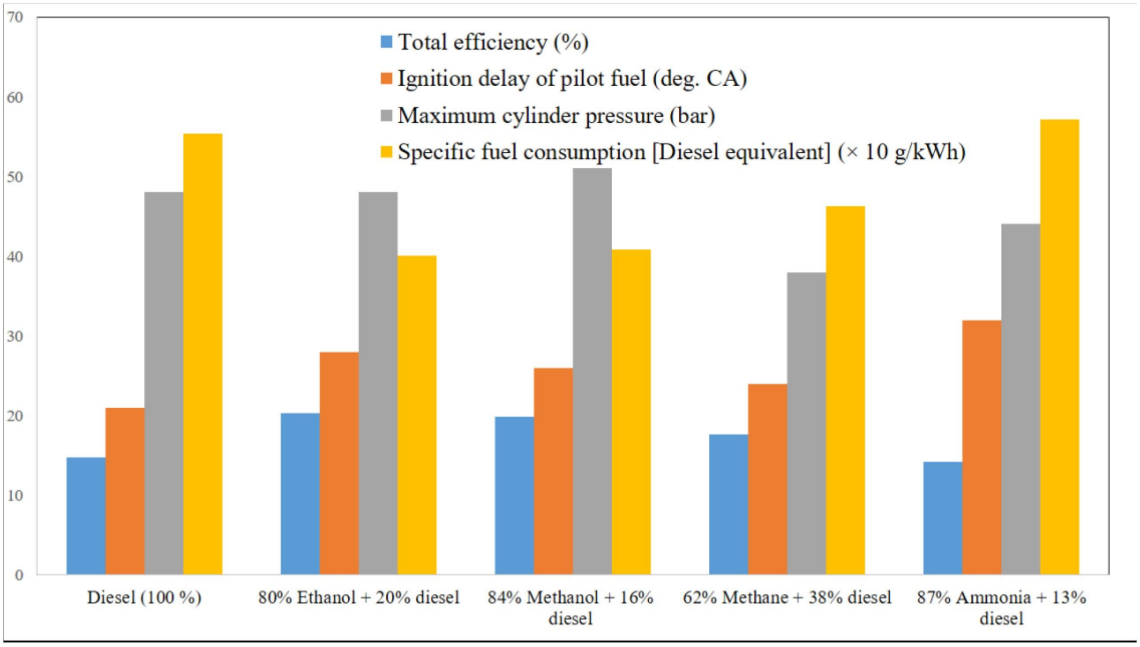

Figure 2.11: Results of comparative study on alternate fuels for diesel dual fuel combustion at 1500 rpm and 1.6 kW (performed in 1977)[88]. Reprinted by [17]

In the modern era, Reiter and Kong performed experimental investigations to explore the feasibility for using ammonia as a fuel for CI engine by introducing ammonia vapor to the intake port of a four-cylinder Common Rail Direct Injection(CRDI) diesel engine (4.5 L capacity) [5]. **The experimental work of Reiter and Kong is used as the reference study of the present thesis, and will be extensively reviewed in the following chapters**. As a general remark however, the overall CO_2 emissions were decreased as the ammonia energy share in the fuel fraction increased. The authors successfully operated the engine under various engine speeds, loads and ammonia energy share ratios up to 95%. Reasonable fuel economy with a combustion efficiency of around 95% was obtained for ammonia rates between 40 and 80% while NOx emission formation was reduced compared to the diesel-only operation for ammonia rates up to 60%. The NOx reduction occurred despite the fuel-bound nitrogen. According to the authors, this is likely due to the lower combustion flame temperatures and the effect of ammonia in NOx reduction as observed in the modern after-treatment systems. However, the relatively low combustion temperatures deteriorated the hydrocarbon (HC) emissions while unburned ammonia emissions between **1000 and 3000 ppm** were observed at the exhaust of the engine.

Lee and Song [89] applied multiple injection methods to a neat NH_3 engine. It was demonstrated that when the mass fraction of the pilot fuel is less than or equal to the main injection, SOI of at least 12 ^{o}CA before Top Dead Center(bTDC) is required to elevate engine in-cylinder pressure to a competitive level of ≈170 bar. Conversely, when the mass fraction for the pilot fuel is higher than that of the main injection, SOI could be retarded to 4 ^{o}CA bTDC before a noticeable in-cylinder pressure drop takes place. When compared with 8 ^{o}CA bTDC SOI, NO emissions were reduced up to a factor of 5 when SOI was retarded to 12 ^{o}CA bTDC, owing to the reduction in peak cylinder temperature. Lamas and Rodriguez [90] showed that parabolic fuel injection profiles resulted in the highest NOx reduction (≈75%) when compared with rectangular and triangle ammonia injection nozzle profiles (≈65%) at 40 ^{o}CA aTDC. It was also shown that prolonged injection duration (10 ^{o}CA) resulted in poorer NOx reduction. Retarded fuel injection led to drastic NO reduction, owing to the heat loss during the expansion stroke. However, it is expected that fuel efficiency will be lowered due to the late fuel injection strategy. Conversely, advanced injection of 10–18 ^{o}CA bTDC is seemingly a more practical approach. Although NOx and N_2O showed an increasing trend from 0 to 10 ^{o}CA bTDC injection[60], it was reported that further advances in fuel injection could reduce NOx drastically [91];[81].

The idea of **aqueous ammonia solution (NH_3 + water (H_2O))** was investigated by Pyrc et al. [92] using a CI engine. Conventional diesel was chosen as the baseline. The engine heat release increased by 12 J/^{o}CA at full load operation when fuelled with the water ammonia solution (WAS), owing to the increased ignition delay and prolonged combustion duration. As a result of the increased heat release, the engine Break Thermal Efficiency(BTE) was found to increase by ≈3%. Although WAS increased the engine $COV_{\mathbf{IMEP}}$(Coefficient of Variation of the Indicated Mean Effective Pressure) by about 0.3%, the overall $COV_{\mathbf{IMEP}}$ was lower than 5% (acceptable $COV_{\mathbf{IMEP}}$[80]). NOx emissions for the diesel/WAS engine were 520 ppm lower than diesel at full load, owing to the lower combustion temperature. Nonetheless, this resulted in 70 ppm higher unburned hydrocarbons (UHCs) than the diesel engine. Schönborn [93] showed that aqueous ammonia was more difficult to ignite than neat ammonia in a CI engine. To ignite ammonia in an aqueous solution, a minimum CR of 27 was necessary for a typical CI engine operation.

Ammonium nitrate or hydrogen are two potential ammonia derivatives that were identified as capable of enhancing aqueous ammonia ignition whilst reducing the required CR to 24. Şahin et al. [94] reported that as compared to a neat diesel engine, the fuel efficiency of diesel/aqueous NH_3 engine reduced by $\approx$20% when the aqueous NH_3 volume fraction increased by 10%. Hydrocarbon (HC) and CO generally show decreasing trends as the NH3 fraction increased. NOx increased as NH_3 proportion increased [81].

Ammonia combined with Dimethyl Ether(DME) and Biodiesel Combustion

Dimethyl ether and ammonia dual-fuel combustion was tested by researchers from the Iowa State University [95];[96] and Kunsan National University [97]. Dimethyl ether is a high cetane number fuel with a high vapour pressure that needs to be pressurised to remain in liquid form, similar to ammonia. The researchers benefited of the miscible characteristics of ammonia and dimethyl ether (DME) to develop stable mixtures of ammonia-DME solutions that they were directly injected into the cylinders of the compression ignition engine using a newly developed injector. Three mixtures of 20%NH_3-80%DME, 40%NH_3-60%DME [96] and 60%NH_3-40%DME [97] were tested, and the results were compared to pure DME operation. The obtained results were similar to the diesel-ammonia literature such as long ignition delay and decreased combustion temperature with higher CO and HC emissions. The NOx formation of the engine deteriorated compared to the DME-only operation due to the formation of fuel-NOx. The exhaust ammonia emissions were in the range of a few hundred ppm under most conditions tested. The authors observed engine performance deterioration as the ammonia energy share ratio was increased, while operating with high ammonia rates (60%) led to significant cycle-to-cycle variations[7].

Soy-based biodiesel was adopted by Reiter and Kong [77] as the ignition source. The experimental results obtained for the biodiesel-ammonia operation were similar to those of diesel-ammonia. In detail, the NOx formation of the engine was reduced for the dual-fuel operation for low to mid-ammonia energy share ratios due to the lower combustion temperatures. At high ammonia energy share ratios (80%), NOx emissions were higher than biodiesel-only operation. Hydrocarbon emissions were deteriorated for low to medium ammonia energy share ratios but improved at the highest ammonia fuelling rate. In a numerical simulation environment, Tay et al. [91] investigated the performance of an ammonia-fumigated compression ignition engine with diesel, diesel-kerosene and kerosene pilot injections. They observed that by changing the pilot fuel from diesel to kerosene led to an advanced start of ignition benefiting of complete ammonia combustion (Fig.2.13). Carbon emissions were drastically reduced for ammonia energy share ratios of over 60%, but this high level led to a substantial increase in NOx emissions [7].

Hydrogen as a combustion promoter - Partial NH_3 decomposition into H_2

Ammonia decomposition that was considerably successful in the SI engine was also tried out in CI engines. Wang et al. [98] utilised catalytic NH_3 decomposition in the CI engine. It was shown that the BTE of the diesel/H_2/NH_3 engine was very similar to that of the Ultra-Low Sulphur Diesel (ULSD) engine, regardless of the variation in H_2/NH_3 volume fraction. HC and CO were reduced by ≈7.5% as H_2/NH_3 volume fraction increased from 2.47 to 11.03. The NO emission of the H_2/NH_3 engine was comparable with the ULSD engine despite NO_2 was found to be marginally higher than that of the ULSD engine. Gill et al. [59] examined combustion of gaseous neat NH_3, H_2, and dissociated NH_3 in a CI engine. Brake Specific Fuel Consumption (BSFC) for a 75/1/24 H_2/NH_3/N_2 blend was found lower than for neat NH3, indicating a better fuel efficiency than the former. **It was hypothesised that emissions from ammonia may be reduced through preheating the chemical (e.g. waste heat from the exhaust gas can be used to partly decompose ammonia)**[81].

Recently, the operation of a homogeneous charge compression ignition (HCCI) engine with ammonia-hydrogen blends was tested by Pochet et al. [99]. The hydrogen induction aimed to promote and stabilise the operation of the engine while the combustion of the mixture was achieved at intake gas pressure of 1.5 bar and temperature in the range of 428–473 K. The authors operated the engine with an ammonia content rate of up to 70%, but as highlighted, this would require the combustion temperatures to stay above 1300 K to maintain hydrogen-like combustion efficiencies. The researchers proposed that higher compression ratios and intake pressures should be used with ammonia to minimise the requirement of intake gas heating and increase the engine's efficiency. However, due to the tendency of hydrogen to preignition, a variable compression ignition system could be beneficial for extending the engine's operation for various ammonia/hydrogen rates [99];[7].

Alternative techniques for Ammonia combustion

Alternative combustion techniques such as homogeneous charge compression ignition (HCCI) and premixed-charge compression ignition (PCCI) have been employed with ammonia fumigation. As reported earlier, Pochet et al. [99] developed an HCCI engine operating with ammonia and hydrogen blends under a variable blending ratio. The authors applied the HCCI strategy as an alternative to SI engines aiming at operation with high compression ratios and low in-cylinder temperatures. The authors [100] previously found that in a naturally aspirated engine with a compression ratio of 16:1, the auto-ignition temperature of ammonia proper combustion timing was around 610 K while this temperature reduced to 440 K for hydrogen gas. Therefore, the implementation of hydrogen was aiming at reducing the required intake gas temperature and enhancing the combustion efficiency of the engine. Moreover, Pochet et al. [99] were one of the first research groups to implement exhaust gas recirculation (EGR) for controlling the NOx emissions of an ammonia-fuelled engine. The EGR technology revealed itself as a promising NOx reduction technique due to the decrease of the in-cylinder oxygen availability. However, the oxygen reduction led to lower combustion temperatures and resulted in a noticeable negative effect on combustion efficiency[7].

Lee and Song [89] developed in a simulation environment a premixed-charged combustion strategy with a compression ratio of 35:1 and intake gas temperature suitable for ammonia combustion without the need for a secondary fuel. The PCCI-alike strategy involved a pilot ammonia injection (ϕ = 0.1–0.3) during the compression stroke to form a homogeneous lean mixture. The auto-ignition of the lean mixture increases the in-cylinder temperature and pressure and prepares a suitable environment for the combustion of the main ammonia spray injected right after the start of combustion. The pilot injection quantity was found to be a significant parameter on the overall engine performance with increased pilot amounts leading to elevated in-cylinder combustion temperatures and enhanced combustion efficiency of the main ammonia spray. A schematic of the ammonia combustion strategy proposed by Lee and Song can be seen in Fig.2.12.

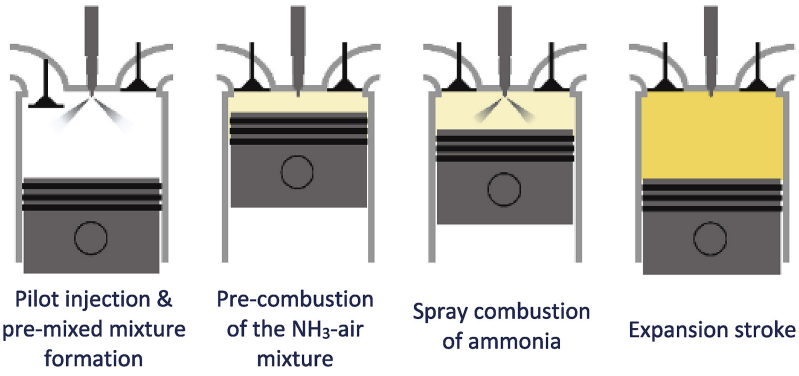

Figure 2.12: Schematic of the ammonia combustion strategy proposed by Lee and Song[89]. Reprinted by [7].

Summarizing, the utilization of ammonia as a fuel for CI engines is a challenging task, mainly due to the chemical's high resistance to auto-ignition and the consequent need for extremely high CR. Many researchers have focused their work on the matter, and significant progress has been made over the last years. For a conventional CI engine to operate smoothly on pure ammonia or dual-fuel ammonia-containing mixtures, the proper adaptation of various engine parameters is essential. In Fig.2.13, a summary of the adjustments of the engine parameters for NH_3 accommodation is presented. The research and the development of new strategies and combustion techniques is a work in progress, and all in all, the future of ammonia fueled engines seems brighter than ever.

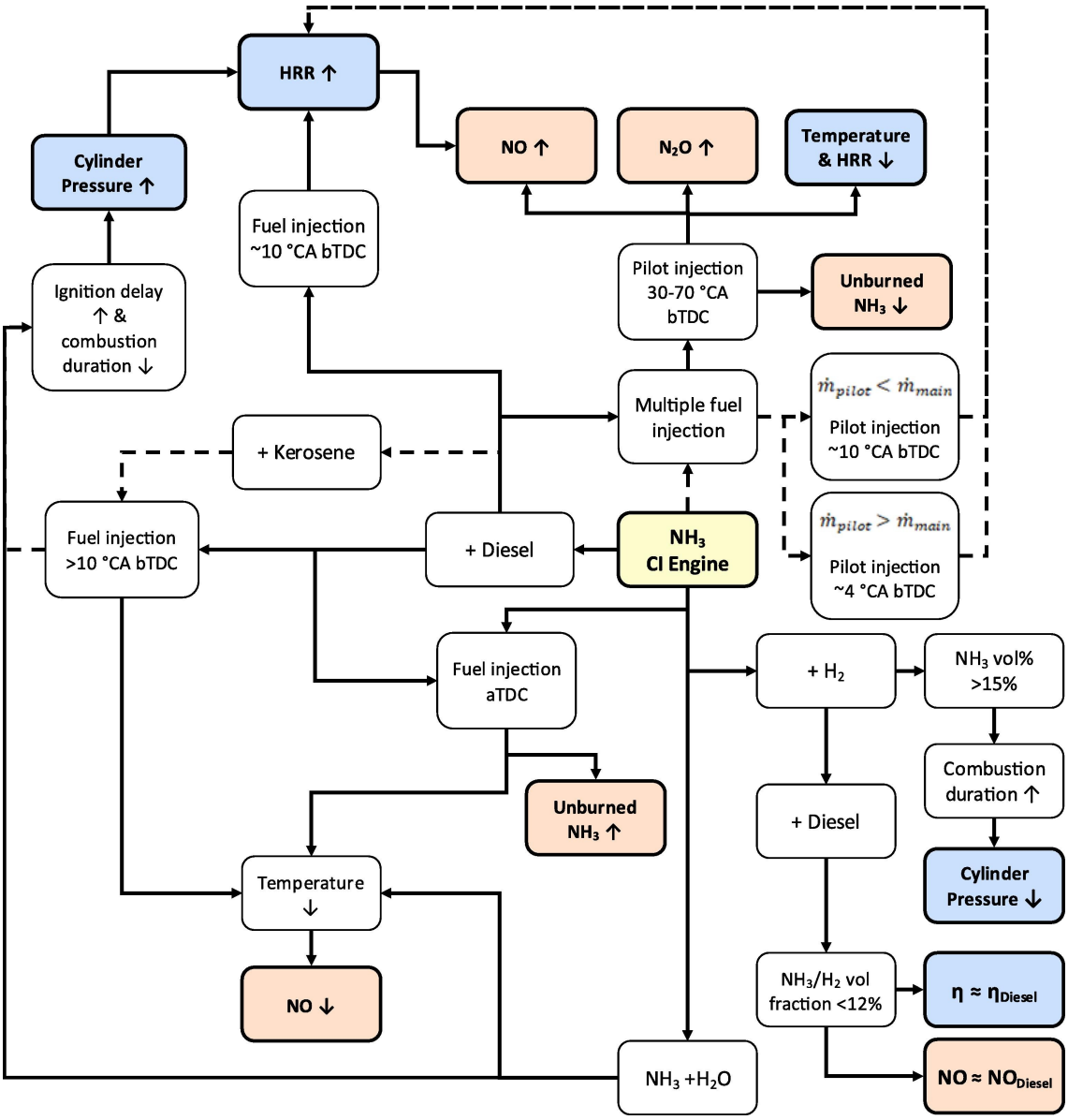

Figure 2.13: CI engine parameters adjustment to accommodate NH_3 operation. Reprinted by [81].

Chapter 3

Model Development

3.1 Reference study description

The present work was based on the experimental results of a study conducted on a 4-stroke, heavy duty, CRDI engine. Reiter and Kong [5] appropriately modified and operated their experimental engine under a dual-fuel operation stencil; the first fuel was diesel(considered as n-dodecane in the frame of the present work) directly injected into the cylinder, and the second was a lean premixed mixture of NH_3/air. Ammonia was port inducted, and as the authors mention, in order to introduce gaseous ammonia into the engine, some modifications were required to the original engine intake setup. An FNPT flush-mount pipe fitting was welded into the intake tube after the compressor and before the intake manifold. A stainless steel tube was then piped to the ammonia flow control system [5](Fig.3.1).

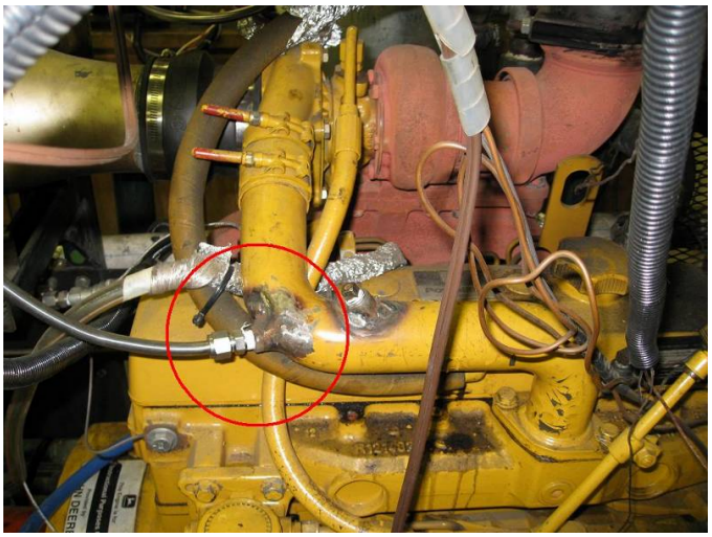

Figure 3.1: Ammonia intake location. Reprinted by [95].

3.1.1 Engine Specifications

The engine used in the experiment(and modeled in the present work) is a John Deere, heavy duty engine (Fig.3.2. The engine's technical specifications can be seen in Table3.1.

Table 3.1: **Engine technical specifications**

Engine Model	John Deere 4045TT068
Engine Type	In-line 4, 4-stroke
Bore (mm)	106
Stroke (mm)	127
Compression Ratio	17:1
Dual-Fuel Operation	Diesel Direct Injection - Lean premixed NH_3/air Mixture
Speed (RPM)	**1000**
Power per Cyl. (kW)	**10**

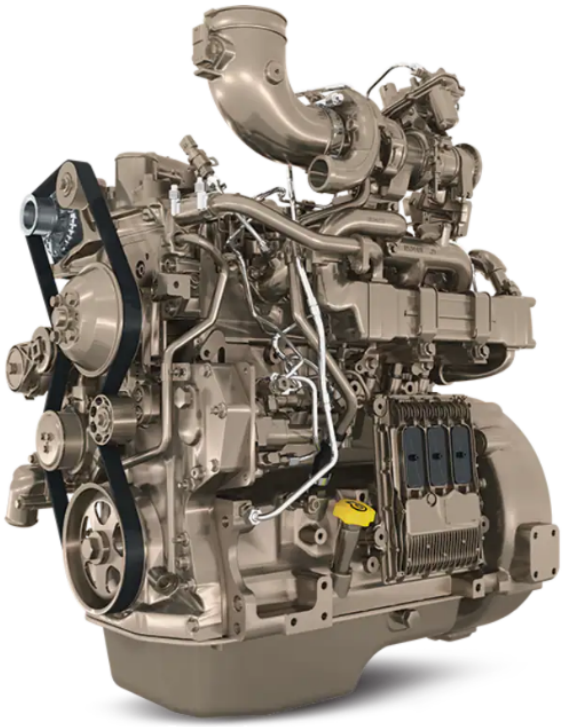

Figure 3.2: John Deere 4045-line engine overview.

3.1.2 Test protocol

During the experiment, the researchers operated the engine in both variable power output and steady power output modes. However, in the frame of the present work, the "Constant Speed - Constant Power" operation stencil in 100% load was chosen. More specifically, in an energy based fuel fraction (Eq.3.1), the amount of NH_3 introduced was progressively increased, whereas the amount of diesel injected was reduced respectively. Overall, a steady power output was maintained. In Fig.3.3, the operating principle of the engine is presented. As can be seen, the role of ammonia is basically to "bridge" the power gap between the dual-fuel operation and the theoretical diesel-only operation (in which diesel fueling would be gradually reduced).

$$\mathbf{NH_{3_{RATIO}}} = \frac{\mathbf{m_{NH_3}} \cdot \mathbf{LHV_{NH_3}}}{\mathbf{m_{NH_3}} \cdot \mathbf{LHV_{NH_3}} + \mathbf{m_{diesel}} \cdot \mathbf{LHV_{diesel}}} \cdot \mathbf{100\%} \tag{3.1}$$

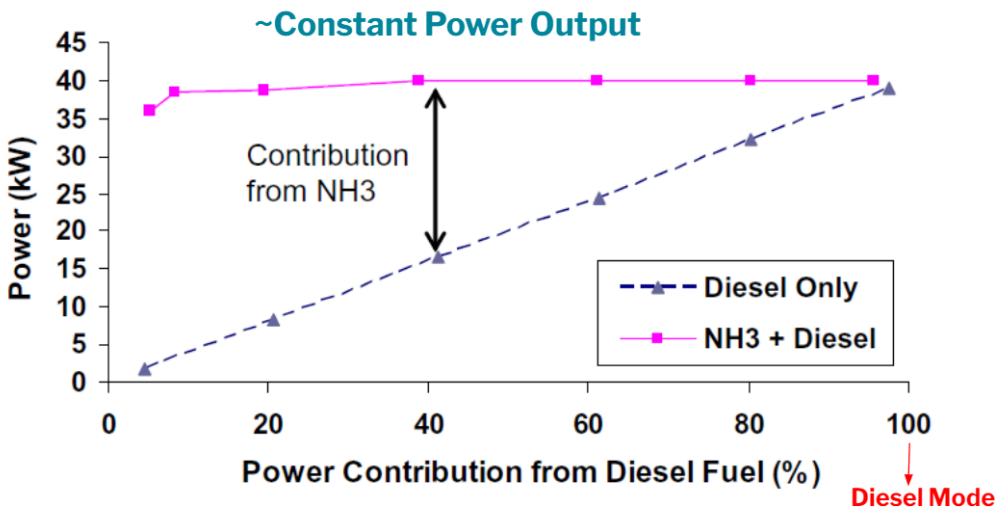

Figure 3.3: Test operating principle.

In total, five cases were tested and modeled, each one of them representing a different percentage of ammonia participation in the total fuel energy fraction, as calculated in Eq.3.1. The five cases, as can be seen in Fig.3.3, are the following:

1. 100% Diesel (Diesel-only mode)
2. 80% Diesel/20% NH_3
3. 60% Diesel/40% NH_3
4. 40% Diesel/60% NH_3
5. 20% Diesel/80% NH_3

For each case, cylinder pressure traces and emission species measurements were drawn from the reference study. The former were used as the basic input and the latter as a means of validation for the developed model.

3.2 Building the model in GT-POWER

3.2.1 Introduction to GT-POWER Software

An Overview of the GT-POWER tool

GT-SUITE, which includes the GT-POWER Engine Library, is the leading engine and vehicle simulation tool used by engine makers and suppliers. It is suitable for analysis of a wide range of issues related to vehicle and engine performance.

The engine performance and acoustics library is designed for steady-state and transient simulations and can be used for analyses of engine and powertrain control. It is applicable to all types of internal combustion engines and provides the user with many components to model almost any advanced concept.

The solution is based on one-dimensional fluid dynamics, representing the flow and heat transfer in the piping and other flow components of an engine system. In addition to the fluid flow and heat transfer capabilities, the code contains many other specialized models required for system analysis. All aspects of the engine in the schematic shown below (Fig.3.4) and more can be modeled. By being comprehensive, the code is well suited for integration of all aspects arising in engine and vehicle development[101].

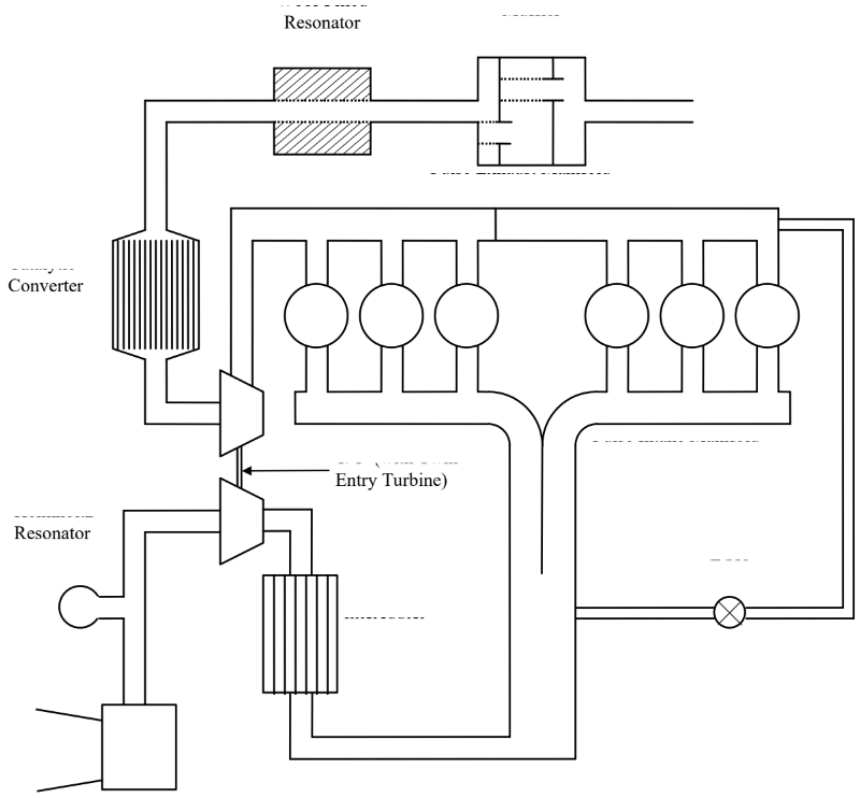

Figure 3.4: Engine aspects offered as modeling options in the GT-POWER tool.

Combustion theory in GT-POWER

The proper treatment of combustion within an engine model is critical to achieve a well calibrated model that is appropriate for the simulation task at hand. To properly discuss the handling of combustion in GT-POWER it is necessary to define some of the terminology used in this section:

- **Combustion** - In GT-POWER, combustion refers to the transfer of a defined amount ofunburned fuel mass and air along with the associated enthalpy from an unburned zone to a burned zone in the cylinder, the release of the chemical energy in the fuel-air mixture and the calculation of species and concentrations that result.

- **Burn Rate** – The instantaneous rate of fuel consumption within the cylinder combustion process. In a GT-POWER simulation, this is the rate at which fuel and air molecules are transferred to the burned zone from the unburned zone and begin to participate in the chemical reactions (although they do not necessarily burn completely to the final products of combustion). In GT-POWER, the combustion rate is controlled by the burn rate. This burn rate input may either be imposed or predicted, depending on the combustion model selected.

- **Heat Release Rate(HRR)** – The instantaneous rate at which the energy stored in the fuel molecules is released in the cylinder as thermal energy. This quantity differs from the burn rate because the fuel-air mixture entering the equilibrium equations does not break down instantly into its final products of combustion. If any intermediate products of combustion are formed before the complete combustion occurs, some of the energy contained in the fuel will not be released until later. This causes the heat release rate to lag the burn rate. In addition, if the mixture of fuel and air in the cylinder is not perfectly homogeneous, the equivalence ratio of the burning mixture will not be constant. The energy released per mass of fuel changes as the equivalence ratio and temperature change, causing a difference between the burn rate and heat-release rate. In GT-POWER, heat release rate is never used as a simulation input. The apparent heat release (see below) is available as a simulation result.

- **Apparent Burn Rate** – This refers to the GT-POWER burn rate that would need to be imposed in a simulation using the general non-predictive combustion profile option ('EngCylCombProfile') to reproduce a measured cylinder pressure trace. The term "apparent burn rate" is specific to GT-POWER where it is possible to use identical code in both the **forward run** combustion calculation (burn rate $\rightarrow$ pressure) and the **reverse run** combustion calculation (pressure $\rightarrow$ burn rate). Two different tools exist within GT-POWER to calculate the apparent burn rate from cylinder pressure.

- **Apparent Heat Release Rate(aHRR)**– The calculated instantaneous rate of thermal energy release based on measurements of cylinder pressure. The actual heat release rate is impossible to measure by conventional means because the instantaneous chemical composition in the cylinder is difficult to determine. Therefore, the heat release rate must be inferred from measurements of cylinder pressure. To calculate heat release rate from cylinder pressure, it is necessary to make simplifying assumptions. The calculated heat release rate will differ from the actual heat release rate due to these assumptions and is therefore labeled "apparent".

Apparent heat release is available as a simulation result. The method of calculation and the simplifying assumptions are documented in a following section. There are different tools available to calculate heat release from cylinder pressure and each may make different assumptions. Therefore, it is not necessarily valid to compare an apparent heat release curve calculated by GT-POWER to a heat release curve calculated with another tool.

- **Forward Run Combustion Calculation** – Combustion calculation where the burn rate is an input, and the result of the calculation is the cylinder pressure. This is the normal mode of operation in a typical GT-POWER simulation. Fuel (and air) are transferred from the unburned to burned zone as specified by the burn rate, and the cylinder pressure is a result of the energy release from combustion.

- **Reverse Run Combustion Calculation** – Combustion calculation where the cylinder pressure is an input, and the result of the calculation is the GT-POWER apparent burn rate that would be necessary to reproduce the same pressure in a forward run. In GT-POWER, the reverse run calculation is actually done by employing the same calculation methods used in a standard forward run. Within each timestep of the calculation, the amount of fuel transferred from the unburned to burned zone is iterated until the measured cylinder pressure is matched.

- **Predictive Combustion** – A combustion model where the burn rate is predicted from the appropriate inputs (pressure, temperature, equivalence ratio, residual fraction, etc.) and then applied in the simulation.

- **Non-Predictive Combustion**– A combustion model where the burn rate is directly imposed as a simulation input. With a non-predictive combustion model, the burn rate does not depend on variables such as residual fraction or cylinder pressure. The fuel and air will simply burn at the prescribed rate.

- **Two-Zone (two-temp or single-temp) Combustion** – A combustion model with two distinct zones – unburned and burned. All combustion models in GT-POWER are two-zone except for 'EngCylCombHCCI', 'EngCylCombDIPulse' and 'EngCylCombDIJet'. The two zones are normally modeled with a separate temperature for each zone but can optionally be specified to have the same temperature.

- **Equilibrium Chemistry** – A method of calculating the concentrations of the species by assuming that the concentrations of the species are equal to that which would occur if the current pressure and temperature were held constant for long periods of time. The engine simulation community has used for a long time this method for the calculation of in-cylinder species. GT-POWER uses this method for the prediction of in-cylinder species, unless the user requests a different method for a specific species.

- **Chemical Kinetics** - A method of calculating the concentrations of the species by taking into account the time required for the species to combine and react. This method is required when calculating NOx and has been shown to improve the prediction of CO.

Two-Zone Combustion Methodology

This section will provide details on the combustion calculations that occur during two-zone combustion. The model developed in the present work uses a two-zone combustion approach, thus the following description is useful for comprehending the modeling process. In GT-POWER, combustion occurs in the following manner:

1. **At the start of combustion** (the start of injection in the DI engine) the cylinder is divided into two zones: an unburned zone and a burned zone. All of the contents of the cylinder at that time start in the unburned zone, including residual gases from the previous cycle and EGR.

2. **At each time step**, a mixture of fuel and air is transferred from the unburned zone to the burned zone. The amount of fuel-air mixture that is transferred to the burned zone is defined by the burn rate. This burn rate is prescribed (or calculated by) the combustion model.

3. **Once the unburned fuel and associated air has been transferred from the unburned zone to the burned zone** in a given time step, a chemical equilibrium calculation is carried out for the entire ”lumped” burned zone. This calculation takes into account all of the atoms of each species (C, H, O, N, S, Ar) present in the burned zone at that time and obtains from these an equilibrium concentration of the 13 products of combustion species (N_2, O_2, H_2O, CO_2, CO, H_2, N, O, H, NO, OH, SO_2, Ar). The equilibrium concentrations of the species depend stronglyon the current burned zone temperature and to a lesser degree, the pressure.

4. **Once the new composition of the burned zone has been obtained**, the internal energy of each species is calculated. Then, the energy of the whole burned zone is obtained by summation over all of the species. Applying the principle that energy is conserved, the new unburned and burned zone temperatures and cylinder pressure are obtained. In the two zone model, the following energy equations are solved in each time step:

► **Unburned Zone:**

$$\frac{\mathbf{d}(\mathbf{m_u} \cdot \mathbf{e_u})}{\mathbf{dt}} = -\mathbf{p} \cdot \frac{\mathbf{dV_u}}{\mathbf{dt}} - \mathbf{Q_u} - (\frac{\mathbf{dm_{f,b}}}{\mathbf{dt}} \cdot \mathbf{h_f} + \frac{\mathbf{dm_{a,b}}}{\mathbf{dt}} \cdot \mathbf{h_a}) + \frac{\mathbf{dm_{f,i}}}{\mathbf{dt}} \cdot \mathbf{h_{f,i}} \tag{3.2}$$

where:

- $\mathbf{m}_u$: unburned zone mass
- $\mathbf{V}_u$: unburned zone volume
- $\mathbf{m}_{f,b}$: fuel mass transferred to the burned zone
- $\mathbf{m}_{a,b}$: air mass transferred to the burned zone
- $\mathbf{m}_{f,i}$: injected fuel mass
- $\mathbf{e}_u$: unburned zone energy
- $\mathbf{p}$: cylinder pressure
- $\mathbf{h}_f$: specific enthalpy of fuel mass
- $\mathbf{h}_a$: specific enthalpy of air mass
- $\mathbf{h}f, i$: specific enthalpy of injected fuel mass
- $\mathbf{Q}_u$: unburned zone heat transfer rate

► **Burned Zone:**

$$\frac{\mathbf{d}(\mathbf{m_b} \cdot \mathbf{e_b})}{\mathbf{dt}} = -\mathbf{p} \cdot \frac{\mathbf{dV_b}}{\mathbf{dt}} - \mathbf{Q_b} + (\frac{\mathbf{dm_{f,b}}}{\mathbf{dt}} \cdot \mathbf{h_f} + \frac{\mathbf{dm_{a,b}}}{\mathbf{dt}} \cdot \mathbf{h_a}) \tag{3.3}$$

where subscript ”b” denotes burned zone.

In the above energy equation for the unburned zone, there are four terms on the right-hand side of the equation. These terms handle pressure work, heat transfer, combustion, and addition of enthalpy from injected fuel, respectively. The third term (combustion) contains the instantaneous rate of fuel consumption or burn rate ($\mathrm{dm}_{f,b}$ /dt).

Non-predictive combustion modeling

A non-predictive combustion model simply imposes a burn rate as a function of crank angle. This prescribed burn rate will be followed regardless of the conditions in the cylinder, assuming that there is sufficient fuel available in the cylinder to support the burn rate. Therefore, the burn rate will not be affected by factors such as residual fraction or injection timing. This may be appropriate as long as the intended use of the model is to study a variable which has little effect on the burn rate. For example, a model built to study the influence of intake manifold runner length on volumetric efficiency or a model built to study the acoustic performance of different muffler designs would not require any prediction of burn rate. In these cases, the variables of interest have a minimal effect on the burn rate.

The option adopted in the present modeling work, is a general option that allows a burn rate to be imposed directly as a function of crank angle:

Imposed Combustion Profile (’EngCylCombProfile’)

This template allows the user to impose a burn rate profile directly as a function of crank angle. It can be used with any type of fuel or injection. This reference template is particularly useful if the cylinder pressure from the engine has been measured in the laboratory(as is the case here) because the burn rate can be calculated from the cylinder pressure. If measured cylinder pressure is available, this is the recommended method of implementing a non-predictive combustion model. It is also possible to change the combustion profile from cycle-to-cycle or from case-to-case by using the RLTDependence and the Profile Dependency Object.

Calculating Burn Rate from Measured Cylinder Pressure

Calculating a burn rate from measured cylinder pressure is sometimes referred to as a ”reverse run”, because the inputs and outputs of the calculation are reversed from the typical combustion calculations in engine simulation. In a ”forward run”, the burn rate is the input, and the cylinder pressure is the result. In a reverse run, the cylinder pressure is the input, and the burn rate is the result. Both forward and reverse run calculation use all the same equations described in the previous section on Two-Zone Combustion Methodology. This means that reverse run calculations include the full thermodynamics and chemistry that is included in a forward run. There are no simplifying assumptions that are applied only to the reverse run. In a reverse run calculation, the amount of fuel that is transferred from the unburned to the burned zone is iterated within each time step until the cylinder pressure matches the measured cylinder pressure. Within GT-SUITE, there are two approaches available to calculate the apparent burn rate from a measured cylinder pressure trace. Both methods have the same basic function – to determine the burn rate from cylinder pressure. Both methods utilize the ’EngBurnRate’ template (called from within the engine cylinder) to enter the measured cylinder pressure. Both methods produce the same set of result plots, tables, and RLT variables, as well as the ’EngCylCombProfile’ objects that can be used in a forward run simulation. The two approaches differ in the way they acquire the necessary additional input data beyond the cylinder pressure (trapped air and fuel mass, heat transfer, etc.). However, in the frame of the present study, only one of the methods will be described, as it is the one applied in the developed model:

Closed Volume Analysis (CPOA) / Calibration, Closed Volume (M+P)

The method is essentially a stand-alone calculation that can be done with only the measured cylinder pressure, either from a single cycle or an ensemble average of many cycles, and a few basic cycle average results (volumetric efficiency, etc.) and engine cylinder geometry. A very simple model should be built that need only include the EngCylinder and EngineCrankTrain (and an injector for DI diesel or GDI applications). The model will run 2 cycles, but essentially repeating the first cycle twice in order to properly converge on results, so valves, ports, and beyond are not necessary. This simulation requires engine geometry, cylinder wall temperatures, a heat transfer model, and initial conditions similar to any other engine simulation. These inputs are all entered in the expected locations within the ’EngCylinder’ template. The initial conditions are of particular importance because they represent the trapped conditions at IVC (the simulation focuses on the closed volume portion of the cycle, so these are the trapped conditions for the combustion event). An ’EngCylInit’ reference object should be defined in the Initial State Object within the cylinder to define these trapped conditions. The cylinder pressure itself is entered in an ’EngBurnRate’ object defined for the Measured Cylinder Pressure Analysis Object attribute. The attribute named Cylinder Pressure Analysis Mode in the EngCylinder object should be set to ”Analysis, Closed Volume (CPOA)” or ”Calibration, Closed Volume (M+P)”.

The simulation methodology is the following:

1. At beginning of a cycle, a rough calculation of combustion burn rate is done making some assumptions about heat transfer (Woschni).
2. The resulting burn rate is applied during the forward simulation cycle and the true heat transfer rate is stored.
3. A final burn rate calculation is done with the true heat transfer from the simulation and all results stored.
4. The final burn rate is applied and imposed back into the model in the 'Combustion Object' during the forward simulation cycle in order to provide a comparison of measurement versus simulation.

The benefit of this approach is that it is fast and only requires one measured instantaneous pressure trace (cylinder pressure). The main downside of this approach is that it requires the estimation of certain input parameters that are difficult or impossible to measure in the test (cylinder trapping ratio and residual fraction). Therefore, this approach is appropriate when the trapping ratio and residual fraction are known (from prior engine simulations) or easily estimated. For example, an engine running at full load with typical valve timings will generally have a trapping ratio of 1.0 and a residual fraction of approximately 4%. In the present work, logical estimations were made concerning these parameters, and a proper calibration was also conducted.

Woschni Heat Transfer Model

Lastly, a description of the applied heat transfer model is made. The 'EngCylHeatTr' reference object allows the user to define which heat transfer model is used to calculate the in-cylinder heat transfer coefficient. The chosen model is described below, accompanied by the main equations for the convective heat transfer coefficient.

WoschniGT indicates that the in-cylinder heat transfer will be calculated by a formula which closely emulates the classical Woschni correlation without swirl (as described in Section 12.4.3 of "Internal Combustion Engine Fundamentals" by John B. Heywood [80]. The temperature exponent was implemented as -0.5 for computational efficiency. This is no longer necessary with modern computers, but the value has not been changed to keep results consistent.). The most important difference lies in the treatment of heat transfer coefficients during the period when the valves are open, where the heat transfer is increased by inflow velocities through the intake valves and also by backflow through the exhaust valves. This option is recommended when measured swirl data is not available.

The convective heat transfer coefficient for the Woschni model is defined as follows:

$$\mathbf{h_{c_{(Woschni)}}} = \frac{\mathbf{K_1 \cdot p^{0.8} \cdot w^{0.8}}}{\mathbf{B^{0.2} \cdot w^{K_2}}} \tag{3.4}$$

Where:

- h_c: convection coefficient (W/m^{2}K)
- B: cylinder bore (m)
- K_1=3.01426, K_2=0.5
- p: cylinder pressure (kPa)
- T: cylinder temperature (K)
- w: average cylinder gas velocity as given below (m/s)

$$\mathbf{w} = \mathbf{C_1} \cdot \mathbf{\overline{S}_p} + \mathbf{C_2} \cdot \frac{\mathbf{V_d \cdot T_r}}{\mathbf{p_r \cdot V_r}} \cdot (\mathbf{p} - \mathbf{p_m}) \tag{3.5}$$

Where:

- w: average cylinder gas velocity (m/s)
- C_1 C_2: constants given below
- $\overline{S}_p$: mean piston speed (m/s)
- T_r: working fluid temperature prior to combustion (K)
- p: instantaneous fluid pressure (kPa)
- p_m: motoring fluid pressure at same angle as p (kPa)
- p_r: working fluid pressure prior to combustion (kPa)
- V_d: displaced volume (m^3)
- V_r: working fluid volume prior to combustion (m^3)

$$\mathbf{C_1} = \mathbf{2.28} + \mathbf{3.9} \cdot \mathbf{MIN}(\frac{\mathbf{m_{in}}}{\mathbf{m_{cyl} \cdot f}}, \mathbf{1}) \tag{3.6}$$

Where:

- $\dot{m}_{in}$: instantaneous mass flow rate summed over valves and orifices through which flow is currently entering cylinder (kg/s)
- m_{cyl}: instantaneous cylinder mass (kg)
- f: engine frequency (revs/sec)

$\mathbf{C_2}$ = 0, during cylinder gas exchange and compression and, $\mathbf{C_2} = \mathbf{3.24 \cdot 10^{-3}}$, during combustion and expansion.

3.2.2 Model Setup

The model was built in the most simple yet efficient way. As mentioned before, a single-cylinder, Closed Volume Analysis approach was chosen. In the GT environment, the engine consists of three main components: (a) the engine crankshaft, (b) the diesel fuel injector, and (c) the engine cylinder.

Engine Cranktrain

Inside the **engine cranktrain** component, the main geometric characteristics (Bore, Stroke, Compression Ratio etc.) as well as the engine speed and the start of cycle are defined.

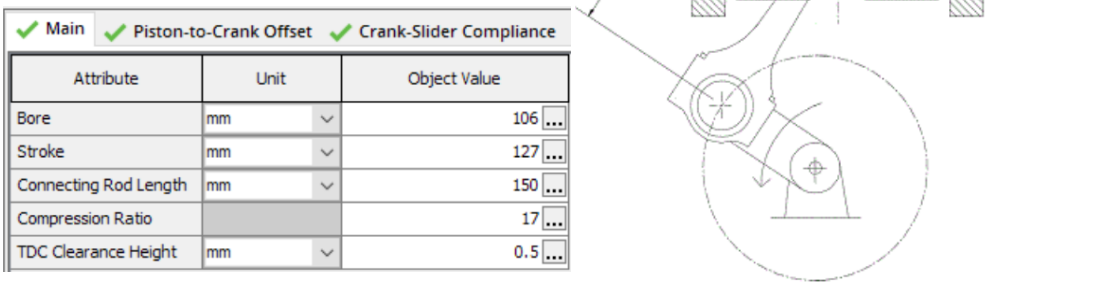

Figure 3.5: Cylinder geometric specifications.

For the application at hand, due to the piston's special morphology (bowl-in piston), a piston-to-crank offset dimension had to be defined (Fig. **??**), as shown below:

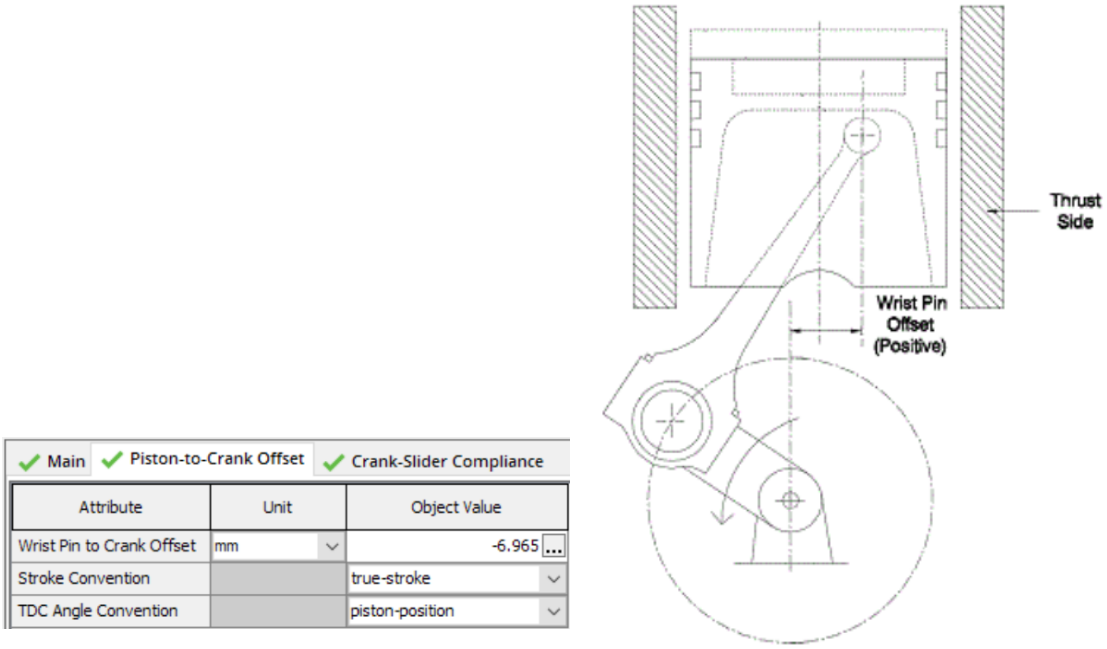

Figure 3.6: Piston-to-crank offset.

Diesel fuel Injector

The diesel fuel injector was chosen from a built-in library, in order to match the engine's fuel flow characteristics. The injection pressure of the common rail system of the engine was specified at **750bar**. The diesel fuel mass injected per pulse was set to **65 mg** for the diesel-only case (according to the experimental data), and it was gradually decreased over the range of the rest cases.

The injection profile was chosen from the GT-POWER library, again in order to satisfy the fueling needs. A typical, rectangular-shaped pulse was used. The Start of Injection(SOI) and fuel mass injected per pulse parameters, were defined in the injector component as shown below:

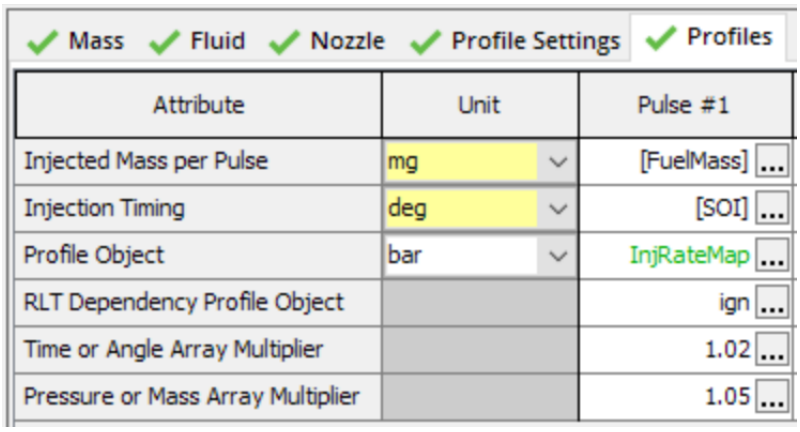

Figure 3.7: Injector parameters definition

The selected liquid fuel was **n-dodecane**(representing diesel fuel), and its thermodynamic properties were imported manually from the DCKM CHEMKIN file.

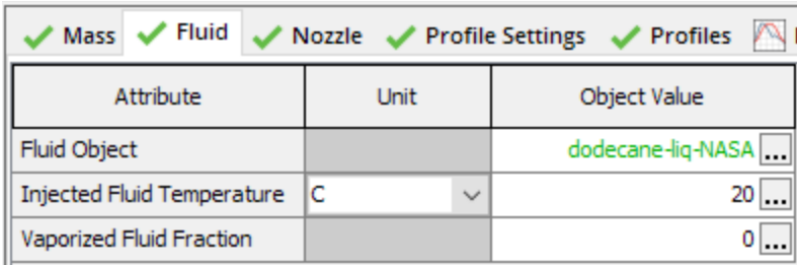

Figure 3.8: n-dodecane importation in the injector component.

Engine Cylinder

The engine cylinder component is the most significant, as it includes the whole combustion modeling. The interface of the 'EngineCylinder' template is presented in Fig.3.9.

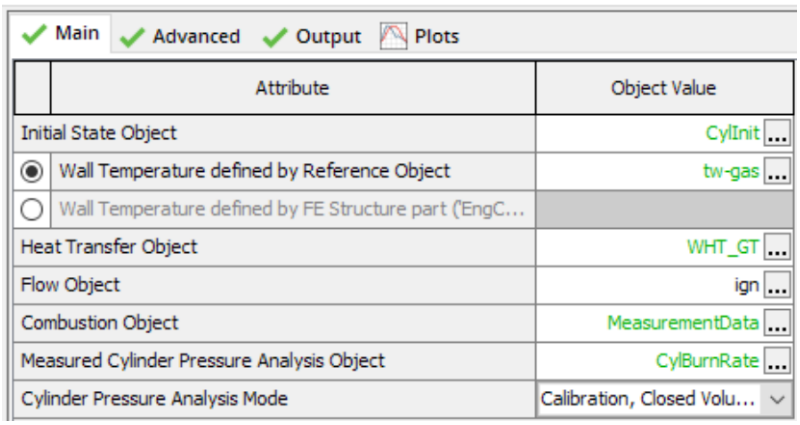

Figure 3.9: Engine cylinder template layout

The model requires the initial conditions within the cylinder to be specified. The main parameters (Air Volumetric Efficiency, Trapping Ratio, Trapped Fuel Vapor Fraction), and temperature at various cylinder locations were calibrated properly, as discussed in the following sections. In the initial conditions, the NH_3 (as a vapor) fuel object is inserted (Fig.3.10).

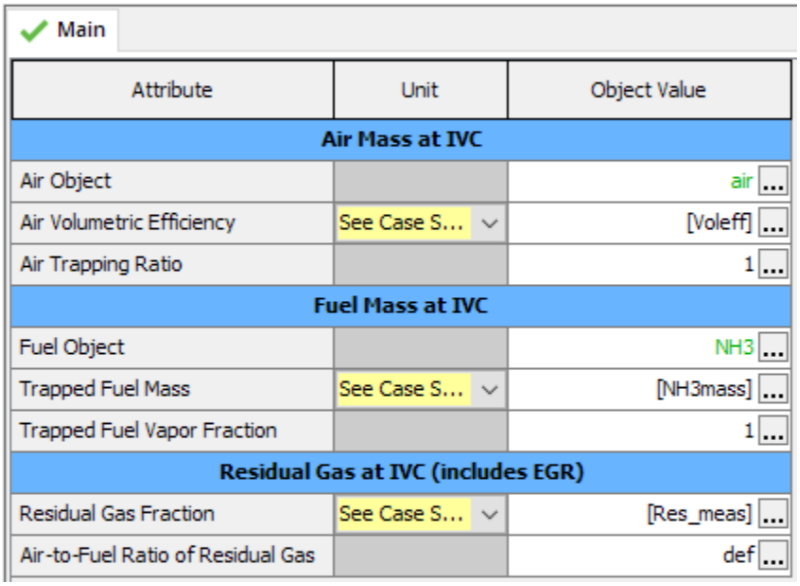

Figure 3.10: Cylinder Initial Conditions.

In addition, a heat transfer object was defined. For this particular application, the Woschni heat transfer model (as discussed earlier) was chosen with its parameters being properly adjusted. The overall convection multiplier was set equal to 0.65 for all cases considered.

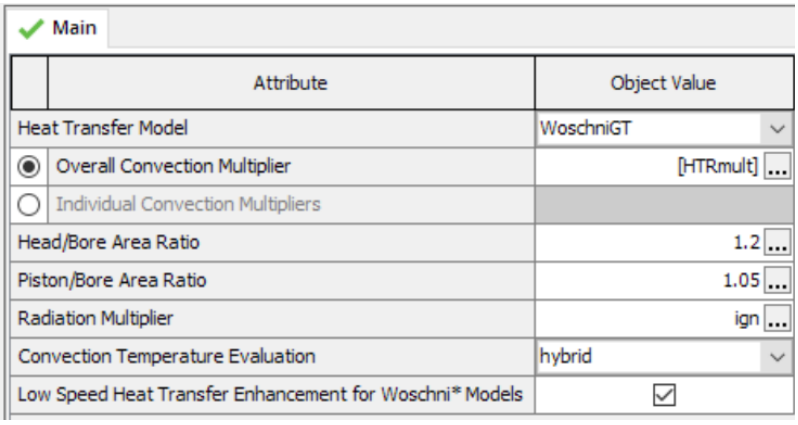

Figure 3.11: Heat transfer object parameters.

The temperature at the different cylinder locations were defined inside the respective object, as shown below:

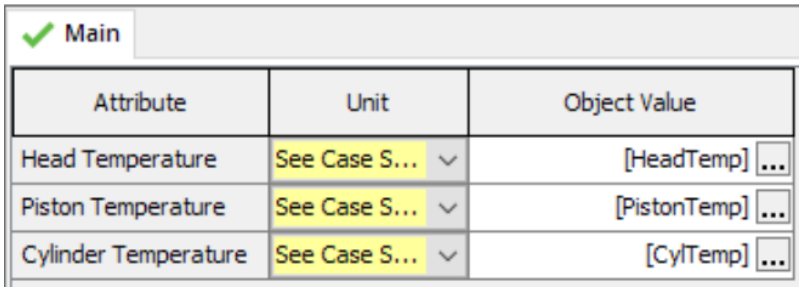

Figure 3.12: Temperature in various cylinder locations

Table 3.2: **Piston, head and cylinder temperature.**

Head Temp.(^{o}C)	325
Piston Temp.(^{o}C)	275
Cyl.Temp.(^{o}C)	175

As previously discussed, the present model is of the two-zone type. This basically means that the cylinder area is divided into two discrete areas: the burned and the unburned. In GT-POWER, the transfer of a defined amount of air and unburned fuel along with the associated enthalpy from the unburned zone to the burned zone in the cylinder, the release of the chemical energy in the fuel-air mixture and the calculation of species and concentrations that result, is the definition of combustion.

The main input of the model is the measured pressure trace (Fig. 3.13, in bar/^{o}CA). In the combustion object defined, a “reverse run” is made at first. During this first run, the model takes the measured cylinder pressure as an input, and solving the reverse problem, it calculates a burn rate. Subsequently, and once the burn rate is stored, it is then imposed into the model, in the Measured Cylinder Pressure Analysis Object. Then, based on the imposed burn rate and the (properly adjusted) combustion parameters, the model recreates a new “predicted” pressure curve. The whole process is called “Calibration, Closed Volume (M+P)”, and its ultimate objective is to achieve the best matching between the Measured(M) and Predicted(P) pressure curves, in order to ensure that the simulation is as close as possible to the experiment. So, basically, the matching between the pressure curves is used as a means for validating the model, and ensuring that the emissions prediction (which is the main goal here) is as accurate as possible.

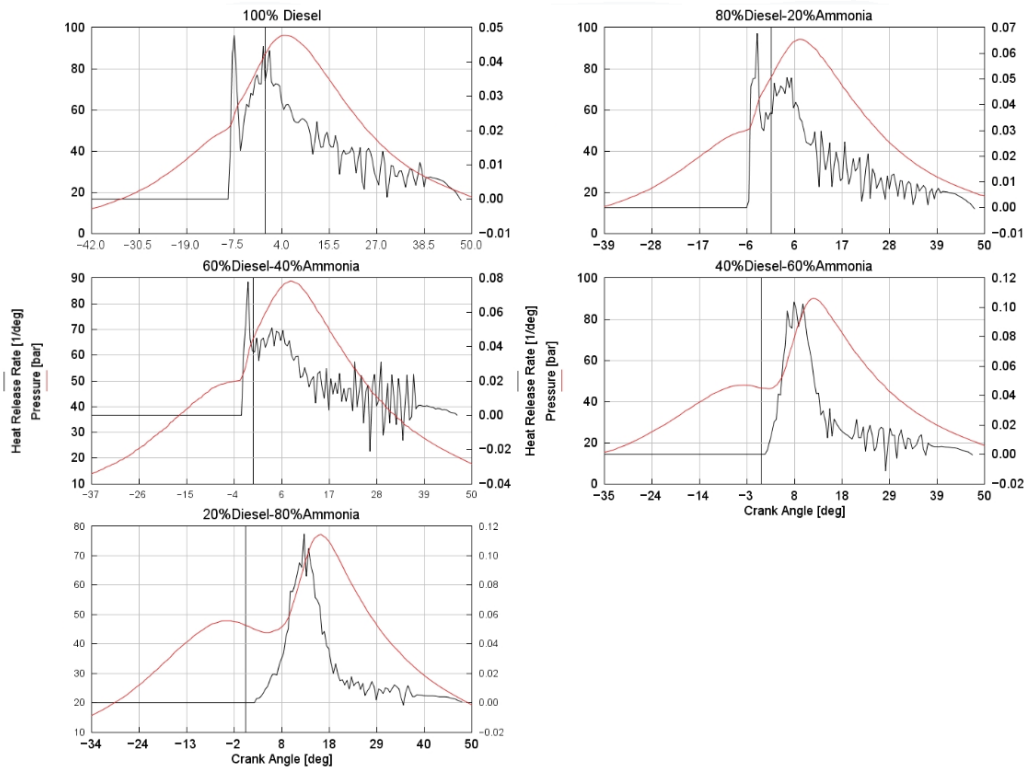

Figure 3.13: Measured(experimental) pressure traces and resulting Heat Release Rates.

3.2.3 ”Constant Speed-Constant Power”

As previously mentioned, the operating principle of the engine was to maintain a steady power throughput in all five cases considered. This was accomplished by maintaining a constant speed (1000rpm) alongside with a constant chemical fuel energy entering the cylinder in every case. The total fuel energy was continuously kept equal to Q=2895.9J while appropriately altering the ammonia participation percentage (Ratio$_{NH_3}$ = 20, 40, 60, 80%) in the total energy fuel fraction(Fig.3.14). In Eq.3.7 and Eq.3.8, the ammonia and diesel fuel mass calculation formulas are presented(Fig.3.15:

$$\mathbf{m_{NH_3}(mg)} = \frac{\mathbf{Q(J)}}{\mathbf{LHV_{NH_3}(MJ/kg)} \cdot (\mathbf{1} + \frac{\mathbf{1-0.01 \cdot Ratio_{NH_3}}}{\mathbf{0.01 \cdot Ratio_{NH_3}}})} \tag{3.7}$$

$$\mathbf{m_{diesel}(mg)} = \frac{(\mathbf{1 - 0.01 \cdot Ratio_{NH_3}}) \cdot \mathbf{m_{NH_3}(mg)} \cdot \mathbf{LHV_{NH_3}(MJ/kg)}}{\mathbf{0.01 \cdot Ratio_{NH_3}} \cdot \mathbf{LHV_{diesel}(MJ/kg)}} \tag{3.8}$$

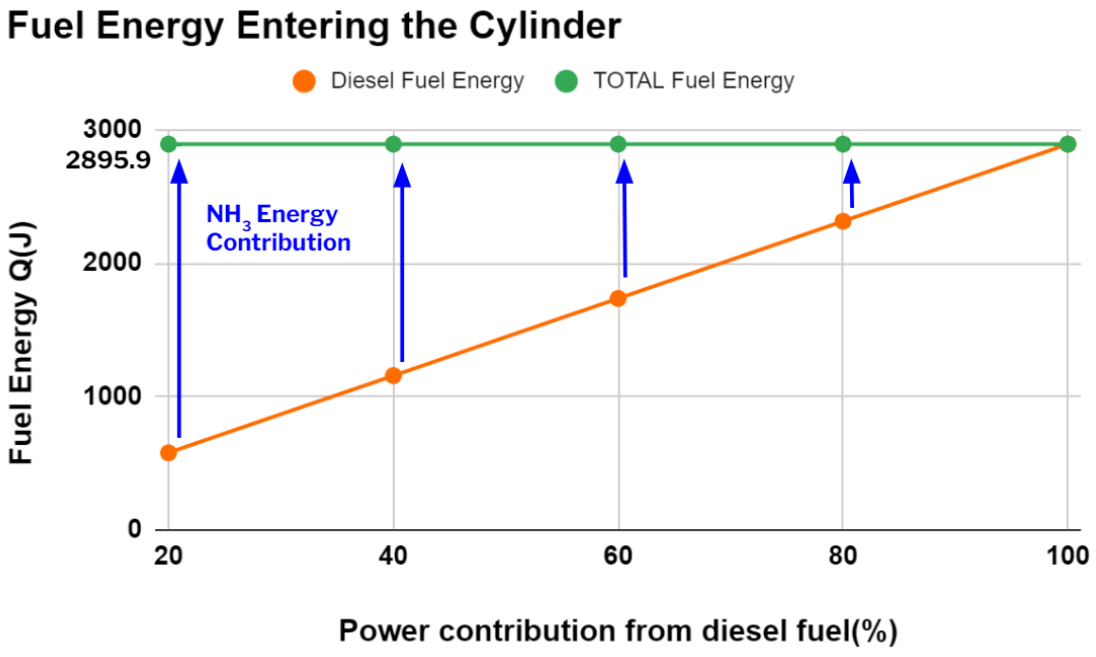

Figure 3.14: Energy contribution from ammonia fuel.

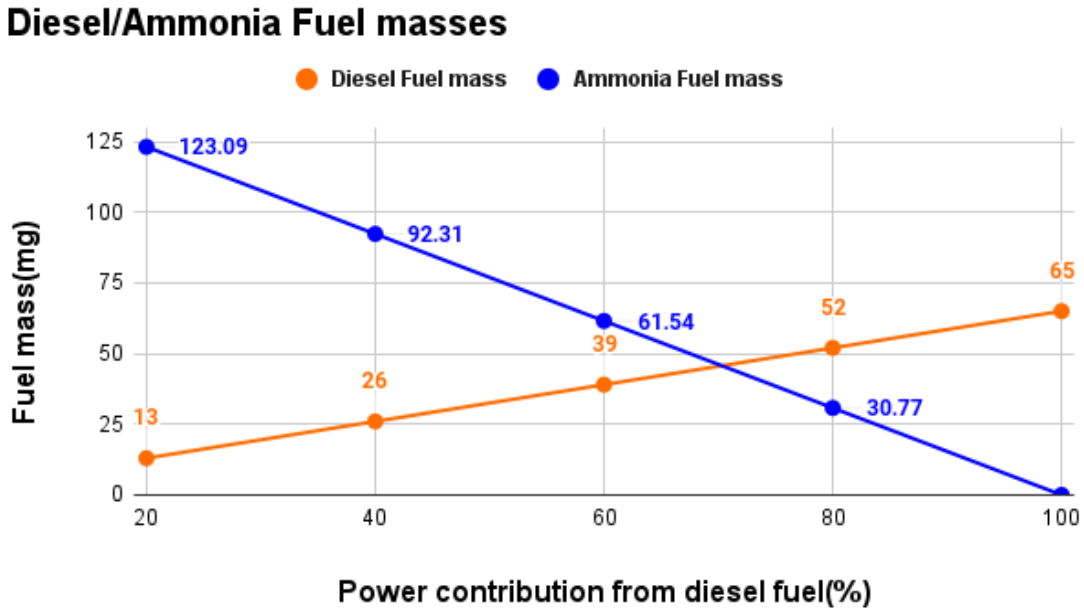

Figure 3.15: Fuel masses at start of combustion.

3.2.4 Importing the DCKM

GT-POWER gives the user the option to import a custom Chemical Kinetics Mechanism, in CHEMKIN-II format, to calculate the species concentration inside the cylinder's burned zone. The mechanism used is a DCKM for n-dodecane oxidation [102], assembled with NOx/NH_3 chemistry[103]. The mechanism, which consists of 190 species and 2800 elementary reactions, was synthesized by the NTUA research group [104] and was modified in an appropriate manner to fit the application at hand.

The DCKM was imported as two separate files in the combustion object; the first file contained the elementary reactions and the respective rate constants, and the second included the thermodynamic properties of all the different species used in the mechanism(Fig.3.16).

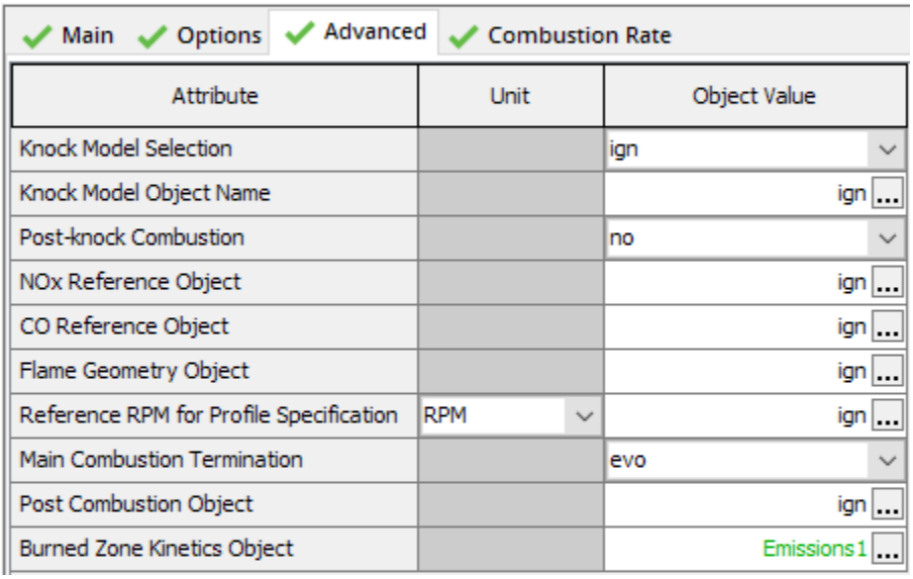

Figure 3.16: Importing the DCKM in the "Emissions1" object.

For the model to run correctly, it is of utmost importance the fuel and air objects to be defined appropriately. The two fuels (n-dodecane and NH_3) were selected from the imported DCKM thermodynamic file, and the air was defined as a mixture of O_2 and N_2 species, again in agreement with the imported species library. Otherwise, no combustion would be observed, as the fuel(s)/air mixture wouldn't match with the chemistry file. The options concerning the DCKM usage in the model can be seen in Fig.3.17.

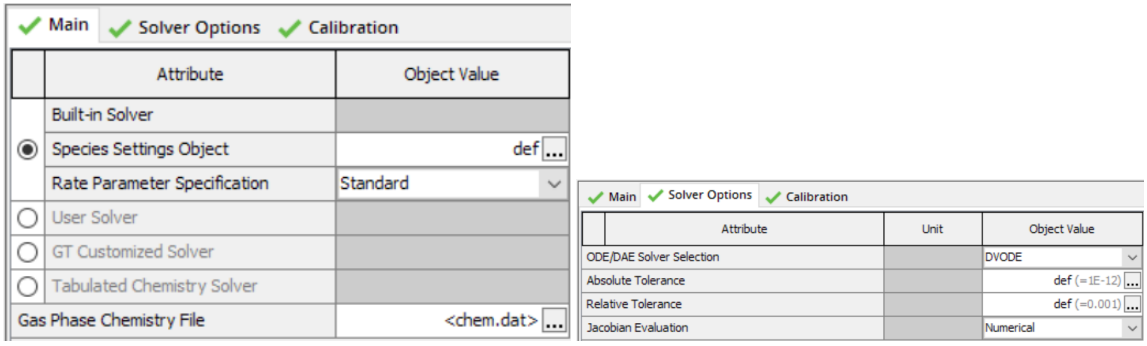

Figure 3.17: CHEMKIN file importation and solver options.

3.2.5 Model Calibration

Due to constraints regarding the limited availability of experimental data, some assumptions were made in order for the model to run smoothly. The main engine parameters, for which no experimental data were available, were calibrated to achieve maximum simulation accuracy. The parameters' values, always kept within logical boundaries, are presented in Table3.3. The Start of Injection(SOI) and Start of Combustion(SOC) values were drawn from the experimental data source.

Table 3.3: **Main parameters calibration**

	100% Diesel	**80%D-20%A**	**60%D-40%A**	**40%D-60%A**	**20%D-80%A**
SOI(deg)	-42	-39	-37	-35	-34
SOC(deg)	-8.5	-5.24	-2.5	1.2	2.5
Residual Gas Fraction	0.03	0.03	0.03	0.04	0.045
Air VolEff	1.45	1.25	1.36	1	0.95

The air volumetric efficiency was gradually decreased as the ammonia vapor amount was increased. Only in Case No.3(60%diesel/40%NH_3) did the Air VolEff increase as it was observed that in lower values, the model could not run properly, in terms of pressure prediction.

After the calibration was done, the simulated engine was found to operate under the following conditions, regarding the air and fuel masses, and the equivalence ratios for each of the two fuels(the stoichiometric AF ratios for NH_3 and diesel were considered equal to **6.05:1** and **14.5:1** respectively):

Table 3.4: **Air mass trapped inside the cylinder at SOC**

Air Mass Trapped at IVC	
Diesel power contribution(%)	Mass(mg)
100	1765.9626
80	1635.1505
60	1700.5565
40	1308.1205
20	1242.7144

Table 3.5: **Ammonia mass at SOC**

Ammonia Mass at IVC	
Diesel power contribution(%)	Mass(mg)
100	0
80	30.77128
60	61.54255
40	92.31383
20	123.0851

Table 3.6: **Diesel fuel mass at SOC**

DIESEL Fuel Consumption	
Diesel power contribution(%)	Mass(mg)
100	65
80	52
60	39
40	26
20	13

Table 3.7: **Ammonia equivalence ratio - φ at SOC**

Equivalence Ratio - φ (NH_3)	
Diesel power contribution(%)	φ
100	0
80	0.1138526662
60	0.2189474019
40	0.4269474192
20	0.5992244517

Table 3.8: **Diesel fuel equivalence ratio - φ at SOC**

Equivalence Ratio - φ (Diesel)	
Diesel power contribution(%)	φ
100	0.5337032619
80	0.4611196339
60	0.3325382015
40	0.2881997492
20	0.1516840877

Overall, the engine was operated using fuel-lean mixtures, regarding both ammonia and diesel fuels, as was anticipated (classic diesel engine operating under abundance of air, and ammonia fueling percentage only reaching $\varphi \approx 0.6$).

An overview of the Graphic User Interface(GUI) of the model developed is presented below:

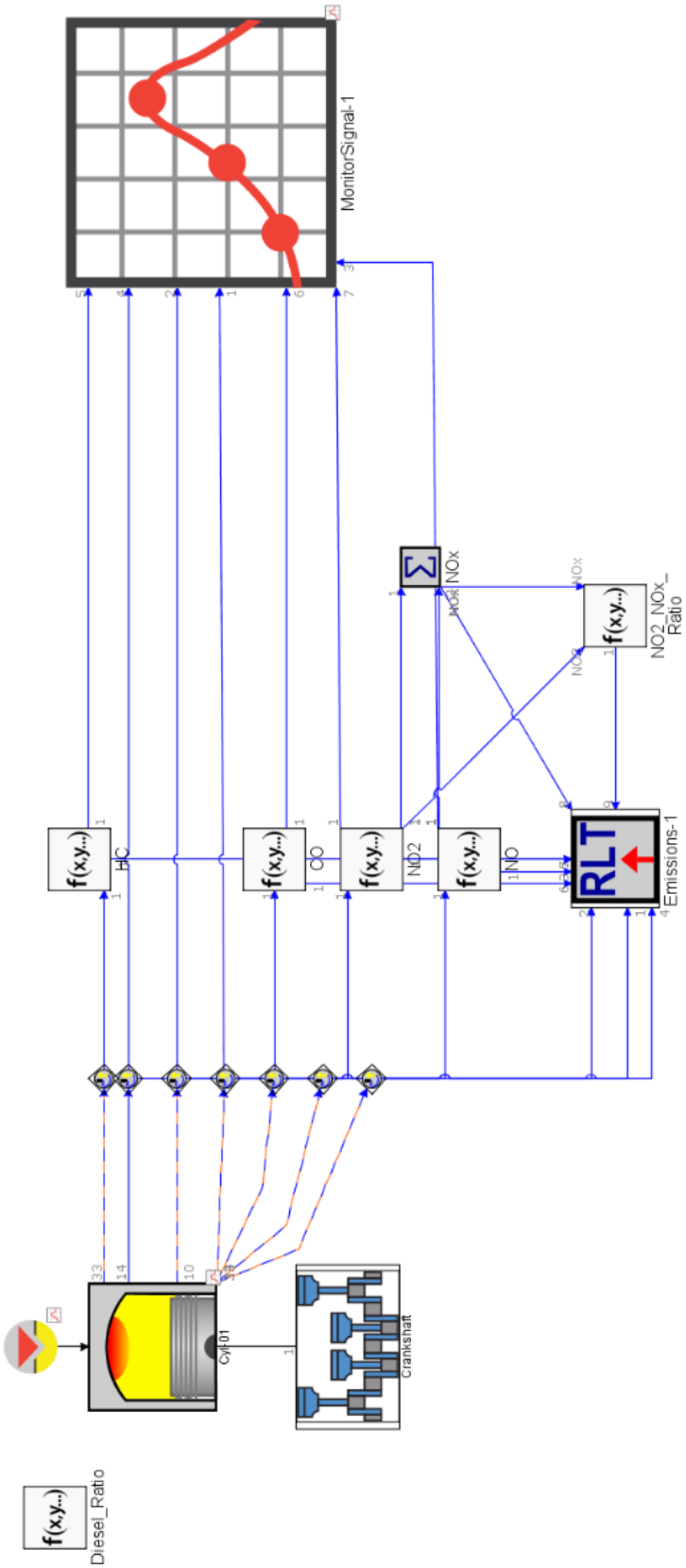

Figure 3.18: Model GUI overview.

Chapter 4

Results and Discussion

In this chapter, the results concerning the matching of the pressure curves as well as the main emission species are presented and discussed.

4.1 Model Validation - Matching the Pressure Traces

As previously mentioned, the main means of validation used was the matching between the measured(experimental) and the predicted(simulated) pressure trace curves. Ultimately, with the proper calibration done, an overall good agreement between the experiment and the simulation was achieved (Fig.4.1).

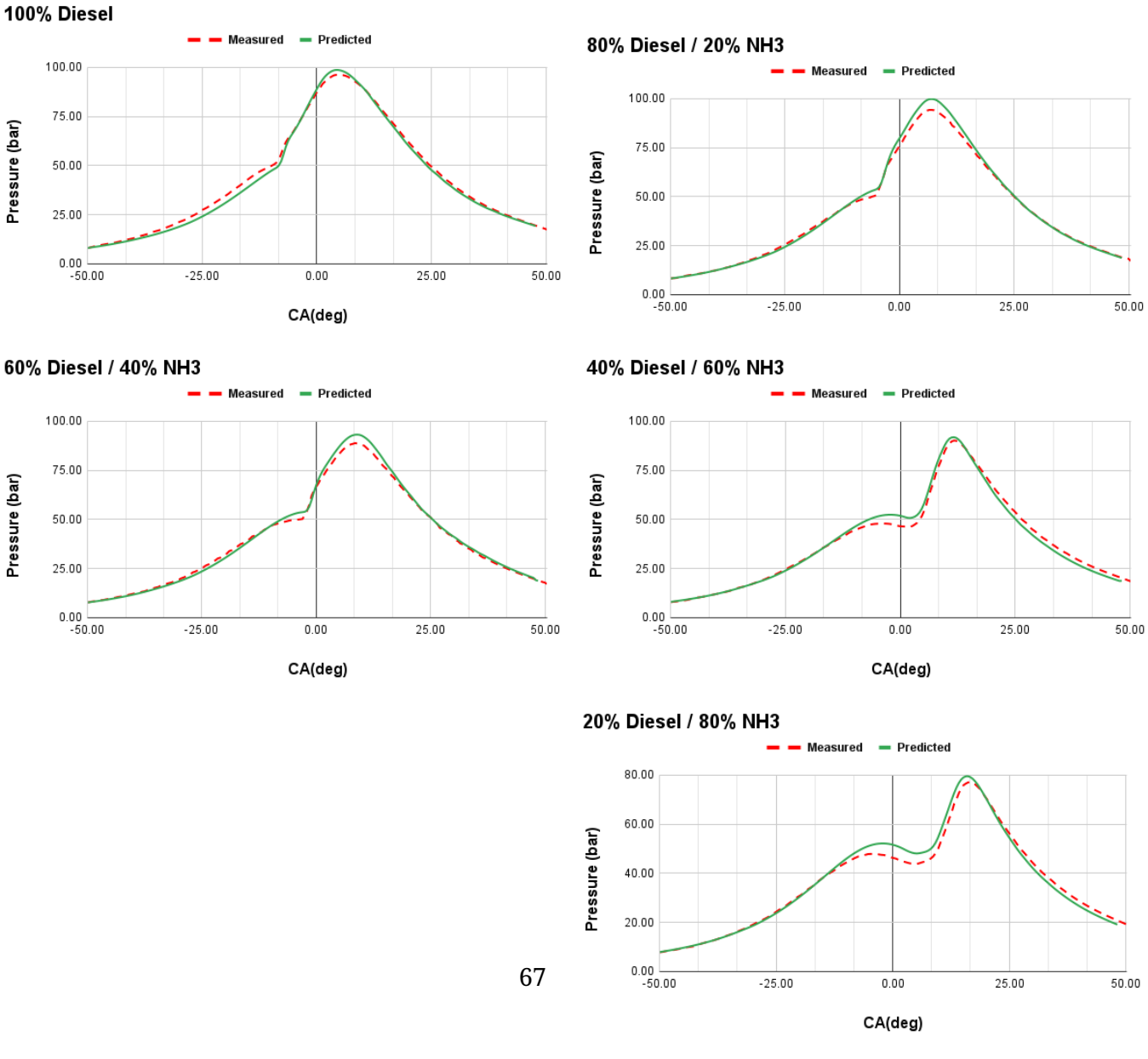

Furthermore, in order to ensure that the “physical problem” was as close as possible to the “simulated” one, a pre-defined un-burned ammonia fraction (in the form of burned fuel fraction) was imposed in the model(Fig.4.2.

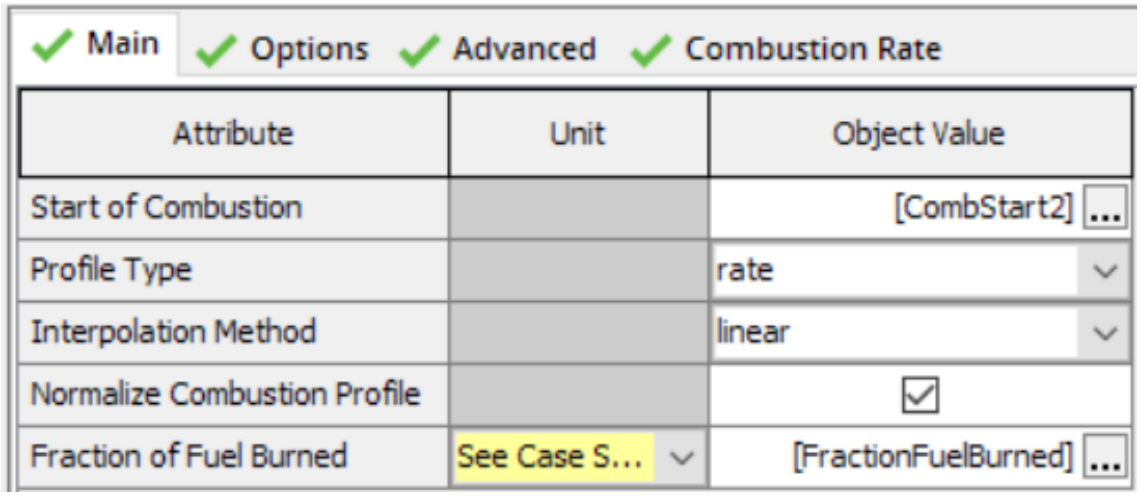

Figure 4.2: Burned Fuel Fraction definition.

Overall, a good match between the measured and the imposed unburned ammonia concentration in the exhaust was achieved, as can be seen in Fig.4.3.

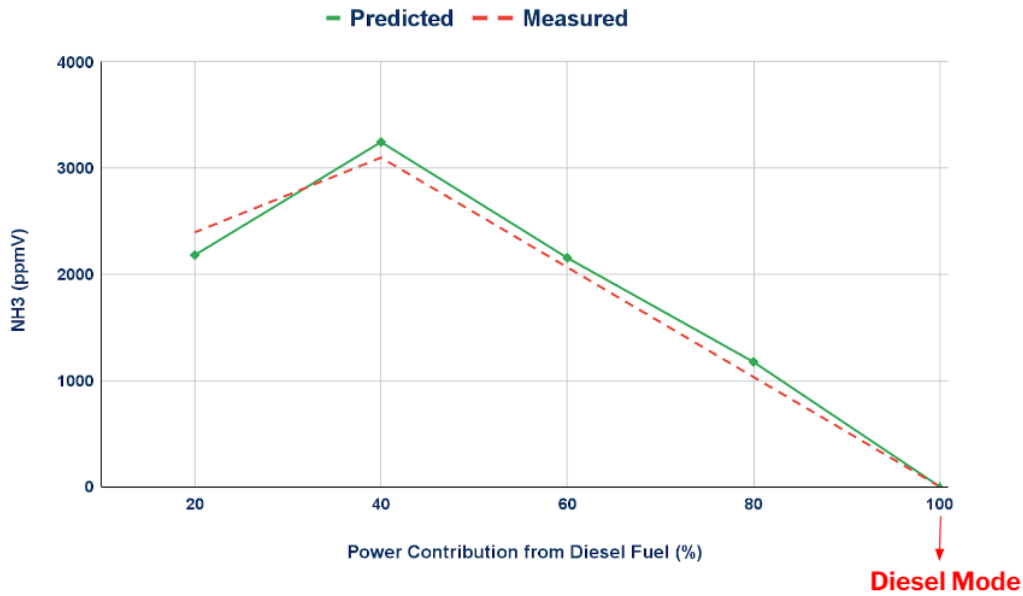

Figure 4.3: Imposed ammonia burned fuel fraction.

4.2 GHG Emission Species

4.2.1 CO_2 Emission Species

As can be seen in Fig.4.4, the overall trend of the CO_2 emission species is satisfactorily captured throughout the whole testing range. As it was anticipated, the gradual increase of the ammonia participation percentage in the fuel mixture (and the consequent decrease of the diesel fueling amount), lead to the significant abatement of the amount of carbon dioxide emitted.

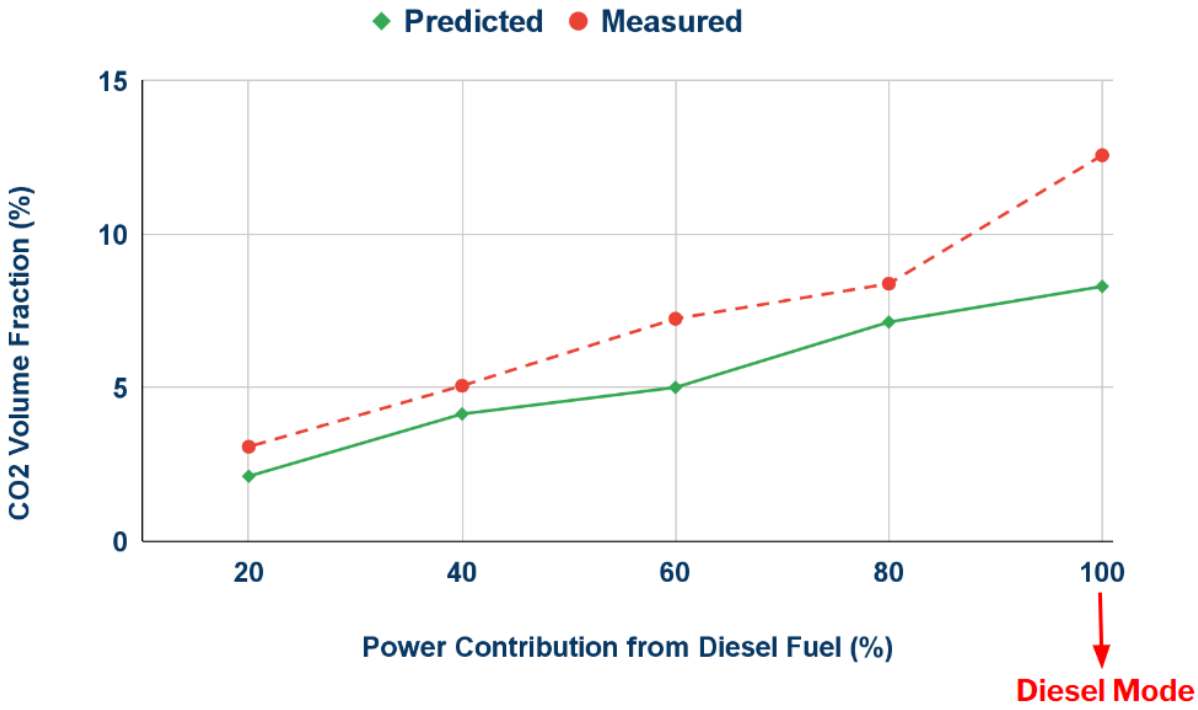

Figure 4.4: CO_2 emission species prediction.

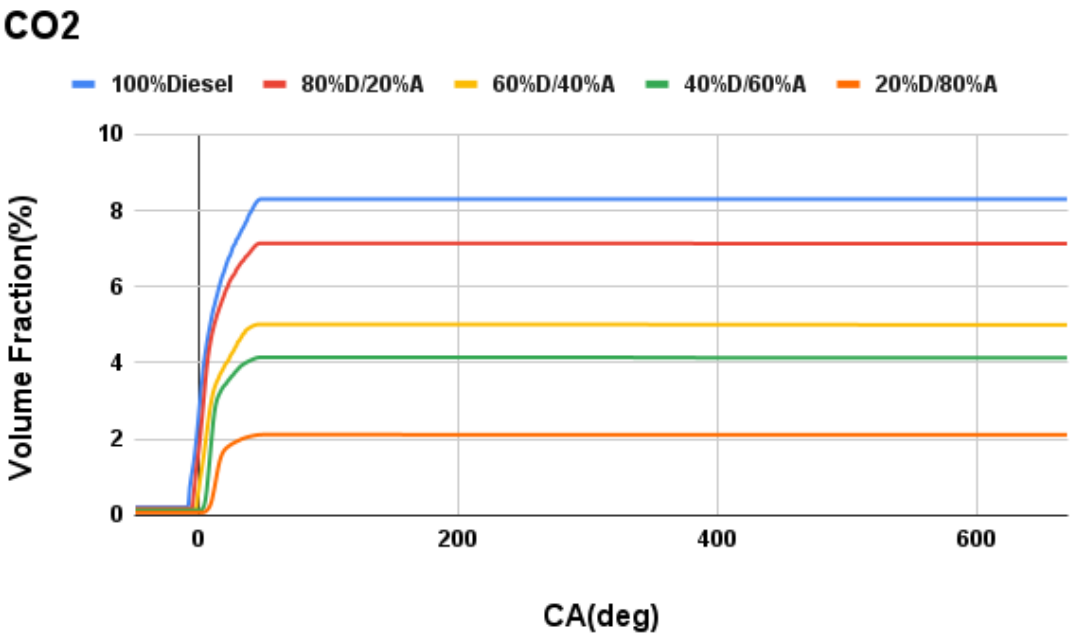

Figure 4.5: CO_2 emission species prediction.

As can be seen in Fig.4.5, at lower ammonia fueling percentages, the volume fraction curves show a steeper slope near TDC, reaching lower values as the substitution percentage increases. This is due to the all-decreasing carbon content of the fuel mixture (leading to overall lower CO_2 exhaust concentration) as well as the SOC timing, which as the ammonia percentage increases, it is constantly shifted towards higher CA(initially towards TDC and gradually surpassing it).

4.2.2 N_2O Emission Species

The predicted levels of nitrous oxide emission species were quite low. However, no experimental data were available for validating the results. As can be seen in Fig.4.6, the maximum N_2O concentration is observed at 60% diesel fueling(40% ammonia). This can be attributed to the ammonia fuel percentage reaching a significant value, leading to both lower in-cylinder temperature (which as previously mentioned favours the N_2O formation) as well as increased nitrogen content in the fuel mixture.

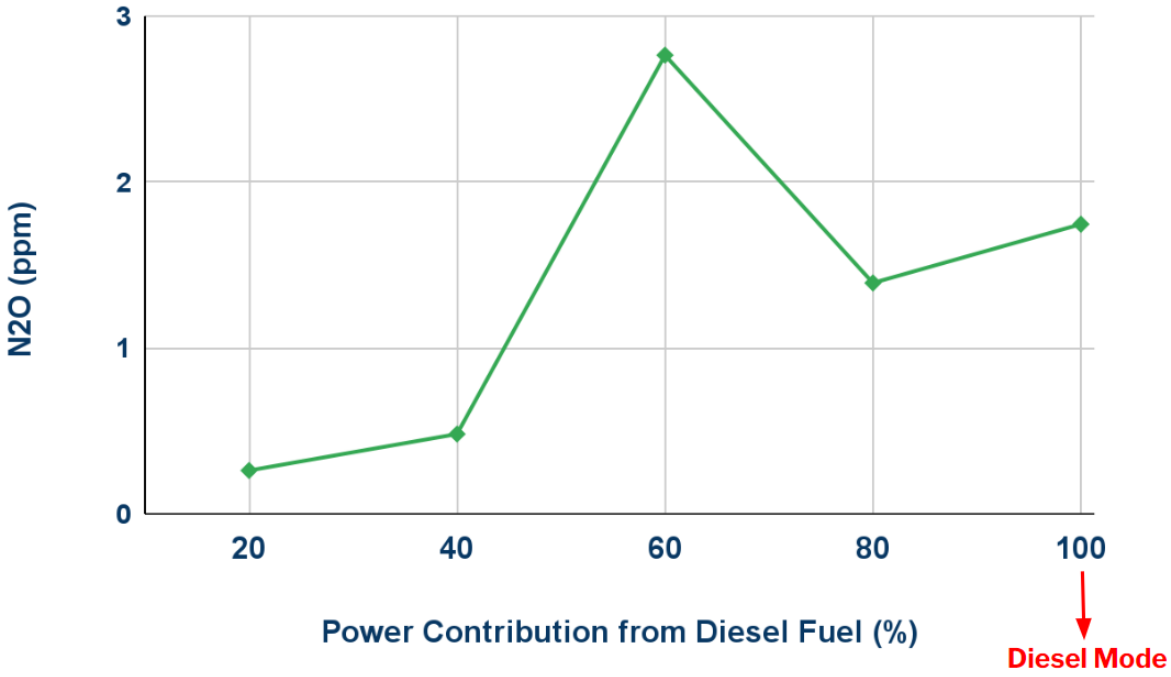

Figure 4.6: N_2O emission species prediction.

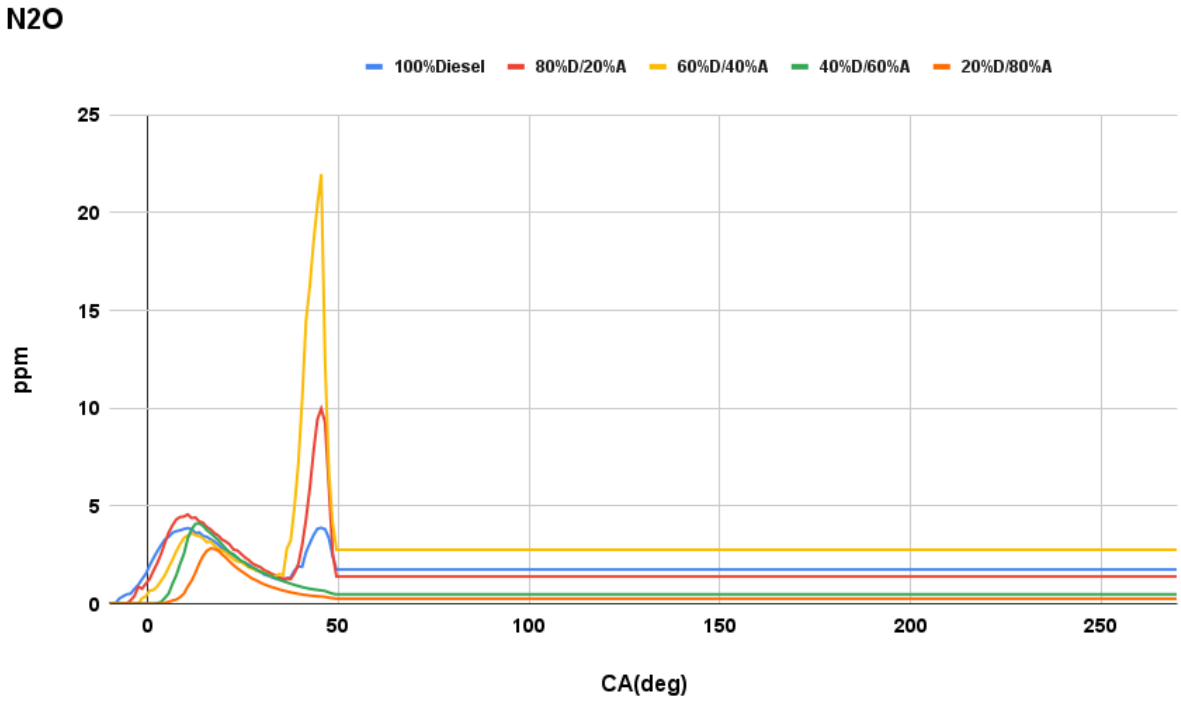

Figure 4.7: N_2O emission species over Crank Angle (TDC=0).

4.3 NOx Emission Species

4.3.1 NO Emission Species

The main observations concerning the NO species prediction are the following:

1. The overall trend is captured quite well in most of the range considered(Fig.4.8).

2. The initially decreasing and subsequently increasing trend of the measured curve for diesel fueling percentages between 60% and 100% is actually captured by the model with a slight shift to the left. More specifically the shame trend in the predicted curve is depicted between 40% and 80% of diesel fueling percentages. A possible explanation for this trend is the following: for lower ammonia substitution percentages(20-40% ammonia fuel energy), the overall combustion temperature is decreased (due to ammonia's lower flame temperature), and thus the thermal NOx formation is inhibited. However, as the ammonia fueling percentage is increased, the total NOx also tend to increase due to the fuel bound nitrogen.

3. Maximum discrepancy is observed at 20% diesel fueling point. This is probably due to incapability of the DCKM to properly predict the emission species under such an extremely elevated ammonia fueling percentage(and consequently decreased presence of diesel fuel).

4. The maximum NO species concentration during the combustion process is observed near Top Dead Center(TDC) in all cases(Fig.4.9). This was well anticipated, as during this phase of the process maximum in-cylinder temperature is observed as well, leading to the strong formation of NO.

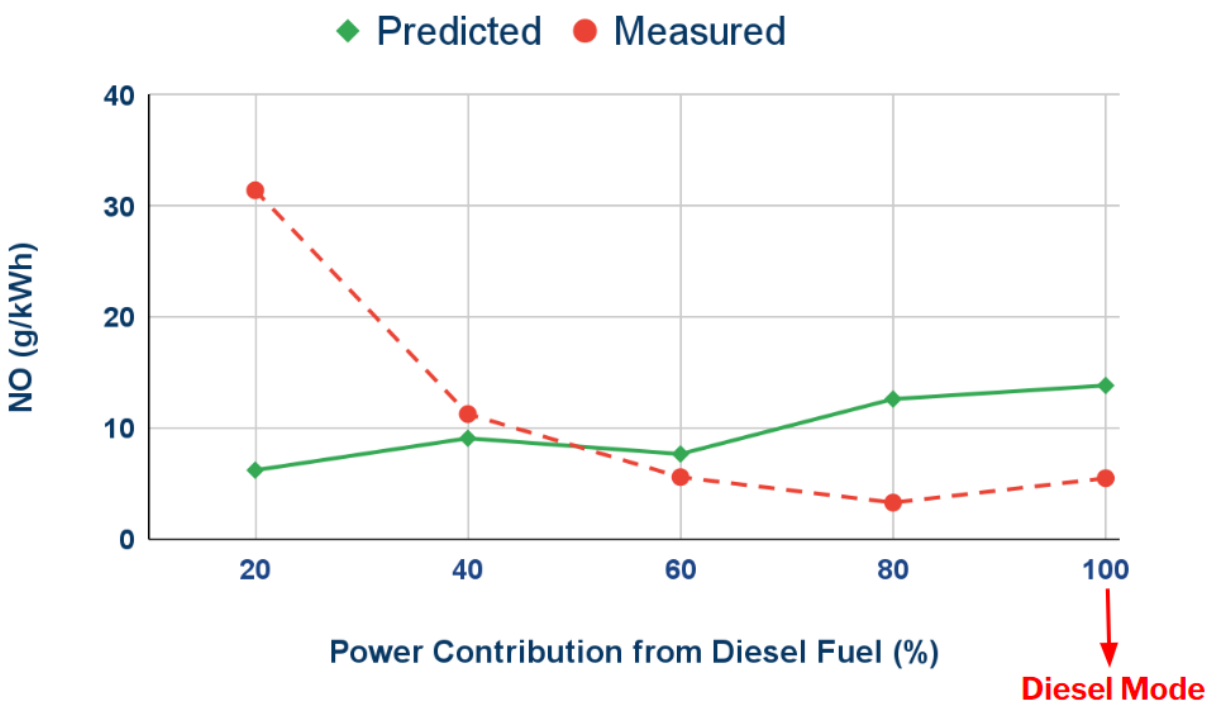

Figure 4.8: NO emission species prediction.

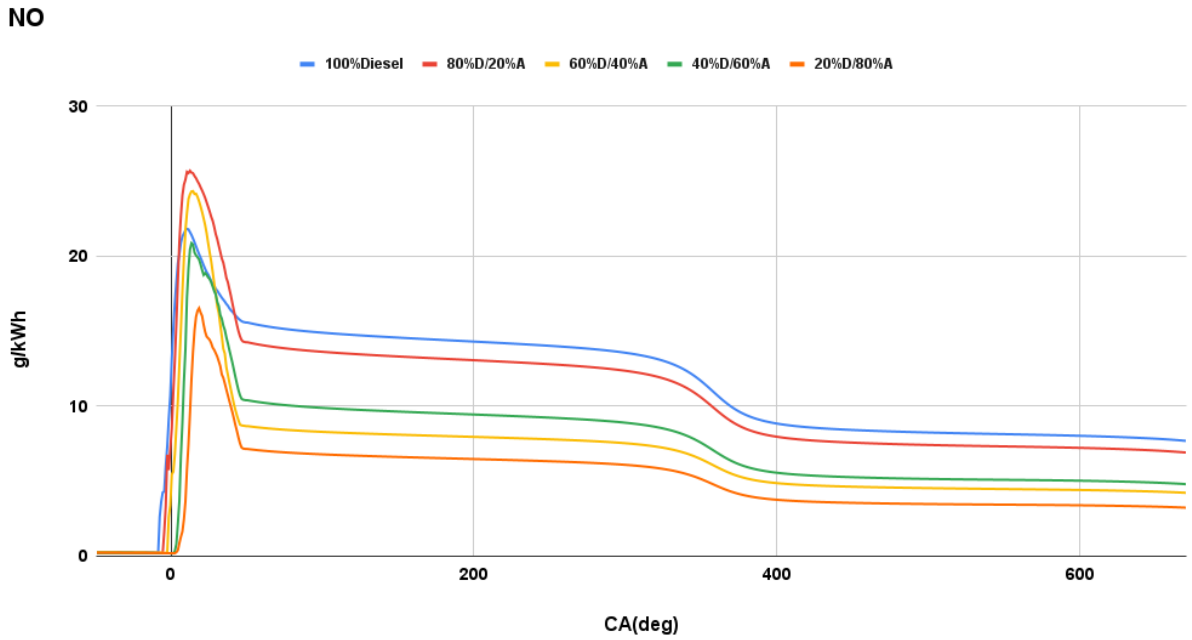

Figure 4.9: NO emission species over Crank Angle (TDC=0).

4.3.2 NO_2 Emission Species

Relatively low levels of NO_2 species concentration in the exhaust gasses were predicted (Fig.4.10), with no experimental data available for validation.

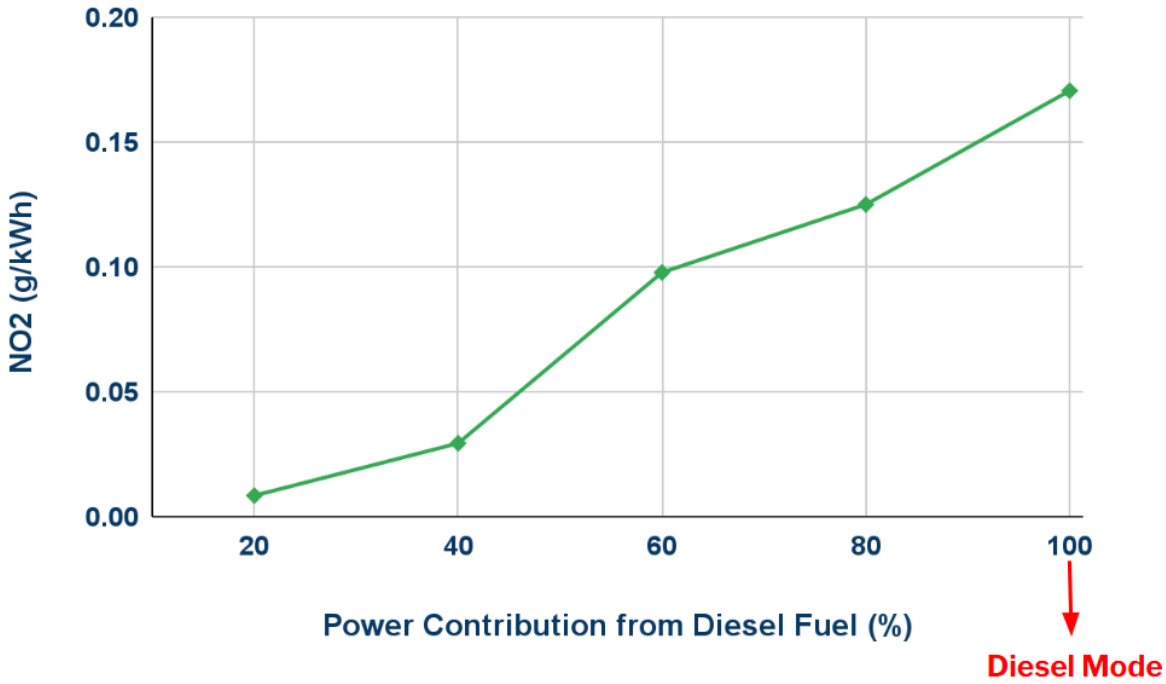

Figure 4.10: NO_2 emission species prediction.

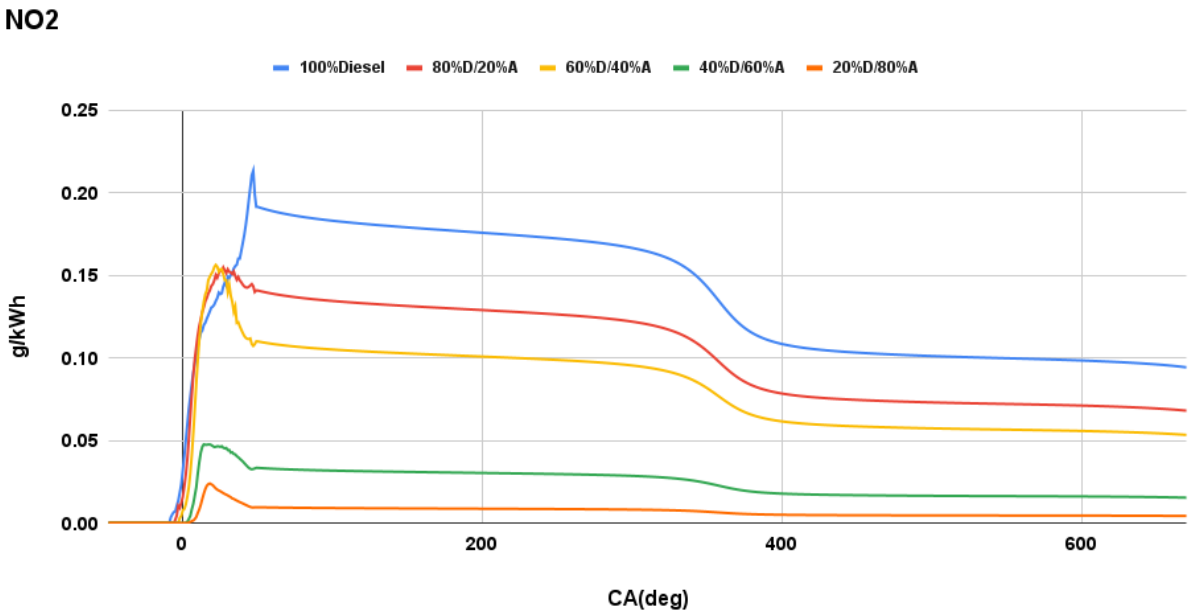

Figure 4.11: NO_2 emission species over Crank Angle (TDC=0).

4.3.3 Total NOx and NO_2/NOx ratio

For completeness purposes, the total NOx emission species prediction is presented (Fig.4.12), as well as the NO_2 / NOx ratio(Fig.4.13).

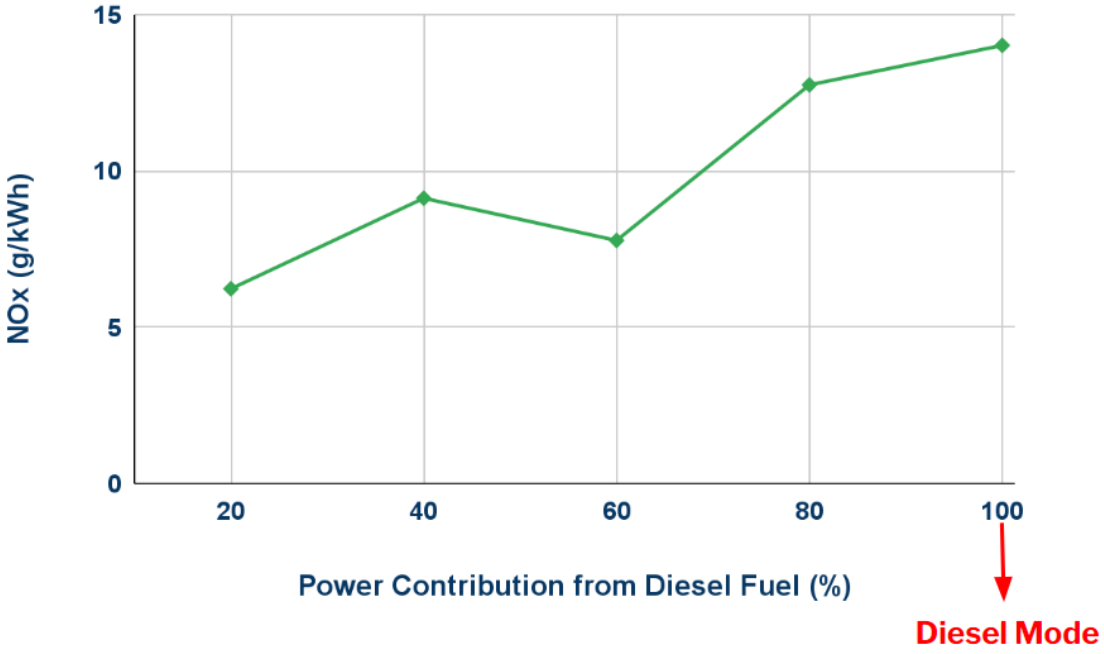

Figure 4.12: Total NOx emissions prediction.

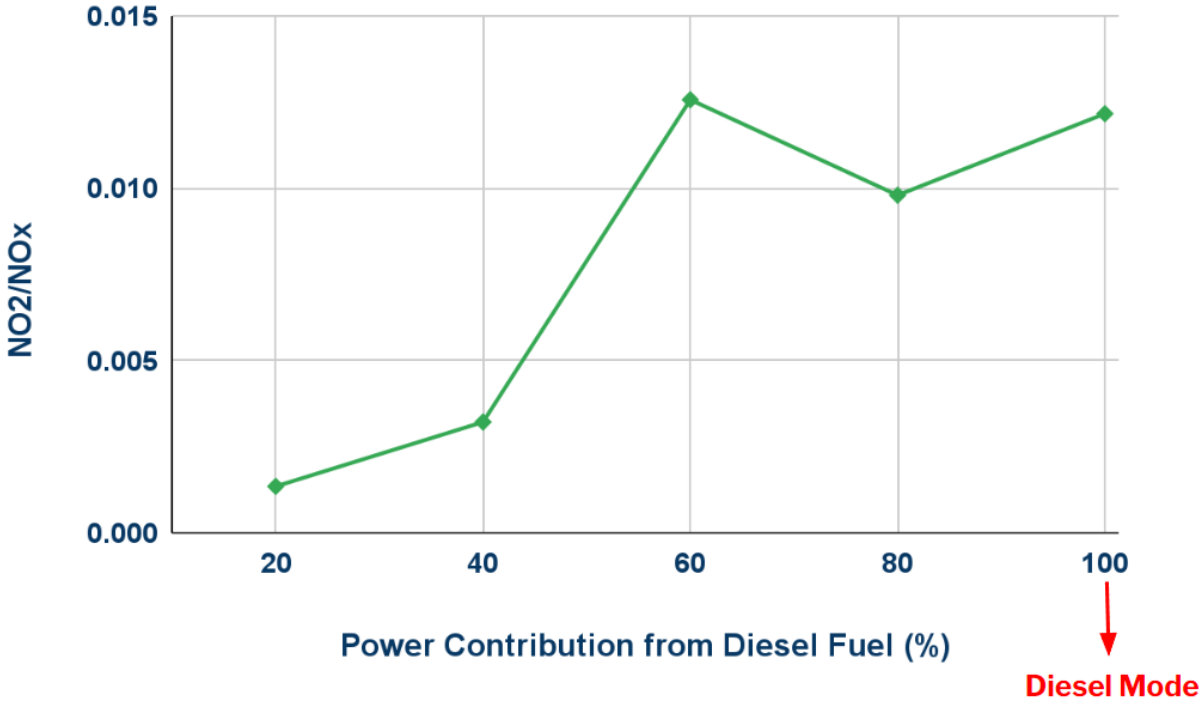

Figure 4.13: NO_2/NOx ratio prediction.

Chapter 5

Conclusions and future work

5.1 Conclusions

5.1.1 General Conclusions

Overall, ammonia was found to be a viable option for minimizing CO_2 emissions. Its satisfactory fuel properties, well established production, storage and distribution network, as well as its carbon-free structure, makes it an attractive choice for decarbonizing the maritime sector. However, the use of ammonia comes with some challenges, mainly associated with its high toxicity and corrosiveness, as well as with a number of unfavorable thermochamical characteristics (high autoignition temperature, narrow flammability limits, low laminar burning velocity). Ammonia slip is one of the major issues that must be addressed when using ammonia in ICE applications. Moreover, during the combustion of ammonia, there is an additional source of NOx due to the fuel bound nitrogen, which will ultimately be oxidized into NOx. One way for coping with these problems, is with the use of exhaust gas aftertreatment systems (e.g. Selective Catalytic Reduction - SCR for NOx reduction). The use of such systems is considered as a viable way for dealing with ammonia slip, since SCR systems have already installed onboard many vessels worldwide. Furthermore, this could be a doubly beneficial, as ammonia is extensively used as an NOx reduction agent.

5.1.2 Conclusion of the present modeling

The main conclusions drawn from the present modeling work can be summarized as follows:

1. The present results yield a good prediction of emitted CO_2.
2. For an energy share of diesel fuel between 40% and 100%, the NO emissions trend is captured satisfactorily by the present modeling.
3. Further validation of the DCKM is necessary for low percentage of diesel fuel (20% and lower) in the diesel-ammonia mixture.
4. Low levels of exhaust concentration were predicted for NO_2 and N_2O, and the results need to be further validated with experiments.

5.1.3 Future Work

First, a wider database of documented experiments is necessary, as the experimental data associated with ammonia combustion in IC engines are still rather limited in the open literature. Further, a more detailed documentation of experiments (Valve Timing, Air Volumetric Efficiency, In-cylinder temperature, etc.) is essential for the development of realistic and accurate models. In comparison to the current availability of emission measurements, addition of NO_2 and N_2O will be required. Regarding the chemical scheme used in the present study, further development and optimization of the ammonia chemistry part should be undertaken. Finally, experimental documentation for large two-stroke marine engines is needed, so that a direct comparison of modeling studies with the actual application is enabled. In the frame of modeling studies, future work can be extended to CFD studies, which can account for a more detailed characterization of combustion and emission formation processes, and possibly for improved prediction of exhaust emissions.

Bibliography

[1] IMO. “Amendments to the Annex of the Protocol of 1997 to amend the International Convention for the Prevention of Pollution from Ships, 1973, as modified by the Protocol of 1978 relating there to (2021 Revised MARPOL Annex VI)”. In: RESOLUTION MEPC.328(76).10 (2021).

[2] IMO. *”Fourth IMO GHG Study”, (2020)*.

[3] DNV. *”DNV Maritime Forecast to 2050”, (2022)*.

[4] Gamma Technologies. *GT-SUITE Integrated Multi-physics Systems Simulation*. URL: https://www.gtisoft.com/gt-suite/.

[5] Aaron J.Reiter and Song-Charng Kong. “Combustion and emissions characteristics of compression-ignition engine using dual ammonia-diesel fuel”. In: *Fuel* 90.1 (2011), pp. 87–97. DOI: https://doi.org/10.1016/j.fuel.2010.07.055.

[6] study.com. *”What is Ammonia?”*. URL: https://study.com/learn/lesson/ammonia-formula-symbol-structure.html.

[7] Dimitriou Pavlos and Rahat Javaid. “A review of ammonia as a compression ignition engine fuel”. In: *International Journal of Hydrogen Energy* 45.11 (2020), pp. 7098–7118. DOI: https://doi.org/10.1016/j.ijhydene.2019.12.209.

[8] The Fertilizer Institute. “Health Effects of Ammonia (2020)”. In: ().

[9] Martin Cames, Nora Wissner, Jürgen Sutter. “Ammonia as a marine fuel”. In: *Institute for Applied Ecology* (2021).

[10] Steven S. Zumdahl. *ammonia chemical compound*. URL: https://www.britannica.com/science/ammonia.

[11] A. Valera-Medina, H. Xiao, M. Owen-Jones, W.I.F.David, P.J.Bowen. “Ammonia for power”. In: *Progress in Energy and Combustion Science* 695 (2018), pp. 63–102. DOI: https://doi.org/10.1016/j.pecs.2018.07.001.

[12] statista. *”Ammonia production worldwide from 2010 to 2021”*. URL: https://www.statista.com/statistics/1266378/global-ammonia-production/.

[13] Venkat Pattabathula, Jim Richardson. “Introduction to Ammonia Production ”. In: *American Institute of Chemical Engineers (AIChE)* (2016). DOI: https://www.aiche.org/sites/default/files/cep/20160969.pdf.

[14] Pragya Berwal, Sudarshan Kumar, Bhupendra Khandelwal. “A comprehensive review on synthesis, chemical kinetics, and practical application of ammonia as future fuel for combustion”. In: *Journal of the Energy Institute* 99 (2021), pp. 273–298. DOI: https://doi.org/10.1016/j.joei.2021.10.001.

[15] Jim Clark. *The Haber Process*. URL: https://chem.libretexts.org/Bookshelves/Physical_and_Theoretical_Chemistry_Textbook_Maps/Supplemental_Modules_(Physical_and_Theoretical_Chemistry)/Equilibria/Le_Chateliers_Principle/The_Haber_Process.

[16] DNV. *"Smells like sustainability: Harnessing ammonia as ship fuel". In: MARITIME IMPACT, February 2022*. URL: https://www.dnv.com/expert-story/maritime-impact/Harnessing-ammonia-as-ship-fuel.html.

[17] Caneon Kurien, Mayank Mittal. "Review on the production and utilization of green ammonia as an alternate fuel in dual-fuel compression ignition engines". In: *Energy Conversion and Management* 251 (2022), p. 114990. DOI: https://doi.org/10.1016/j.enconman.2021.114990.

[18] J.H.Lee, J.H.Kim, J.H.Park, O.C.Kwon. "Studies on properties of laminar premixed hydrogen-added ammonia/air flames for hydrogen production". In: *International Journal of Hydrogen Energy* 35.3 (2010), pp. 1054–1064. DOI: https://doi.org/10.1016/j.ijhydene.2009.11.071.

[19] Akihiro Hayakawa, Takashi Goto, Rentaro Mimoto, Yoshiyuki Arakawa, Taku Kudo, Hideaki Kobayashi. "Laminar burning velocity and Markstein length of ammonia/air premixed flames at various pressures". In: *Fuel* 159 (2015), pp. 98–106. DOI: https://doi.org/10.1016/j.fuel.2015.06.070.

[20] Kenji Takizawa, Akifumi Takahashi, Kazuaki Tokuhashi, Shigeo Kondo, Akira Sekiya. "Burning velocity measurements of nitrogen-containing compounds". In: *Journal of Hazardous Materials* 155.1-2 (2008), pp. 144–152. DOI: https://doi.org/10.1016/j.jhazmat.2007.11.089.

[21] U.J Pfahl, M.C Ross, J.E Shepherd, K.O Pasamehmetoglu, C Unal. "Flammability limits, ignition energy, and flame speeds in H2–CH4–NH3–N2O–O2–N2 mixtures". In: *Combustion and Flame* 123.1-2 (2000), pp. 140–158. DOI: https://doi.org/10.1016/S0010-2180(00)00152-8.

[22] Zakaznov, V.F., Kursheva, L.A.,Fedina, Z.I. "Determination of normal flame velocity and critical diameter of flame extinction in ammonia-air mixture". In: *Combustion Explosion and Shock Waves* 14 (1978), pp. 710–713. DOI: https://doi.org/10.1007/BF00786097.

[23] Paul D. Ronney. "Effect of Chemistry and Transport Properties on Near-Limit Flames at Microgravity". In: *Combustion Science and Technology* 59.1-3 (1988), pp. 123–141. DOI: https://doi.org/10.1080/00102208808947092.

[24] Hideaki Kobayashi, Akihiro Hayakawa, K.D. Kunkuma A. Somarathne, Ekenechukwu C. Okafor. "Science and technology of ammonia combustion". In: *Proceedings of the Combustion Institute* 37.1 (2019), pp. 109–133. DOI: https://doi.org/10.1016/j.proci.2018.09.029.

[25] Engineering Toolbox. *Air- Composition and Molecular Weight*. URL: https://www.engineeringtoolbox.com/air-composition-d_212.html.

[26] LYON RICHARD K. *Method for the reduction of the concentration of NO in combustion effluents using ammonia*. 1975. URL: https://www.freepatentsonline.com/3900554.html.

[27] Richard K. Lyon. "The NH3-NO-O2 reaction". In: *International Journal of Chemical Kinetics* 8 (1976), pp. 315–318. DOI: https://doi.org/10.1002/kin.550080213.

[28] B.S.Haynes. "Reactions of ammonia and nitric oxide in the burnt gases of fuel-rich hydrocarbon-air flames". In: *Combustion and Flame* 28 (1977), pp. 81–91. DOI: https://doi.org/10.1016/0010-2180(77)90010-4.

[29] M.A.Cremer, C.J. Montgomery, D.H.Wang, M.P.Heap, J.-Y.Chen. "Development and implementation of reduced chemistry for computational fluid dynamics modeling of selective non-catalytic reduction". In: *Proceedings of the Combustion Institute* 28.2 (2000), pp. 2427–2434. DOI: https://doi.org/10.1016/S0082-0784(00)80656-6.

[30] James A.Miller, Craig T.Bowman. “Mechanism and modeling of nitrogen chemistry in combustion”. In: *Progress in Energy and Combustion Science* 15.4 (1989), pp. 287–338. DOI: https://doi.org/10.1016/0360-1285(89)90017-8.

[31] James A.Miller, M.C. Branch, Robert J.Kee. “A chemical kinetic model for the selective reduction of nitric oxide by ammonia”. In: *Combustion and Flame* 43 (1981), pp. 81–98. DOI: https://doi.org/10.1016/0010-2180(81)90008-0.

[32] James A. Miller, Mitchell D. Smooke, Robert M. Green, Robert J. Kee. “Kinetic Modeling of the Oxidation of Ammonia in Flames”. In: *Combustion Science and Technology* 34.1-6 (1983), pp. 149–176. DOI: https://doi.org/10.1080/00102208308923691.

[33] D.I.Maclean, H.Gg.Wagner. “The structure of the reaction zones of ammonia-oxygen and hydrazine-decomposition flames”. In: *Symposium (International) on Combustion* 11.1 (1967), pp. 871–878. DOI: https://doi.org/10.1016/S0082-0784(67)80213-3.

[34] Robert M.Green, James A.Miller. “The measurement of relative concentration profiles of NH2 using laser absorption spectroscopy”. In: *Journal of Quantitative Spectroscopy and Radiative Transfer* 26.4 (1981), pp. 313–327. DOI: https://doi.org/10.1016/0022-4073(81)90126-6.

[35] C. P. Fenimore, G. W. Jones. “OXIDATION OF AMMONIA IN FLAMES”. In: *J. Phys. Chem.* 65.2 (1961), pp. 313–327. DOI: https://doi.org/10.1021/j100820a027.

[36] R. C. Murray, A. R. Hall. “Flame speeds in hydrazine vapour and in mixtures of hydrazine and ammonia with oxygen”. In: *Transactions of the Faraday Society* 47 (1951), pp. 743–751. DOI: DOIhttps://doi.org/10.1039/TF9514700743.

[37] Alka Karan, Guillaume Dayma, Christian Chauveau, Fabien Halter. “High-pressure and temperature ammonia flame speeds”. In: *13th Asia-Pacific Conference on Combustion (ASPACC)* (2021).

[38] Klippenstein, Stephen J., Mark Pfeifle, Jasper Ahren W., Peter Glarborg. “Theory and modeling of relevance to prompt-NO formation at high pressure”. In: *Combustion and Flame* 195 (2018), pp. 3–17. DOI: 10.1016/j.combustflame.2018.04.029.

[39] Philippe Dagaut, Peter Glarborg, Maria U.Alzuetac. “The oxidation of hydrogen cyanide and related chemistry”. In: *Progress in Energy and Combustion Science* 34.1 (2008), pp. 1–46. DOI: https://doi.org/10.1016/j.pecs.2007.02.004.

[40] Yingjia Zhang, Olivier Mathieu, Eric L Petersen, Gilles Bourque. “Assessing the predictions of a NO x kinetic mechanism on recent hydrogen and syngas experimental data”. In: *Combustion and Flame* 182 (2017), pp. 122–141. DOI: 10.1016/j.combustflame.2017.03.019.

[41] Krishna Prasad Shrestha, Lars Seidel, Thomas Zeuch, Fabian Mauss. “Detailed Kinetic Mechanism for the Oxidation of Ammonia Including the Formation and Reduction of Nitrogen Oxides”. In: *Energy Fuels* 32.10 (2018), 10202□10217. DOI: 10.1021/acs.energyfuels.8b01056.

[42] Hisashi Nakamura Susumu Hasegawa. “Combustion and ignition characteristics of ammonia/air mixtures in a micro flow reactor with a controlled temperature profile”. In: *Proceedings of the Combustion Institute* 36.3 (2017), pp. 4217–4226. DOI: https://doi.org/10.1016/j.proci.2016.06.153.

[43] Ekenechukwu Chijioke Okafor, Yuji Naito, Sophie Colson, Akinori Ichikawa, Taku Kudo, Akihiro Hayakawa, Hideaki Kobayashi. “Measurement and modelling of the laminar burning velocity of methane-ammonia-air flames at high pressures using a reduced reaction mechanism”. In: *Combustion and Flame* 204 (2019), pp. 162–175. DOI: https://doi.org/10.1016/j.combustflame.2019.03.008.

[44] Junichiro Otomo , Mitsuo Koshi , Teruo Mitsumori, Hiroshi Iwasaki , Koichi Yamada. “Chemical kinetic modeling of ammonia oxidation with improved reaction mechanism for ammonia/air and ammonia/hydrogen/air combustion”. In: *International Journal of Hydrogen Energy* 43.5 (2018), pp. 3004–3014. DOI: https://doi.org/10.1016/j.ijhydene.2017.12.066.

[45] Alessandro Stagni, Carlo Cavallotti, Suphaporn Arunthanayothin, Yu Song, Olivier Herbinet, Frédérique Battin-Leclerc, Tiziano Faravelli. “An experimental, theoretical and kinetic-modeling study of the gas-phase oxidation of ammonia”. In: *Reaction Chemistry Engineering* 5 (2020), pp. 696–711. DOI: https://doi.org/10.1039/C9RE00429G.

[46] Olivier Mathieu, Eric L.Petersen. “Experimental and modeling study on the high-temperature oxidation of Ammonia and related NOx chemistry”. In: *Combustion and Flame* 162.3 (2015), pp. 554–570. DOI: https://doi.org/10.1016/j.combustflame.2014.08.022.

[47] A.A. Konnov. “Implementation of the NCN pathway of prompt-NO formation in the detailed reaction mechanism”. In: *Combustion and Flame* 156.11 (2009), pp. 253–276. DOI: https://doi.org/10.1016/j.combustflame.2009.03.016.

[48] A.A. Konnov. *Konnov’s mechanism v0.6*. URL: https://chemistry.cerfacs.fr/en/chemical-database/mechanisms-list/konnovs-mechanism-v2/.

[49] R. P. Lindstedt, F. C. Lockwood, M. A. Selim. “Detailed Kinetic Modelling of Chemistry and Temperature Effects on Ammonia Oxidation”. In: *Combustion Science and Technology* 99.4-6 (1994), pp. 253–276. DOI: https://doi.org/10.1080/00102209408935436.

[50] Zhenyu Tian, Lidong Zhang, Yuyang Li, Tao Yuan, Fei Qi. “An experimental and kinetic modeling study of a premixed nitromethane flame at low pressure”. In: *Proceedings of the Combustion Institute* 32.1 (2009), pp. 311–318. DOI: https://doi.org/10.1016/j.proci.2008.06.098.

[51] Berkley combustion team. *GRI-Mech 3.0*. URL: https://chemistry.cerfacs.fr/en/chemical-database/mechanisms-list/gri-mech-3-0/.

[52] Peter Glarborg Øyvind Skreiberg Pia Kilpinen. “Ammonia chemistry below 1400 K under fuel-rich conditions in a flow reactor”. In: *Combustion and Flame* 136.4 (2004), pp. 501–518. DOI: https://doi.org/10.1016/j.combustflame.2003.12.008.

[53] Peter Glarborg Teresa Mendiara. “Ammonia chemistry in oxy-fuel combustion of methane”. In: *Combustion and Flame* 156.10 (2009), pp. 1937–1949. DOI: https://doi.org/10.1016/j.combustflame.2009.07.006.

[54] David Stern Anthony M. Dean Mau-Song Chou. “Kinetics of rich ammonia flames”. In: *International Journal of Chemical Kinetics* 16.6 (1984), pp. 633–653. DOI: https://doi.org/10.1002/kin.550160603.

[55] Anthony M. Dean, Joseph W. Bozzelli. “Combustion Chemistry of Nitrogen”. In: *Gas-Phase Combustion Chemistry* (2000), pp. 125–341. DOI: https://doi.org/10.1007/978-1-4612-1310-9_2.

[56] Stephen J.Klippenstein, Lawrence B.Harding, Peter Glarborg, James A.Miller. "The role of NNH in NO formation and control". In: *Combustion and Flame* 158.4 (2011), pp. 774–789. DOI: https://doi.org/10.1016/j.combustflame.2010.12.013.

[57] Borisovich Zeldovich. "Selected Works of Yakov Borisovich Zeldovich, Volume I". In: Addison-Wesley, 1992. Chap. 25. The Oxidation of Nitrogen in Combustion and Explosions.

[58] C.Duynslaegher, H.Jeanmart, J.Vandooren. "Flame structure studies of premixed ammonia/hydrogen/oxygen/argon flames: Experimental and numerical investigation". In: *Proceedings of the Combustion Institute* 32.1 (2009), pp. 1277–1284. DOI: https://doi.org/10.1016/j.proci.2008.06.036Getrightsandcontent.

[59] S.S.Gill, G.S.Chatha, A.Tsolakis, S.E.Golunski, A.P.E.York. "Assessing the effects of partially decarbonising a diesel engine by co-fuelling with dissociated ammonia". In: *International Journal of Hydrogen Energy* 37.7 (2012), pp. 6074–6083. DOI: https://doi.org/10.1016/j.ijhydene.2011.12.137.

[60] Niki Y., Nitta Y., Sekiguchi H., Hirata K. "Diesel Fuel Multiple Injection Effects on Emission Characteristics of Diesel Engine Mixed Ammonia Gas Into Intake Air." In: *ASME. J. Eng. Gas Turbines Power* 141.6 (2019). DOI: https://doi.org/10.1115/1.4042507.

[61] Seamus P., Kane William F. Northrop. "Thermochemical Recuperation to Enable Efficient Ammonia-Diesel Dual-Fuel Combustion in a Compression Ignition Engine". In: *Energies* 14.22 (2021), p. 7540. DOI: https://doi.org/10.3390/en14227540.

[62] RH Thurston. *A History of the Growth of the Steam-Engine*. 1878.

[63] D. Clerk. *GAS OR OTHER INTERNAL COMBUSTION ENGINE, Patent No. 769,589, 1904*. URL: https://patents.google.com/patent/US769589A/en.

[64] Norsk Hydro. *Ammonia running truck*. URL: https://www.flickr.com/photos/hydrogencarsnow/8136698514.

[65] M. Zavka. *Device for operating internal combustion engines with mixtures of Ammonia, Hydrogen and Nitrogen prepared from Ammonia, 1938*.

[66] E. Kroch. *Ammonia - a fuel for motor buses*. 1945.

[67] P.G. Grimes. "Energy Depot Fuel Production and Utilization". In: *SAE Transactions* 74 (1966), pp. 281–299, 316–326. DOI: https://www.jstor.org/stable/44460523.

[68] A.B. Rosenthal. "Energy Depot - A Concept for Reducing the Military Supply Burden". In: *SAE Transactions* 74 (1966), pp. 274–280, 316–326. DOI: https://www.jstor.org/stable/44460522.

[69] Thomas J. Pearsall, Charles G. Garabedian. "Combustion of Anhydrous Ammonia in Diesel Engines". In: *SAE Transactions* 76 (1968), pp. 3213–3221. DOI: https://www.jstor.org/stable/44562853.

[70] Meyer CM. "Ammonia made by renewable energy". In: (2019).

[71] *NH3 car*. URL: http://nh3car.com.

[72] Paul Bond. *Marangoni GT 86-R Eco Explorer*. URL: https://www.autoexpress.co.uk/toyota/gt-86/63372/marangoni-gt-86-r-eco-explorer.

[73] Jay Schmuecker, Pinehurst Farm Schmuecker. *My Solar Hydrogen and Ammonia, and Ammonia Tractor Fuel and Fertilizer System*. URL: https://www.ammoniaenergy.org/paper/my-solar-hydrogen-and-ammonia-and-ammonia-tractor-fuel-and-fertilizer-system/.

[74] M.F Ezza, I. Dincer. “Development and assessment of a new hybrid vehicle with ammonia and hydrogen”. In: *Applied Energy* 219 (2018), pp. 226–239. DOI: https://doi.org/10.1016/j.apenergy.2018.03.012.

[75] MAN Energy Solutions. *MAN BW two-stroke engine operating on ammonia*. URL: https://www.man-es.com/docs/default-source/document-sync/man-b-w-two-stroke-engine-operating-on-ammonia-eng.pdf?sfvrsn=c4bb6fea_0.

[76] WinGD. *WinGD and Hyundai Heavy Industries collaborate on ammonia two-stroke engine delivery*. URL: https://www.wingd.com/en/news-media/press-releases/wingd-and-hyundai-heavy-industries-collaborate-on-ammonia-two-stroke-engine-delivery/.

[77] Song-Charng Kong Aaron J. Reiter. “Demonstration of Compression-Ignition Engine Combustion Using Ammonia in Reducing Greenhouse Gas Emissions”. In: *Energy Fuels* 22.5 (2008), pp. 2963–2971. DOI: https://doi.org/10.1021/ef800140f.

[78] Paul Breeze. *Piston Engine-Based Power Plants*. ELSEVIER, 2018. ISBN: 978-0-12-812904-3.

[79] Simone Lion, Ioannis Vlaskos, Rodolfo Taccani. “A review of emissions reduction technologies for low and medium speed marine Diesel engines and their potential for waste heat recovery”. In: *Energy Conversion and Management* 207 (2020), p. 112553. DOI: https://doi.org/10.1016/j.enconman.2020.112553.

[80] John B. Heywood. *Internal Combustion Engine Fundamentals, 2nd Edition*. McGraw-Hill Education, 2018. ISBN: 9781260116106.

[81] Meng-Choung Chiong, Cheng Tung Chong, Jo-Han Ng, Syed Mashruk, William Woei Fong Chong, Nor Afzanizam Samirang, Guo Ren Mong, Agustin Valera-Medina. “Advancements of combustion technologies in the ammonia-fuelled engines”. In: *Energy Conversion and Management* 244 (2021), p. 114460. DOI: https://doi.org/10.1016/j.enconman.2021.114460.

[82] E. S. Starkman, G. E. James, H. K. Newhall. “Ammonia as a Diesel Engine Fuel: Theory and Application”. In: *SAE Transactions* 76 (1968), pp. 3193–3212. DOI: https://www.jstor.org/stable/44562852.

[83] James T. Gray Jr., Edward Dimitroff, Nelson T. Meckel, R. D. Quillian Jr. “Ammonia Fuel — Engine Compatibility and Combustion”. In: *SAE Transactions* 75 (1967), pp. 785–807. DOI: https://www.jstor.org/stable/44563675.

[84] Garabedian Charles G., Johnson John H. “THE THEORY OF OPERATION OF AN AMMONIA BURNING INTERNAL COMBUSTION ENGINE”. In: *ARMY TANK-AUTOMOTIVE CENTER WARREN MI* (1966).

[85] E.S. Starkman, G.E. James, H.K. Newhall. “Ammonia as a diesel engine fuel: theory and application”. In: *SAE Transactions* (1968), pp. 3193–3212. DOI: http://www.jstor.org/stable/44562852.

[86] Pearsall Thomas J. “AMMONIA APPLICATION TO RECIPROCATING ENGINES. VOLUME 1”. In: *CONTINENTAL AVIATION AND ENGINEERING CORP DETROIT MI* (1967).

[87] Wikipedia. *Continental AV1790*. URL: https://en.wikipedia.org/wiki/Continental_AV1790.

[88] Klaus Bro, Peter Sunn Pedersen. “Alternative Diesel Engine Fuels: An Experimental Investigation of Methanol, Ethanol, Methane and Ammonia in a D.I. Diesel Engine with Pilot Injection”. In: *SAE Technical Paper 770794* (1977). DOI: https://doi.org/10.4271/770794.

[89] Lee D., Song H.H. “Development of combustion strategy for the internal combustion engine fueled by ammonia and its operating characteristics”. In: *J Mech Sci Technol* 32 (2018), pp. 1905–1925. DOI: https://doi.org/10.1007/s12206-018-0347-x.

[90] Lamas M. I., C. G. Rodriguez. “NOx Reduction in Diesel-Hydrogen Engines Using Different Strategies of Ammonia Injection”. In: *Energies* 12.7 (2018), p. 1255. DOI: https://doi.org/10.3390/en12071255.

[91] Kun Lin Tay , Wenming Yang, Jing Li, Dezhi Zhoua Wenbin Yu, Feiyang Zhao, Siaw Kiang Chou, Balaji Mohana. “Numerical investigation on the combustion and emissions of a kerosene-diesel fueled compression ignition engine assisted by ammonia fumigation”. In: *Applied Energy* 204 (1476-1488). DOI: https://doi.org/10.1016/j.apenergy.2017.03.100.

[92] Michał Pyrc, Michał Gruca, Romualdas Juknelevičius. “An experimental investigation of the performance, emission and combustion stability of compression ignition engine powered by diesel and ammonia solution (NH4OH)”. In: *Institution of Mechanical Engineers* 22.8 (). DOI: https://doi.org/10.1177/1468087420940942.

[93] ABS. “AMMONIA AS MARINE FUEL”. In: *SUSTAINABILITY WHITEPAPER* (2020).

[94] Zehra Şahin, İmdat Ziya Akcanca, Orhan Durgun. “Experimental investigation of the effects of ammonia solution (NH3OH) on engine performance and exhaust emissions of a small diesel engine”. In: *Fuel* 214 (2018), pp. 330–341. DOI: https://doi.org/10.1016/j.fuel.2017.10.034.

[95] Song-Charng Kong, Matthias Veltman, Christopher Gross. “Performance of a Compression-Ignition Engine Using Direct-Injection of Liquid Ammonia/DME Mixture”. In: *Iowa Energy Center* (2008).

[96] Christopher W.Gross, Song-Charng Kong. “Performance characteristics of a compression-ignition engine using direct-injection ammonia–DME mixtures”. In: *Fuel* 103 (2013), pp. 1069–1079. DOI: https://doi.org/10.1016/j.fuel.2012.08.026.

[97] Kyunghyun Ryu, George E.Zacharakis-Jutz, Song-Charng Kong. “Performance characteristics of compression-ignition engine using high concentration of ammonia mixed with dimethyl ether”. In: *Applied Energy* 113 (2014), pp. 488–499. DOI: https://doi.org/10.1016/j.apenergy.2013.07.065.

[98] Wentao Wang, José M.Herrerosa, Athanasios Tsolakis, Andrew P.E.York. “Ammonia as hydrogen carrier for transportation; investigation of the ammonia exhaust gas fuel reforming”. In: *International Journal of Hydrogen Energy* 38.23 (2013), pp. 9907–9917. DOI: https://doi.org/10.1016/j.ijhydene.2013.05.144.

[99] M. Pochet,H. Jeanmart, F. Contino. “Compression Ratio Ammonia-Hydrogen HCCI Engine: Combustion, Load, and Emission Performances.” In: *Front. Mech. Eng.* (2020). DOI: https://doi.org/10.3389/fmech.2020.00043.

[100] M. Pochet, V. Dias, H. Jeanmart, S. Verhelst, F. Contino. “Multifuel CHP HCCI Engine towards Flexible Power-to-fuel: Numerical Study of Operating Range”. In: *Energy Procedia* 105 (2017). DOI: https://doi.org/10.1016/j.egypro.2017.03.468.

[101] Gamma Technologies. “Engine Performance Application Manual”. In: (2022).

[102] Eliseo Ranzi, Alessio Frassoldati, Alessandro Stagni, Matteo Pelucchi, Alberto Cuoci, Tiziano Faraveli. “Reduced Kinetic Schemes of Complex Reaction Systems: Fossil and Biomass-Derived Transportation Fuels”. In: *International Journal of Chemical Kinetics* 46.9 (2014), pp. 512–542. DOI: https://doi.org/10.1002/kin.20867.

[103] T. Faravelli, Alessio Frassoldati, Eliseo Ranzi. “Kinetic modeling of the interactions between NO and hydrocarbons in the oxidation of hydrocarbons at low temperaturess”. In: *Combustion and Flame* 132.1-2 (2003), pp. 188–207. DOI: https://doi.org/10.1016/S0010-2180(02)00437-6.

[104] D. Kazangas , G. Skevis , L. Kaiktsis. “Effects of NOx -SOx Addition on Methane Ignition: Toward a Kinetic Understanding for Marine Engine Applications”. In: *The Journal of Energy Engineering* (2021). DOI: 10.1061/(ASCE)EY.1943-7897.0000752..